

LATE CRETACEOUS AND EARLY TERTIARY TURTLES FROM
THE BIG BEND REGION, BREWSTER COUNTY, TEXAS

by

SUSAN LEIGH TOMLINSON, B.F.A., M.S.

A DISSERTATION

IN

GEOSCIENCE

Submitted to the Graduate Faculty
of Texas Tech University in
Partial Fulfillment of
the Requirements for
the Degree of

DOCTOR OF PHILOSOPHY

Approved

Accepted

May, 1997

Copyright 1997, Susan L. Tomlinson

ACKNOWLEDGEMENTS

I would like to thank the members of my committee, Dr. Sankar Chatterjee, Dr. George Asquith, Dr. James Barrick, Dr. Richard Strauss, and the committee chairman, Dr. Thomas Lehman for their contributions to this dissertation. In particular, I'd like to thank Dr. James Barrick and Dr. Richard Strauss for their valuable insight in the many discussions we had about certain parts of this study.

Tom Lehman was instrumental in starting me on the path of the turtle. Without his support and invaluable knowledge about Big Bend stratigraphy and vertebrate paleontology, this project would not have been started, nor completed. I look forward to many more years of Big Bend collaboration with him.

There were a number of people who helped in both big and small ways. I thank the Texas Memorial Museum, the Louisiana State University Museum of Natural Science, and the Museum at Texas Tech University for making their collections available to me. Julia Sankey at LSU also helped by tracking down map locations. For their help in the field I thank Bill Straight, James Browning, Dave Evans, Heather Beatty, and Dr. Elisabeth Wheeler. I'd like to thank Dr. Howard Hutchison for sharing the University of California Museum of Paleontology turtle collection with me for my edification (and also for his many explanations). I also thank the following for their help: Anne Weil, Dr. Kathleen Nichols, and Jill Haukos.

Most of all, I thank my husband, Walt Schaller. I wouldn't have finished without his support.

TABLE OF CONTENTS

| | |
|---|-----|
| ACKNOWLEDGMENTS..... | ii |
| ABSTRACT..... | iv |
| LIST OF TABLES..... | v |
| LIST OF FIGURES..... | vi |
| CHAPTER | |
| I. INTRODUCTION..... | 1 |
| II. STRATIGRAPHY..... | 5 |
| III. SYSTEMATIC PALEONTOLOGY..... | 21 |
| IV. STRATIGRAPHIC DISTRIBUTION OF TURTLES..... | 117 |
| V. ECOLOGICAL DIVERSITY OF THE BIG BEND | |
| TURTLE FAUNA..... | 125 |
| VI. MORPHOMETRIC ANALYSIS OF PIT VARIANCE IN | |
| TRIONYCHID SHELLS..... | 148 |
| REFERENCES..... | 177 |
| APPENDIX..... | 184 |

ABSTRACT

Fossil turtles are abundant in the Upper Cretaceous and Lower Tertiary sediments of the Aguja, Javelina, and Black Peaks Formations in Big Bend National Park, Brewster County, Texas. Nine genera of freshwater and terrestrial turtles have been identified from these deposits, including *Bothremys*, "*Baena*", *Neurankylus*, *Compsemys*, *Adocus*, *Basilemys*, "*Aspideretes*", "*?Helopanoplia*" and *Hoplochelys*. A marine turtle from the Aguja Formation represents a new genus.

Turtles are most abundant in the marginal marine, brackish, and freshwater floodplain deposits of the Aguja Formation, and within the Aguja, they are most abundant in the upper shale member. "*Aspideretes*" is the dominant genus in the Upper Cretaceous sediments, followed by "*Baena*". Turtle fossils are rare in the fluvial floodplain deposits of the Javelina Formation, where the dominant genus is also "*Aspideretes*." There is a slight increase in abundance and diversity of turtles in the fluvial floodplain deposits of the overlying Black Peaks Formation, where *Hoplochelys* is the dominant genus. The decrease in numbers and diversity of turtles in the Javelina and Black Peaks formations, compared to the Aguja, was probably the result of a change to dry inland environments less hospitable to turtles.

The diversity level of the upper shale member of the Aguja Formation is comparable to that in the correlative Fruitland and Kirtland formations of the San Juan Basin in New Mexico, and to a modern assemblage of turtles in the Brazos River

drainage basin in Texas. A comparison of the shell morphologies exhibited in the Aguja fauna and in the Brazos River fauna also suggests that the diversity level is comparable. A morphometric technique was used to determine whether variability in the ornamentation patterns in trionychid shells is useful for taxonomic discrimination. Preliminary results suggest that discrete shell ornamentation patterns are discriminatory and non-random. This technique may be useful for identifying levels of fossil trionychid diversity

LIST OF TABLES

| | | |
|-----|--|-----|
| 4.1 | Turtles of the Aguja, Javelina and Black Peaks formations... | 120 |
| 5.1 | Genera of turtles represented in the modern Brazos River drainage of Texas, the Aguja fauna of Big Bend, and the Fruitland and Kirtland fauna of New Mexico..... | 131 |
| 5.2 | Comparison of Brazos River drainage fauna and Aguja fauna..... | 143 |
| 5.3 | Comparison of Brazos River drainage fauna and Aguja fauna..... | 144 |
| 5.4 | Taxa and number of individuals from the upper shale member of the Aguja Formation used for Simpson's Index calculations..... | 146 |
| 6.1 | Variables used in morphometric study..... | 155 |
| 6.2 | TOTTURT data..... | 158 |
| 6.3 | RANDTURTNC data..... | 165 |
| 6.4 | ALLDATA..... | 168 |

LIST OF FIGURES

| | | |
|------|--|----|
| 2.1 | Upper Cretaceous and lower Tertiary strata in Big Bend (after Maxwell et al., 1967 and Lehman, 1985)..... | 7 |
| 2.2 | Stratigraphy of the Upper Cretaceous and lower tertiary sediments (after Maxwell et al., 1967)..... | 8 |
| 2.3 | The Aguja Formation as subdivided by Lehman (1985)..... | 11 |
| 3.1 | Carapace and plastron bones and scutes (diagram after Zangerl, 1969)..... | 22 |
| 3.2 | <i>Bothremys</i> sp., TMM 43381-1, left first costal, dorsal and visceral views..... | 26 |
| 3.3 | <i>Bothremys</i> sp., TMM 43469-2, right hyo- (above) and hypoplastron (below), visceral view..... | 28 |
| 3.4 | <i>Bothremys</i> sp., TMM 43469-2, right hyo (above) and hypoplastron (below), ventral view..... | 29 |
| 3.5 | <i>Bothremys</i> sp..... | 32 |
| 3.6 | A comparison of the plastron of <i>Bothremys</i> , <i>Taphrosphys</i> , and the Big Bend specimen..... | 34 |
| 3.7 | " <i>Baena</i> " cf. " <i>B</i> " <i>ornata</i> , LSUMG V-1136, carapace in dorsal view..... | 37 |
| 3.8 | " <i>Baena</i> " cf. " <i>B</i> " <i>ornata</i> , LSUMG V-1136, plastron in ventral view..... | 39 |
| 3.9 | " <i>Baena</i> " cf. " <i>B</i> " <i>nodosa</i> , TMM 42536-1, carapace in dorsal view..... | 43 |
| 3.10 | " <i>Baena</i> " cf. " <i>B</i> " <i>nodosa</i> , TMM 42536-1, plastron in ventral view..... | 44 |

| | | |
|------|---|----|
| 3.11 | " <i>Baena</i> " cf. " <i>B</i> " <i>nodosa</i> , TMM 43251-1, carapace fragments..... | 45 |
| 3.12 | " <i>Baena</i> " cf. " <i>B</i> " <i>nodosa</i> , TMM 432351-1, plastron fragments..... | 46 |
| 3.13 | " <i>Baena</i> " sp., carapace fragments of TTU 5-104-47 in dorsal view..... | 51 |
| 3.14 | " <i>Baena</i> " sp., TTU 5-104-47, plastron in ventral view..... | 52 |
| 3.15 | " <i>Baena</i> " sp., LSUMG V-1168, plastron in ventral view..... | 56 |
| 3.16 | <i>Neurankylus eximius</i> , TMM 43385-1, carapace in dorsal view..... | 63 |
| 3.17 | <i>Neurankylus eximius</i> , TMM 43385-1, plastron in ventral view..... | 65 |
| 3.18 | Cheloniidae, n. gen., n. sp., TMM 43072-1, lower mandible in oral and side views..... | 68 |
| 3.19 | Cheloniidae, n. gen., n. sp., TMM 43072-1, carapace fragments..... | 70 |
| 3.20 | Cheloniidae, n. gen., n. sp., TMM 43072-1, plastron in ventral view..... | 71 |
| 3.21 | Cheloniidae, n. gen., n. sp., TMM 43072-1, left scapula, ventral view..... | 72 |
| 3.22 | Cheloniidae, n. gen., n. sp., TMM 43072-1, left scapula, dorsal view..... | 73 |
| 3.23 | Cheloniidae, n. gen., n. sp., TMM 43072-1, left and right humeri, dorsal view..... | 75 |
| 3.24 | Cheloniidae, n. gen., n. sp., TMM 43072-1, left and right humeri, ventral view..... | 76 |
| 3.25 | Cheloniidae, n. gen., n. sp., TMM 43072-1, right ulna..... | 77 |

| | | |
|------|--|-----|
| 3.26 | Cheloniidae, n. gen., n. sp., TMM 43072-1, right radius..... | 78 |
| 3.27 | Cheloniidae, n. gen., n. sp., TMM 43072-1, right femur..... | 80 |
| 3.28 | Comparison of plastrons of Chelonioidea..... | 82 |
| 3.29 | Comparison of humeri of Chelonioidea..... | 83 |
| 3.30 | <i>Adocus</i> sp., TMM 4257-3, first costal..... | 87 |
| 3.31 | Trionychidae, TMM43380-5, partial carapace..... | 92 |
| 3.32 | Trionychidae, TMM 42335-8, left nuchal..... | 93 |
| 3.33 | Trionychidae, TMM 43534-2, right fifth costal..... | 95 |
| 3.34 | Trionychidae, TMM 43534-8, right hypoplastron..... | 96 |
| 3.35 | Trionychidae, TMM 422880-6, right hyoplastron..... | 98 |
| 3.36 | Trionychidae, TMM 42539-5, left hypoplastron, left xiphiplastron and the distal end of a humerus..... | 100 |
| 3.37 | Trionychidae, TMM 43057-324, left hypoplastron..... | 102 |
| 3.38 | Trionychidae, TMM 42874-1, right xiphiplastron..... | 103 |
| 3.39 | Trionychidae, TMM 41400-5, left humerus..... | 105 |
| 3.40 | Representative specimens of Trionychidae..... | 107 |
| 3.41 | Representative specimen of Trionychidae..... | 108 |
| 3.42 | Representative specimens of Trionychidae..... | 109 |
| 3.43 | Representative neurals from Hoplochelys sp. specimens..... | 113 |
| 3.44 | Representative costals from Hoplochelys sp. specimens..... | 114 |
| 3.45 | Representative peripherals from Hoplochelys sp. specimens..... | 115 |

| | | |
|-----|--|-----|
| 4.1 | Stratigraphic distribution of turtles in the Aguja, Javelina, and Black Peaks formations..... | 118 |
| 4.2 | Stratigraphic distribution of turtles in the Aguja Formation..... | 119 |
| 5.1 | Drainage area estimated for this study..... | 134 |
| 5.2 | Drainage area estimated for this study... .. | 136 |
| 5.3 | Method of measurement for morphology study..... | 141 |
| 6.1 | Plot of PRIN2*PRIN1, TOTTURT data..... | 159 |
| 6.2 | Plot of PRIN3*PRIN2, TOTTURT data..... | 161 |
| 6.3 | Plot of PRIN2*PRIN1, RANDTURTNC data..... | 165 |
| 6.4 | Plot of PRIN3*PRIN2, RANDTURTNC data..... | 166 |
| 6.5 | Plot of PRIN2*PRIN1, ALLDATA..... | 169 |
| 6.4 | Plot of PRIN3*PRIN2, ALLDATA..... | 171 |

CHAPTER I

INTRODUCTION

General Background of Study

Upper Cretaceous and lower Tertiary sedimentary rocks exposed in Big Bend National Park (Texas) accumulated at the southernmost extreme of the Western Interior Province, and the westernmost extreme of the Gulf Coast Province. These sediments record the final transgressive/regressive sequence of the Western Interior Cretaceous Seaway and the subsequent transition from a marine to a terrestrial environment. The total area of exposure of Upper Cretaceous and lower Tertiary sediments in Big Bend is small compared to correlative exposures of these strata elsewhere in North America. In spite of this, numerous invertebrate and vertebrate fossils have been collected from the park since the first geologic work was done there around the turn of the century. Collection of vertebrate fossils began with Barnum Brown working under the aegis of the American Museum of Natural History, and has continued through the years through the efforts of many workers (Langston, Standhardt, and Stevens, 1989). The Big Bend area represents one of the southernmost exposures of Upper Cretaceous and lower Tertiary sediments in North America, and the rarity of exposures underscores the importance of all the vertebrate material that has been collected and studied from Big Bend.

Fossil turtles are relatively abundant in these strata, but have often been overlooked in preference to other fossil vertebrates. The turtles, while occasionally

collected and identified as parts of various other studies, have never been systematically collected and studied as a group. Turtles were an important part of the Late Cretaceous and early Tertiary terrestrial and aquatic ecosystems. Work by Hutchison and Archibald (1986) suggests that turtles could provide important clues to what happened to flora and fauna during the puzzling K/T transition. And, because they survived the transition, and are in fact a “living fossil” organism, modern turtles offer us an opportunity to understand their ecology in a way that other fossils do not. Therefore, it is useful to study turtles as a group on their own merit in order to gain more knowledge about the ecology of that time. The Big Bend turtle fauna, then, is an important component in that body of work. This study focuses on the identification, stratigraphic distribution, and diversity of the Big Bend turtle fauna in order to add to that knowledge.

Purpose and Scope of Study

The purpose of this report is three-fold. First, it documents the occurrence of fossil turtles in Big Bend National Park. Secondly, this study attempts to assess the level of diversity of the Late Cretaceous and early Tertiary turtle fauna by comparing the Big Bend fauna to turtle faunas both from stratigraphically equivalent intervals and from a modern assemblage. Finally, an exploratory morphometric study is used to determine the level of variability in ornamentation patterns on trionychid turtle shells. This technique may allow discrimination between soft-shelled turtle taxa, and thereby give us a more accurate assessment of the level of diversity.

Methods and Techniques

Existing collections of fossil turtle material from the Texas Memorial Museum (TMM), the Museum of Natural Science at Louisiana State University (LSUMG), and the Museum at Texas Tech (TTU) were borrowed for study, and in some cases, preparation. Complete information on the geographic localities and stratigraphic positions for each of the TMM, TTU, and LSUMG turtle fossil specimens are available at the respective institutions.

In addition to studying collections already in existence, field excursions were made to the park for the purpose of collecting additional turtle fossils. In collecting the new turtle specimens, a deliberate attempt was made not to "high grade" the collection. Rather, any and all material, even fragmentary, was collected, in order to better estimate the relative abundance of turtle genera. Standard field techniques, including the use of stabilizing agents such as "Butvar" (a polymer dissolved in acetone) and plaster jackets, were used in the collection of large turtle fossils before removal and transport from the field. Fossil localities were plotted on USGS topographic quadrangles at 1:24,000 scale. All new localities collected are registered at the Texas Memorial Museum and the specimens were repositied with the Texas Memorial Museum at the conclusion of this study.

The new specimens were prepared at Texas Tech University. An effort was made to reconstruct fragmented fossils where possible, and to stabilize those that were too poorly preserved to reconstruct. Broken fragments were bonded with epoxy and plaster, and surfaces coated with Butvar. In some cases, hard concretionary sandstone

coatings or friable gypsum and calcite coatings obscured surface detail. These coatings were removed, in part, with the use of an airscribe, the sparing use of acetic acid, and careful application of various dental tools.

CHAPTER II

STRATIGRAPHY

Regional Geology

Late Cretaceous and early Tertiary sedimentary rocks are exposed in the fill of a basin that formed in Big Bend National Park during Laramide time. This large intermontane basin, covering much of the Trans-Pecos region, is known as the Tornillo Basin. The Tornillo Basin is bounded on the west by the Chihuahua Tectonic Belt, and on the east by the Marathon Uplift (Lehman, 1985, 1991). The Tornillo Basin is a strongly asymmetric sedimentary basin with the thickest accumulation of sediment along the eastern margin (Lehman, 1991). This basin was disrupted by extensional faulting in late Tertiary time, resulting in the “Big Bend Sunken Block” (Udden, 1907), a large graben in which Big Bend National Park now sits.

In Big Bend, the fault-bounded Sunken Block comprises a valley approximately 25 km wide, bounded on the east by the Sierra del Carmen, a west-dipping faulted monocline, and the Santiago Mountains, a overturned faulted anticline (Maxwell, Lonsdale, Hazzard, and Wilson, 1967). The Sierra del Carmen and the Santiago Mountains border the southwestern margin of the Marathon Uplift. The Sunken Block graben is bounded on the west by Mesa de Anguila, a northwest-trending tilted fault block, and the Terlingua Uplift, a broad arch with a steeply dipping southwestern margin (Maxwell et al., 1967). Most of the major folds and thrust faults bounding the uplifts and within the basin trend northwest and were formed during the

Laramide Orogeny (Maxwell et al., 1967). The Terlingua-Solitario Uplift, a large dome resulting in part from the intrusion of a laccolith in middle Tertiary time, exhibits evidence for left-lateral transpressive deformation during Laramide time (Maxwell et al., 1967; Erdlac, 1990; Lehman, 1991).

Upper Cretaceous and Lower Tertiary Strata

The Upper Cretaceous and lower Tertiary strata in Big Bend National Park have been largely covered by middle Tertiary volcanic rock and Quaternary sediment, have been intruded by numerous middle Tertiary plutons, and disrupted by late Tertiary faulting (Lehman, 1991). However, exposures of these strata occur in numerous areas within the park (Figure 2.1). These sediments record the transition from the last major marine regression of the Western Interior Cretaceous Seaway to the fluvial-dominated terrestrial environments of latest Cretaceous to earliest Tertiary time. Udden (1907) was among the first to map the strata in the Tornillo Basin. At that time, strata that are now known to be Paleocene and Eocene in age (Black Peaks and Hannold Hill Formations) were included with those of the Upper Cretaceous (Udden, 1907). These strata have more recently been subdivided into five formations that are, in ascending order, the Aguja, Javelina, Black Peaks, Hannold Hill, and Canoe Formations (Figure 2.2). These formations (excluding the Aguja) together comprise the “Tornillo Clays” of Udden (1907), and were subsequently renamed the Tornillo Formation by Adkins (1933). Maxwell et al. (1967) redefined the Tornillo Formation as the Tornillo Group, and subdivided the Tornillo Group into the Javelina,

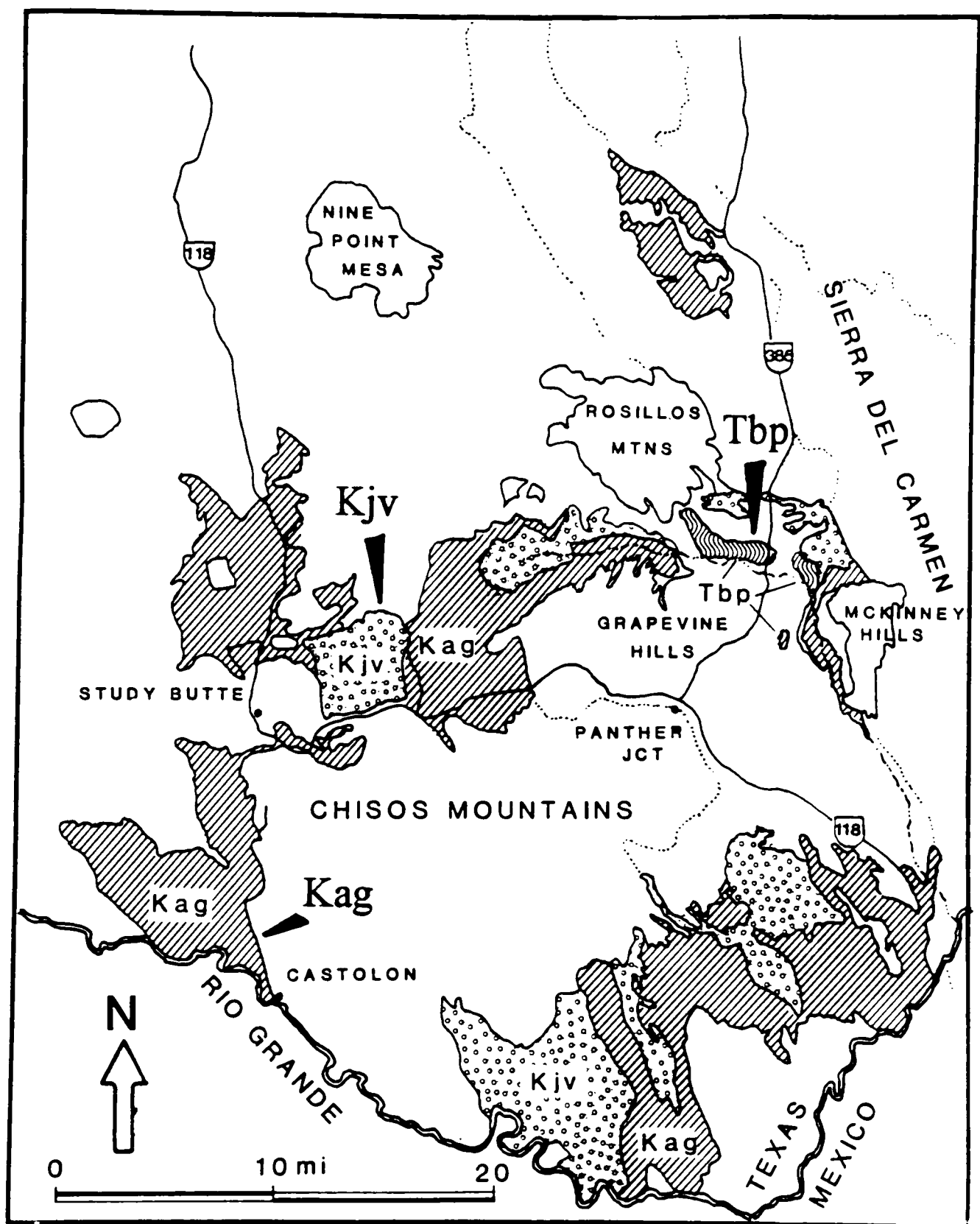


Figure 2.1. Upper Cretaceous and lower Tertiary strata in Big Bend, after Maxwell et al., 1967 and Lehman, 1985. Kag = Aguja Formation; Kjv = Javelina Formation; Tbp = Black Peaks Formation.

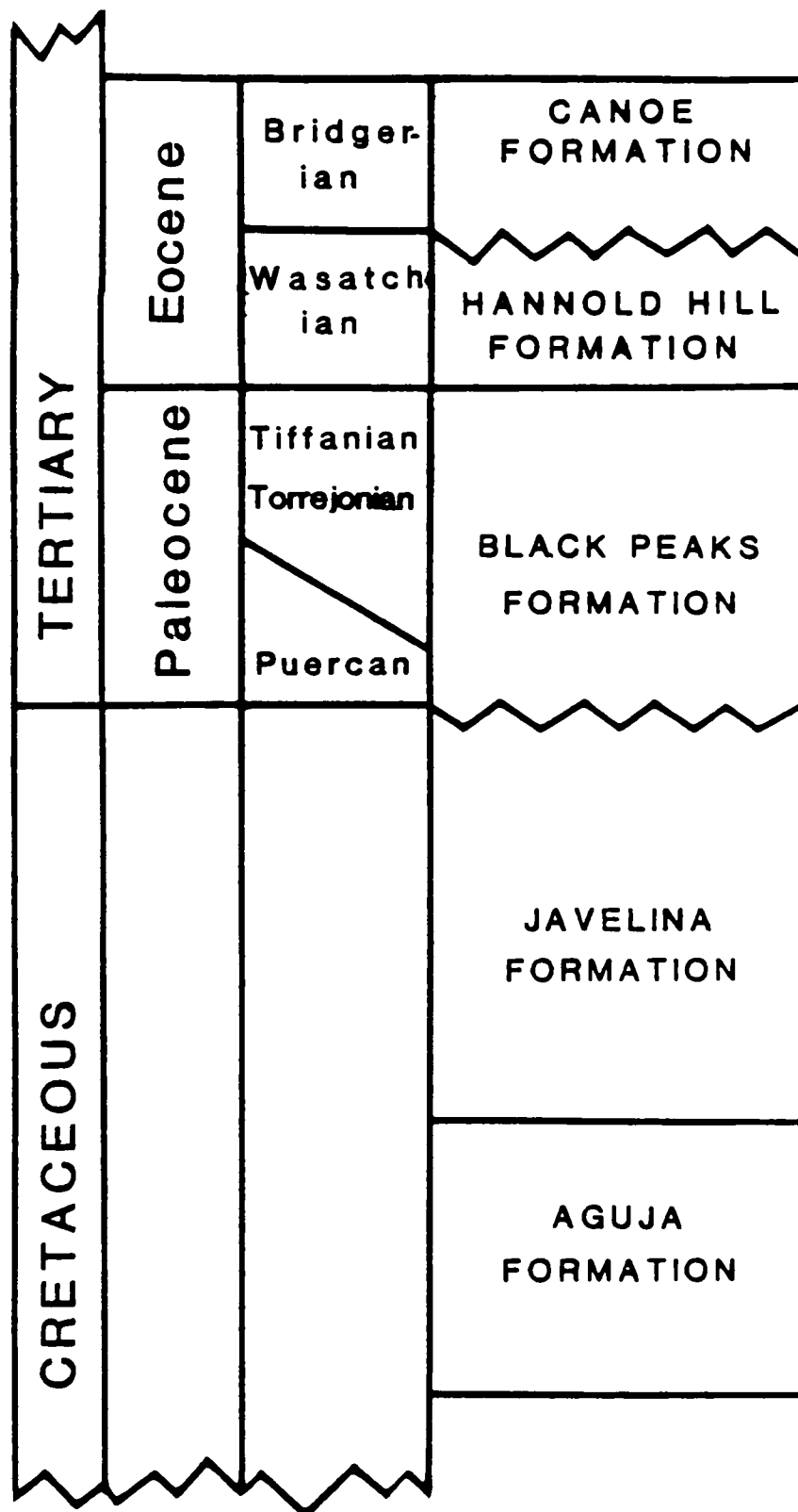


Figure 2.2. Stratigraphy of the Upper Cretaceous and lower Tertiary sediments (after Maxwell, et al., 1967).

Black Peaks, and Hannold Hill Formations. The status of these units (the formations of Maxwell et al., 1967) as formations has recently been disputed (Lawson, 1972; Schiebout, Rigsby, Rapp, Hartnell, and Standhardt, 1987; Lehman, 1988). This dispute has been primarily concerned with the recognition of boundaries and mappability of the units. Schiebout et al. (1987) have proposed that the formational subdivisions of Maxwell et al. be reduced to member status, and that the Tornillo Group be reduced in rank to the Tornillo Formation. However, this issue is largely beyond the scope of this study, and the formations of the Tornillo Group as originally designated by Maxwell et al. (1967), are used for the purpose of determining stratigraphic position of the Late Cretaceous and early Tertiary turtle specimens.

Turtle specimens described in this report were recovered from the Aguja and Javelina Formations, and the lower part of the Black Peaks Formation. The history of the nomenclature and stratigraphic divisions of each formation are described below. Detailed lithologic descriptions are not given because the lithologic descriptions and measured sections of these formations have already been well-documented by numerous workers (Maxwell et al., 1967; Lawson, 1972; Schiebout, 1970; Lehman, 1985; and Straight, 1996). The descriptions of lithologies and contacts given by these authors will be adopted for this study. In all instances, the lithology and contacts between the Aguja, Javelina, and Black Peaks Formations will be as defined and described by Maxwell et al. (1967) and Lehman (1985). Turtle specimens have been found in only certain intervals of each formation, and in differing abundances, and so

the lithology of the sections in which the turtle fauna occurs is discussed more thoroughly below.

The Aguja Formation

The Aguja Formation was originally named the “Rattlesnake Beds” by Udden (1907), and was subsequently renamed by Adkins (1933) because the name was already in use. Adkins (1933) used the name Aguja for these beds, in reference to Sierra Aguja (Needle Peak), which is near Udden’s original type section at Rattlesnake Mountain. However, Adkins did not measure a type section there, rendering study of the original type section difficult. Lehman (1985) proposed that several sections measured by Udden in the Chisos Pen area can be combined to form a composite type section for the Aguja.

The Aguja Formation was first subdivided by Maxwell et al. (1967) into four informal units, consisting of: (1) a basal sandstone unconformably overlying the Pen Formation; (2) a fossiliferous marine clay; (3) a unit of alternating marine sandstone and clay that grades upward into; (4) a unit of non-marine alternating sandstone and clay. Further refinement of subdivisions of the Aguja have been proposed by three workers, Kovschak (1973), Knebusch (1981), and Lehman (1985), all loosely based on Maxwell et al.’s (1967) original lithologic subdivisions. For the purpose of this study, the subdivisions of Maxwell et al. (1967), and Lehman (1985) will be followed.

Lehman (1985) redefined the subdivisions of the Aguja into six informal members (Figure 2.3). In ascending order they are: the basal sandstone member,

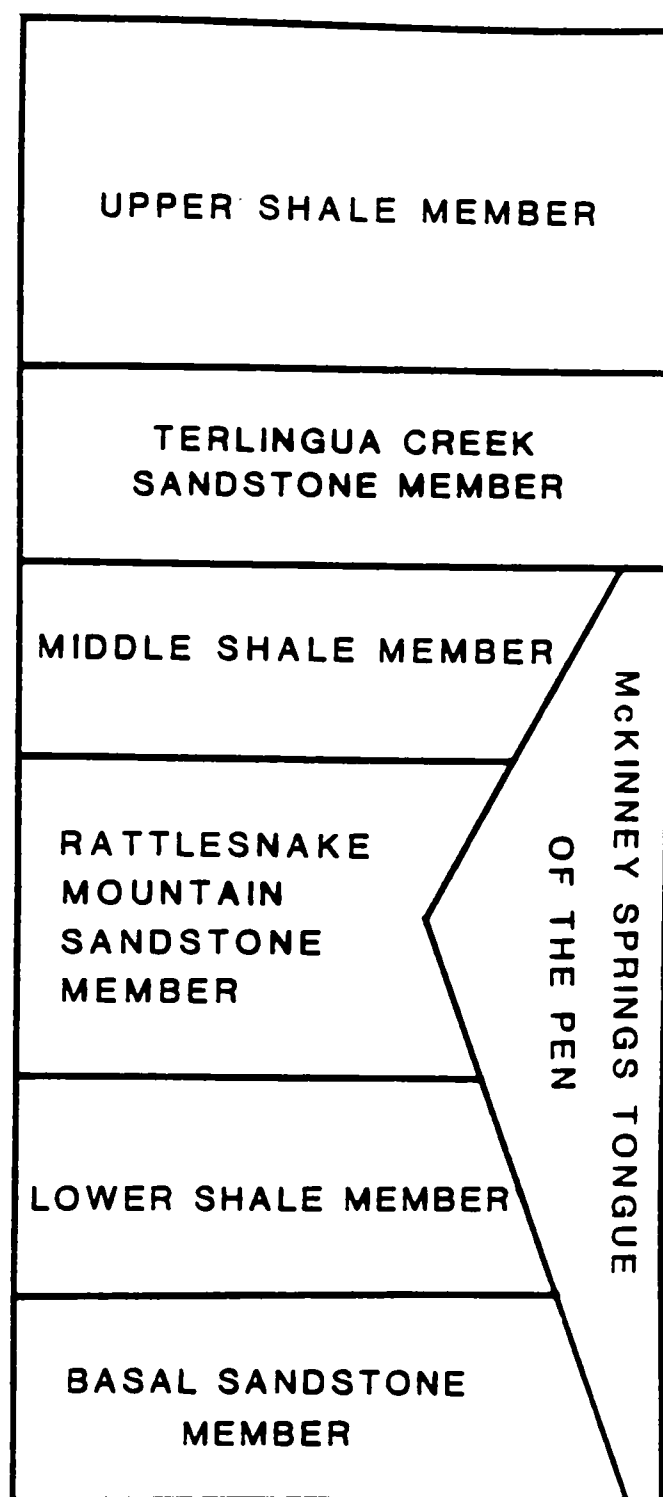


Figure 2.3. The Aguja Formation as subdivided by Lehman (1985).

lower shale member, Rattlesnake Mountain sandstone member, middle shale member, Terlingua Creek sandstone member, and upper shale member. In addition, Lehman recognized that the lower part of the Aguja and the upper part of the Pen were both gradational and intertonguing, and that the fossiliferous marine clay of Maxwell et al. (1967) was a tongue of the underlying Pen Formation. This fossiliferous marine clay was subsequently renamed the McKinney Springs tongue of the Pen Formation by Lehman (1985). Lehman (1985) considered the McKinney Springs tongue of the Pen and the middle shale member of the Aguja to be stratigraphically equivalent. The fauna of the Aguja indicates a middle to late Campanian age (Lehman, 1985). The Aguja records the paralic deposits of the final two transgressive-regressive cycles of the Western Interior Cretaceous Seaway and the subsequent transition to non-marine sedimentation (Lehman, 1985). The contact between the Aguja Formation and the underlying Pen Formation was originally identified as unconformable by Maxwell et al. (1967). Lehman (1985), however, has determined that this contact is gradational and intertonguing rather than unconformable. The contact is placed at the lowest "substantial" sandstone bed in a group of intertonguing sandstones that are present in most places in the uppermost part of the Pen (Lehman, 1985). The contact of the Aguja with the overlying Javelina Formation is placed at the top of the highest sandstone bed above which the mudstones are predominantly variegated (Maxwell et al., 1967; Lehman, 1985). This contact is gradational, and it is not always easy to recognize the transition from the Aguja to the Javelina.

The entire Aguja Formation was measured by Lehman (1985) for a maximum thickness of 242-285 meters in the west part of Big Bend National Park in the Rattlesnake Mountain-Santa Elena Canyon area. It thins to 118-135 meters in the Grapevine Hills-McKinney Springs area in the eastern part of the park. The upper part of the Aguja, the Terlingua Creek sandstone member and the upper shale member (see below), retain a more or less constant thickness of 118-172 meters. These measurements exclude the McKinney Springs tongue of the Pen, which intertongues with the Aguja and is probably equivalent to the middle shale member in the western part of the park. Turtle specimens have been found in the lower shale member, the Rattlesnake Mountain sandstone member, the Terlingua Creek sandstone member, and the upper shale member.

Lower Shale Member

The lower shale member overlies the basal sandstone member. According to Lehman (1985), it is present only on the western side of the park and farther west, outside the study area. The upper contact of this member is with the overlying Rattlesnake Mountain Sandstone Member at the base of a white, fossiliferous, “ledge-forming” sandstone.

The lower shale member consists of carbonaceous claystone, lignite, and coal interbedded with lenticular sandstone. Where exposed, the shale weathers to a brown, tan, and gray badlands topography. Limonite after pyrite is common throughout the clay shale. Red, black, and yellow Fe and Mg oxide-rich “ironstone” concretions

appear in many horizons throughout this member. This unit has been interpreted by Lehman (1985) as a coastal marsh and swamp deposit with associated estuarine channels, shoreface sands, and inner shelf sand sheets. Vertebrate and invertebrate fauna found in this unit include a wide variety of marine and brackish water molluscs, as well as turtles, crocodilians and dinosaurs. These sediments accumulated in two depositional environments: in the interdistributary zones of prograding deltas, and in the delta plains and adjacent coasts after delta abandonment.

Rattlesnake Mountain Sandstone Member

The lower shale member is in sharp contact with the overlying Rattlesnake Mountain sandstone member, a marine sandstone exposed only in the western part of the park. The upper contact of the Rattlesnake Mountain sandstone member is gradational with the overlying middle shale member in the west, and with the McKinney Springs Tongue of the Pen in the east. The Rattlesnake Mountain sandstone member is composed almost entirely of laterally extensive, thin, sheet-like sandstones. Local zones of calcite-cemented fine sandstone and shell hash conglomerate are common. The abundance of fossil oysters, notably *Flemingostrea pratti*, *Flemingostrea subspatulata*, *Crassostrea cusseta*, and *Crassostrea trigonalis*, is highly characteristic, but not necessarily diagnostic, of this member. This faunal assemblage suggests a brackish-water environment. Lehman (1985) and Macon (1994) have interpreted the depositional environment to be an inner shelf sand sheet

and shoal facies, a facies that represents the accumulation of sediment from transgressive erosion of the shoreline and delta plain environments.

Middle Shale Member/McKinney Springs Tongue of the Pen

The middle shale member overlies the Rattlesnake Mountain sandstone member along a sharp contact in the western part of the park. It is laterally gradational with and equivalent to the McKinney Springs tongue of the Pen Formation in the east. The McKinney Springs tongue represents a member of the Pen Formation that extends laterally as a southwesterly-thinning wedge in the lower part of the Aguja. This was formerly included as part of the Aguja Formation (Maxwell et al., 1967).

This member contains dark gray-, brown-, and black-weathering carbonaceous claystones, lignite, and coal interbedded with light gray or yellow shale. The shale and claystone of this member resemble the claystone of the lower shale member. No ironstone concretions are present, however.

Lehman (1985) has interpreted the depositional setting to be coastal swamp and marsh with associated tidal channel deposits in the lower part of the member. These facies grade laterally and upward into an overlying prodeltaic-delta front and muddy shelf facies.

Terlingua Creek Sandstone Member

The Terlingua Creek sandstone member is in gradational contact with the underlying middle shale member and McKinney Springs tongue of the Pen, but the

contact is locally sharp. It is in gradational contact with the overlying upper shale member.

This member is an extensive marine sandstone of varying thicknesses, ranging from 2 meters to over 30 meters. In most areas it is a single sandstone body, but it can locally contain as many as three separate sandstones units. The sandstone is fine-grained, and consists of a lower, friable, white-weathering unit generally overlain by a calcite-cemented dark-brown unit. Reworked oyster hash deposits, “ironstone” concretions, and clasts of gray claystone and lignite are found along erosional surfaces within the sandstone. Lehman (1985) has interpreted the sand bodies of this member to be prodeltaic-delta front, distributary channel and mouth bar, progradational shoreface, and inner shelf sand sheet deposits.

Upper Shale Member

The upper shale member is in gradational contact with the underlying Terlingua Creek sandstone. The contact with the underlying Terlingua Creek sandstone member is placed at the top of a laterally continuous sandstone above which the sediments are predominantly mudstones that contain only lenticular sandstone bodies. The mudstones in the lower part of this member are drab gray to olive in color and contain “ironstone” (sideritic) concretions. The upper part of this unit is banded light or dark gray, purple, and maroon. The mudstones are interbedded with lenticular tan or reddish brown sand bodies that hold up a series of distinctive, easily recognizable hogbacks. The upper contact with the overlying Javelina Formation is gradational and

sometimes difficult to locate precisely. The mudstones of the upper shale member, however, are characteristically different from the overlying mudstones of the Javelina in containing more abundant lenticular sandstones. These sandstones differ in color from the tan, pale green and dark brown sandstones of the Javelina. The color banding is also more drab in the upper shale member than in the highly variegated purple and gray mudstones of the Javelina. In addition, the Javelina mudstones contain abundant calcareous concretions, rather than sideritic concretions. These concretions are easily recognized in the field, and serve as a good marker of location in the section. The contact with the Javelina is arbitrarily placed at the top of the highest sandstone above which the mudstones change from a drab to predominantly variegated banding.

The upper shale member contains a diverse vertebrate fauna and brackish-water molluscan fauna. The upper shale member has been interpreted by Lehman (1985) as the deposits of fluvial environments that are in close association with coastal environments. The lower part of the unit represents deltaic coastal plain deposition and the sediments in the upper part of the unit represent inland fluvial floodplain deposition.

The Javelina Formation

Overlying the Aguja Formation is the Javelina Formation, named for Javelina Creek in the northeastern part of Tornillo Flat (Maxwell et al., 1967). It is the lowest of the three formations included in the original Tornillo Clays of Udden (1907), and

later, included in the Tornillo Formation of Adkins (1932), and the Tornillo Group of Maxwell et al. (1967; Figure 2.3). Udden (1907) believed that all of the Tornillo Clays were Cretaceous in age. However, the discovery of Tertiary mammals in the upper part of the Tornillo Clays indicated that the Cretaceous/Tertiary boundary falls within this unit (see Schiebout, 1974; Schiebout et al., 1987). Consequently, Maxwell et al. (1967) described the Javelina Formation as the Cretaceous part of the Tornillo Group, and the Black Peaks and Hannold Hill Formations as the Paleocene and Eocene parts of the Tornillo Group respectively.

The Javelina Formation conformably overlies the upper shale member of the Aguja Formation. It lies at the top of the highest sandstone above which the mudstones are predominantly variegated. Lehman (1985) divided the Javelina into two broad stratigraphic intervals, with the lower of the two intervals defined as containing significantly more interbedded sandstone, and with mudstones containing abundant distinctive calcareous nodules, while the upper interval is mudstone dominated and lacks nodules. This is significant, because dinosaur bones have been found in the lower interval and Paleocene mammals occur in the upper interval, effectively placing the K/T boundary at this level (see Schiebout, 1974; and Schiebout et al., 1987). Lehman (1985) suggested that the upper boundary with the overlying Paleocene Black Peaks Formation could be readily placed at the top of the sandstone-dominated unit above which the mudstone is more abundant and darker in color, the mudstones have bright maroon-colored bands and darker black and gray bands, and the mudstones lack calcareous nodules. The formational boundary thus coincides roughly with the

Cretaceous/Tertiary boundary. Lehman (1985) has interpreted the Javelina Formation as representing an inland fluvial floodplain deposit.

The Black Peaks Formation

The Black Peaks Formation overlies the Javelina Formation. The Black Peaks Formation was named for three small black peaks on Tornillo Flat, northwest of McKinney Hills (Maxwell et al., 1967). This formation is approximately the middle of Udden's Tornillo Clay, and later, the middle part of Maxwell's Tornillo Group (Maxwell et al., 1967). There is some dispute regarding the nature of the contact between the Black Peaks and the Javelina Formations. Maxwell et al. (1967) show the contact to be unconformable, however, Lehman considers it to be conformable (1985, 1988). The Black Peaks Formation is, like the Javelina, primarily a multi-colored shale and mudstone unit. Sandstone beds are less abundant in the Black Peaks than in the underlying Javelina Formation or the overlying Hannold Hill Formation, and the Black Peaks mostly lacks in calcareous nodules (Maxwell et al., 1967; Lehman, 1985; Schiebout, 1974; Schiebout et al., 1987). Fauna from the Black Peaks Formation indicates a middle to late Paleocene age (latest Torrejonian to Clarkforkian; Schiebout, 1974; Schiebout et al., 1987; Straight, 1996). The absence of an earliest Paleocene fauna is, in part, the reason some workers believe an unconformity exists at the boundary between the Javelina and Black Peaks Formations (Schiebout, 1974; Schiebout et al., 1987).

The lower boundary of the Black Peaks Formation is placed at the top of the ledge-forming sandstone-dominated part of the Javelina, above which there are predominantly more mudstones with distinct black bands and which lack the distinctive calcareous nodules found in the Javelina. This contact includes strata formerly mapped as part of the upper mudstone-dominated part of the Javelina now identified with the Black Peaks.

The Black Peaks Formation contains alternating sandstones and mudstones, which, overall, contains fewer sandstones than the underlying Javelina (Maxwell, et al., 1967). The sandstones are gray and gray-white, and contain distinctive “cannonball” concretions, which split into platy layers (Maxwell et al., 1967).

Numerous vertebrate fossils have been collected from the Black Peaks Formation, most notably Paleocene mammals including *Periptychus*, *Mimetodon*, *Psittacotherium*, *Phenocodus*, and others (Maxwell et al., 1967; Schiebout, 1974). Schiebout (1970) has interpreted the Black Peaks sediments as representing channel and flood-plain deposits of a seasonally wet and dry inland fluvial environment.

CHAPTER III

SYSTEMATIC PALEONTOLOGY

Introduction

Most of the turtle specimens described in this study are fragmentary, and consist of a few carapace or plastron fragments of several individuals. A few limb bones, disarticulated vertebral elements, and skull fragments have also been collected. Current taxonomic and phylogenetic studies rely heavily of skull characters. Therefore, in most instances specimens are identified only to the generic level in this study on the basis of their carapace or plastron features. A diagram showing the terminology of the carapace and plastron is provided to illustrate the placement of these fragments. The terminology for the dermal bones and epidermal scutes follows that of Zangerl (1969, Figure 3.1). Measurements of the specimens are given in centimeters. Measurements are projected straight line distances where the surfaces are curved.

A few of the Late Cretaceous and early Tertiary turtles from Big Bend National Park have been described by previous workers in the course of faunal surveys for other theses and dissertations, but the turtles have not been collectively described. This chapter of the dissertation provides a systematic description of the turtle fauna from the Aguja, Javelina, and lower Black Peaks Formations. It is not the purpose of this study to revise current taxonomy, therefore in most cases I have chosen to use the most recent classification schemes for different groups of turtles, for example, Gaffney (1972) for the Baenidae, and Hirayama (1994) for the Chelonioidae.

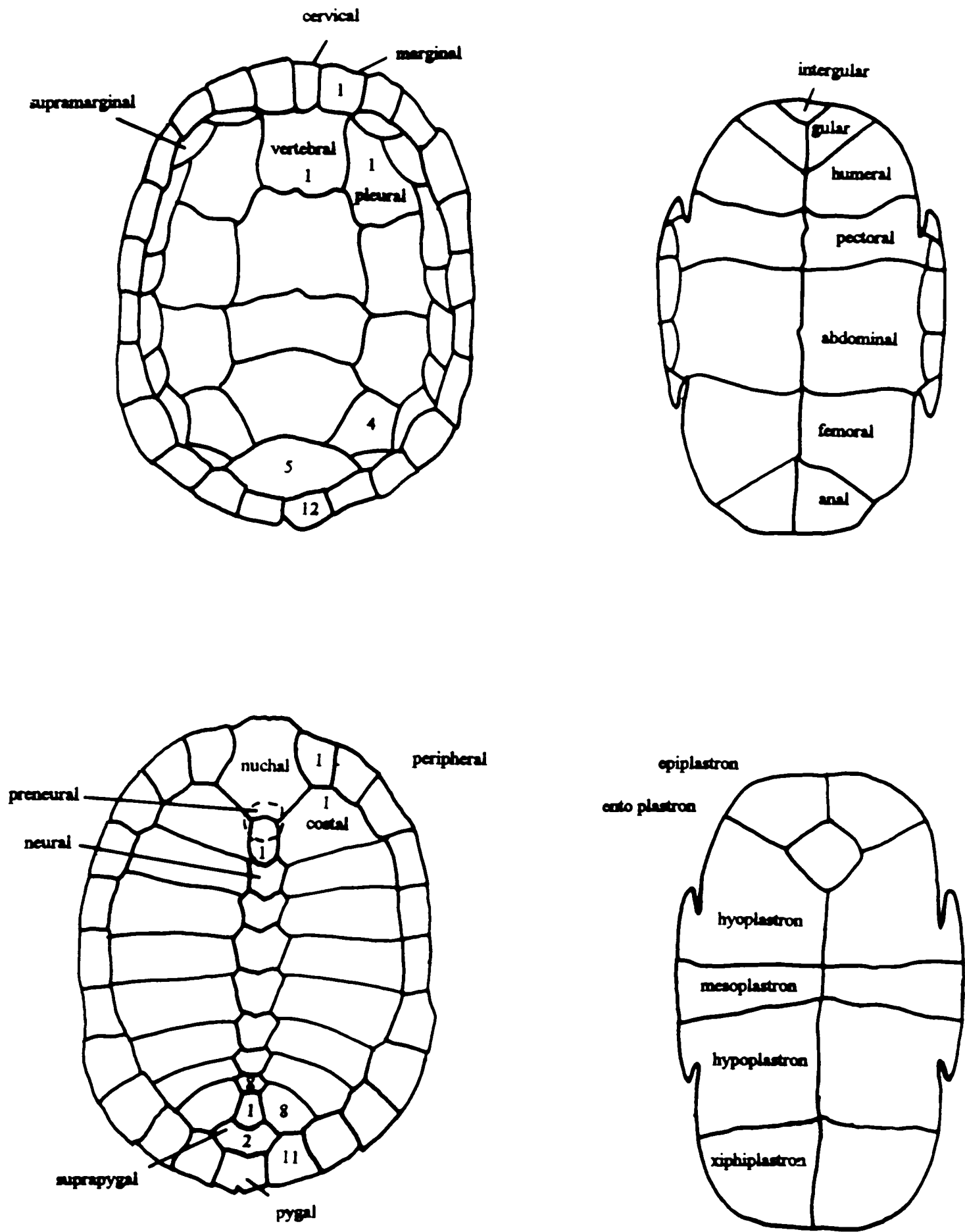


Figure 3.1. Carapace and plastron bones and scutes. (Diagram after Zangerl, 1969).

Not all specimens from Big Bend are described herein, but all taxa found in each of the stratigraphic units are represented. In choosing which specimens to describe, I have concentrated on: (a) the most complete specimens, (b) specimens from taxa that are rarely represented, or (c) specimens that exhibit unusual features. Many of the specimens from Big Bend are simply fragments, but it is nonetheless worth noting their presence for the purpose of gaining a clearer picture of the total diversity. The illustrations given here show the more complete specimens, and the characteristic shell ornamentation is shown in some areas.

The format of the systematic descriptions follows a nested classification of the specimens, with synonymies. All specimens are listed by skeletal position, in numerical order where possible. Localities are listed next, with stratigraphic position noted. The descriptions are followed by a discussion section, and the specimens are discussed in the order in which they appear in the description section. In a few places, I deviate slightly from this order so that a discussion of current taxonomic classification may be inserted.

The following abbreviations are used for museum collections that were studied during the course of this project: TMM, Texas Memorial Museum; LSUMG, Louisiana State University Museum of Paleontology; TTU, Texas Tech University.

Class REPTILIA

Subclass TESTUDINES

Gigaorder CASICHELYDIA Gaffney 1975

Megaorder PLEURODIRA Gaffney 1975

Family PELOMEDUSIDAE Cope 1865

Subfamily PELOMEDUSINAE Gaffney 1975

Bothremys sp. Leidy 1865

Referred Specimens: TMM 42534-7, TMM 42537-2, TMM 43370-1, TMM 43375-4, TMM 43382-1, TMM 43466-1, TMM 43469-1, TMM 43473-1.

Localities: TMM 42534-7 is from the southwest side of Rattlesnake Mountain; TMM 42537-2 is from the northwest side of Grapevine Hills; TMM 43375-4 is from north of McKinney Springs; TMM 43370-1 is from the east end of the River Road; TMM 43382-1 is from Dagger Flats; TMM 43466-1, 8, is from the east end of the River Road.

Stratigraphic Distribution: Aguja Formation, Terlingua Creek Sandstone Member and the lower part of the upper shale member.

Description

Most of the specimens referred here to *Bothremys* sp. consist of fragments of carapace and plastron. Many of these fragments exhibit a distinctive subtle ornamentation of small shallow, vermiform grooves in a broken, polygonal pattern.

Most of the fragments are on the order of 1 cm in thickness, but some probable plastron fragments are as thick as 2 cm. Several fairly complete elements are represented in the collection.

TMM 43466-1 is a large left first costal that is longer than it is wide (maximum length 20 cm, maximum width approximately 11.5 - 12 cm, maximum thickness is 1 cm). If it were complete, it would have a distinctive “wing” shape (Figure 3.2). It is badly weathered and abraded at the sutural edges, and appears to be missing approximately one-fifth of its total area. The visceral surface exhibits a strongly developed costiform process that is partly broken on the left lateral portion of the process. The left antero-lateral suture (for the first costal/second through fourth peripherals) and posterior suture (for the second costal) are present, but the right antero-lateral (for the nuchal and first peripheral) and medial (for first costal/first costal) sutures are broken. The left antero-lateral suture tapers to a thin (4 mm) edge. The dorsal surface of the first costal exhibits the typical shallowly grooved, reticulated vermiform sculpturing found on other specimens, but on a slightly larger scale.

TMM 43469-1 is a partial right first costal, measuring 14 cm in maximum length, 10.5 cm in maximum width, and approximately 0.9 cm in maximum thickness. It appears as if nearly one-third to one-half of the total area is missing from the medial portion of the specimen. If this specimen were complete, it would be the near mirror image of TMM 43466-1 in shape and size. A costiform process is present on the visceral side, but is mostly covered by a sandstone matrix. The portion of the costal

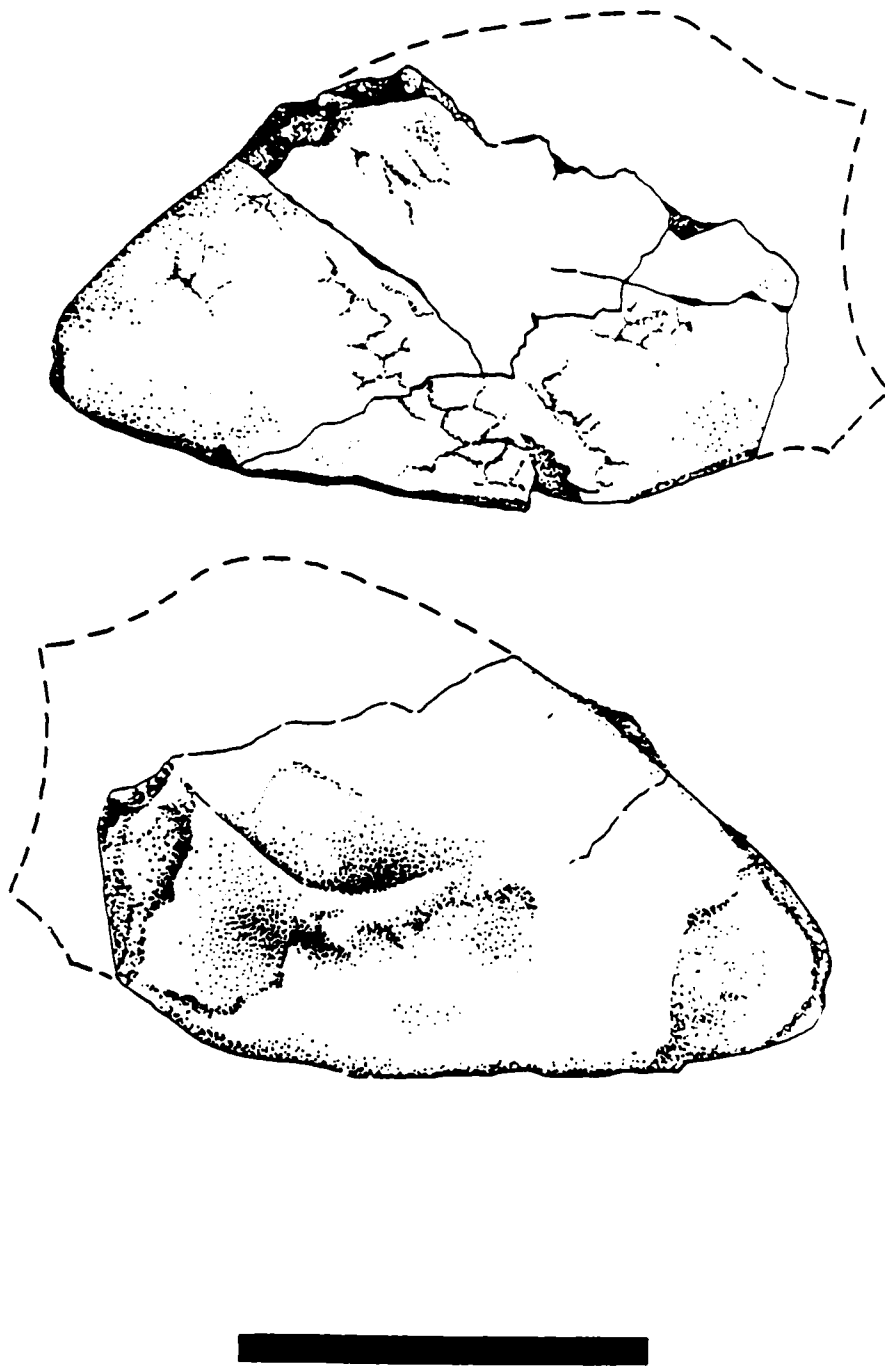


Figure 3.2. *Bothremys* sp., ST 94-1, left first costal, dorsal view and visceral view.
Bar scale is 10 cm.

that is present is nearly complete, with the sutures mostly unbroken and unabraded. The sutural surfaces taper to a thin (~0.5 cm) edge.

TMM 42534-7 is a small peripheral fragment, measuring 4.5 x 2.5 x 1 cm. The fragment is broken on two sides, tapers to an acute edge on one side, and exhibits the terminal edge of a suture on the fourth side.

TMM 43469-2 consists of two large, disarticulated portions of the anterior and posterior plastral lobes, which are apparently the right hyo- and hypoplastron (Figures 3.3, 3.4). These pieces are badly weathered and broken. Portions of the matrix remain on the hyo- hypoplastral suture, the medial suture of the hypoplastron, and the hypo-xiphiplastral suture. The hypoplastron is large (17.5 cm maximum length, 14 cm maximum width, and approximately 1.2 cm maximum thickness, excluding the axillary buttress). The broken process of the axillary buttress is present on the visceral surface, and makes an angle of approximately 80 degrees from the edge of the hyo-/hypoplastral suture. The medial and hyo-hypoplastral suture is intact, but the marginal edge, where the hypoplastron would connect with the bridge is broken, and the suture between the hypoplastron and the entoplastron is badly abraded, or broken entirely. The position of the pectoral/abdominal sulcus is clearly marked on the ventral side of the hypoplastron. This sulcus is approximately 5.5 cm from the hyo-hypoplastral suture, or about one-fourth the total length of the hypoplastron from the suture. The distinctive, subtle, reticulated sculpturing is present and easily seen on the ventral side.



Figure 3.3. *Bothremys* sp., ST 94-8a, right hyo- (above) and hypoplastron (below), visceral view. Bar scale is 10 cm.

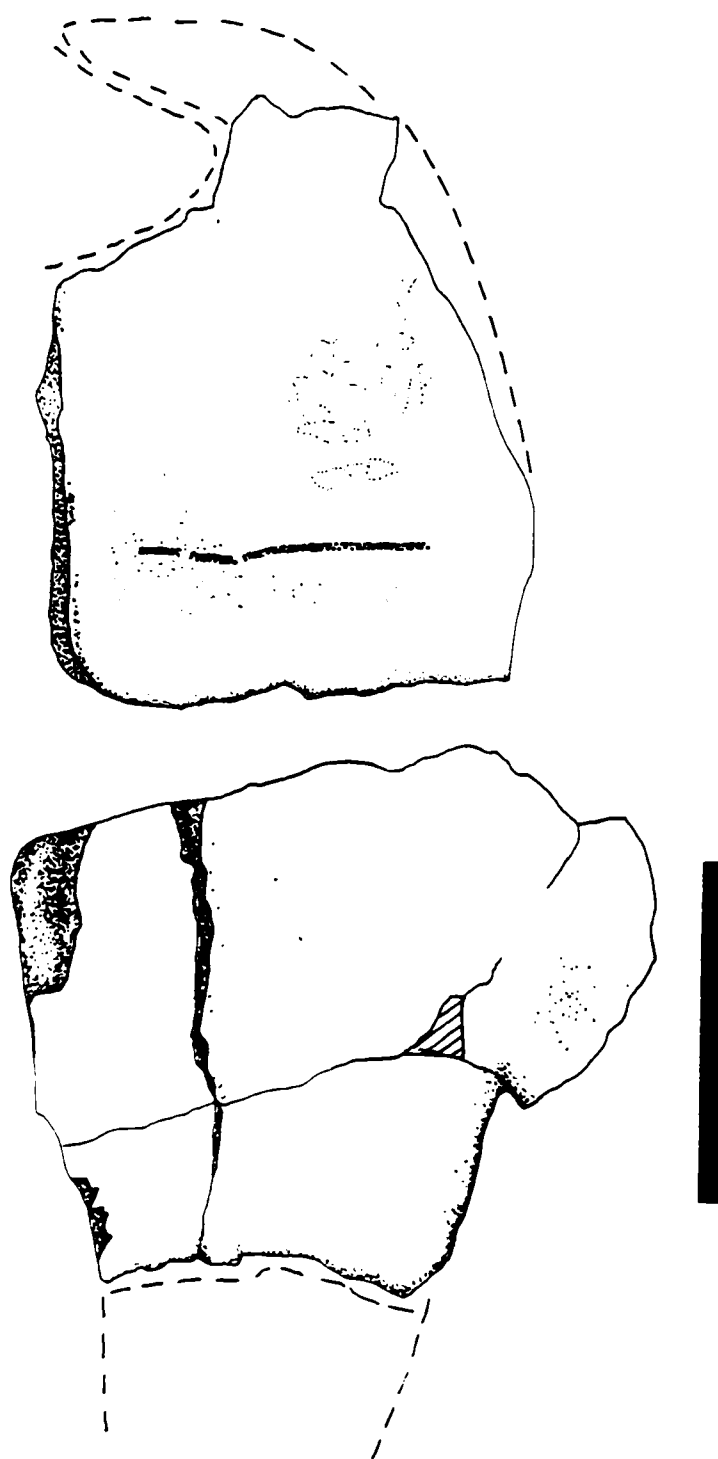


Figure 3.4. *Bothremys* sp., ST 94-8a, right hyo- (above) and hypoplastron (below), ventral view. Bar scale is 10 cm.

The hypoplastron is large, 14 cm in length along the approximated midline, 18.5 cm in maximum width, and approximately 2 cm thick at maximum width, which is at the medial suture at the level of the inguinal buttress. The medial suture is intact, the hyo-hypoplastral suture and the hypo-xiphiplastral sutures are badly abraded and covered with a sandstone matrix. The hypoplastral margin with the inguinal notch is intact and partly coated with sandstone. The distance from the inguinal notch to the broken hyo- hypoplastral suture (measured from the mid-point of the notch and in line with the lateral margin of the plastron), is approximately 8.0 cm, or nearly one-half the total length of the hypoplastron from the xiphiplastral suture. The abdominal/femoral sulcus cannot be located, probably owing to the badly weathered surface on the ventral side of the hypoplastron. A large portion of the inguinal buttress is present, and it exhibits an angle of nearly 90 degrees with the lateral margin of the plastron. The buttress appears thin and somewhat poorly developed in comparison to the overall size of the hypoplastron. On the ventral surface, the subtle, reticulated sculpturing can be seen.

A fragment from TMM 43370-1 is probably a portion of the right hypoplastron. The hypoplastron is broken at a line approximately one third of the distance from the hypoplastral/xiphiplastral suture to the hyoplastral/hypoplastral suture. Part of the inguinal buttress is present, as is the hypoplastral/xiphiplastral and medial hypoplastral sutures. The distance between the inguinal notch and the medial suture is 8.5 cm. Maximum thickness at the medial suture is 1.5 cm. A part of the abdominal/femoral sulcus is present on the antero-medial edge.

TMM 42537-2 is also a large plastron fragment (Figure 3.5). It is flat, 8.5 cm in width, 7 cm in length, and 1 cm thickness. It apparently comes from the bridge of the plastron; one broken side appears to be part of a buttress. The ventral surface shows inframarginal (?) sulci intersecting with the abdominal/pectoral (?) sulcus. The distinctive sculpturing of shallow, vermiform and reticulated grooves mark the ventral surface.

Discussion

That these specimens all pertain to the same taxon is suggested by the distinctive vermiform, reticulate sculpturing on the outer surface of the shell fragments. It is on the basis of this distinctive sculpturing, and the stratigraphic distribution of the specimens, that these fragments are assigned to *Bothremys* sp. This same pattern is illustrated by Hay (1908) and Gaffney (1965), and is shown to occur in the genera *Taphrosphys* and *Podocnemis*, both members of the family Pelomedusidae. This sculpture pattern is not found in any other Cretaceous or Tertiary families. Also, all of these specimens were found in marginal marine deposits, indicating that they may pertain to marine turtles, like the pelomedusids. In addition, the “wing-shaped” first costal seen in these specimens, is found in *Bothremys*, *Taphrosphys*, and the modern *Podocnemis*, all members of the Pelomedusidae (Hay, 1908; Gaffney, 1965). The present specimens can be confidently assigned to that family, in spite of the absence of a preserved xiphiplastron to demonstrate an ischiac scar, or of more diagnostic specimens.

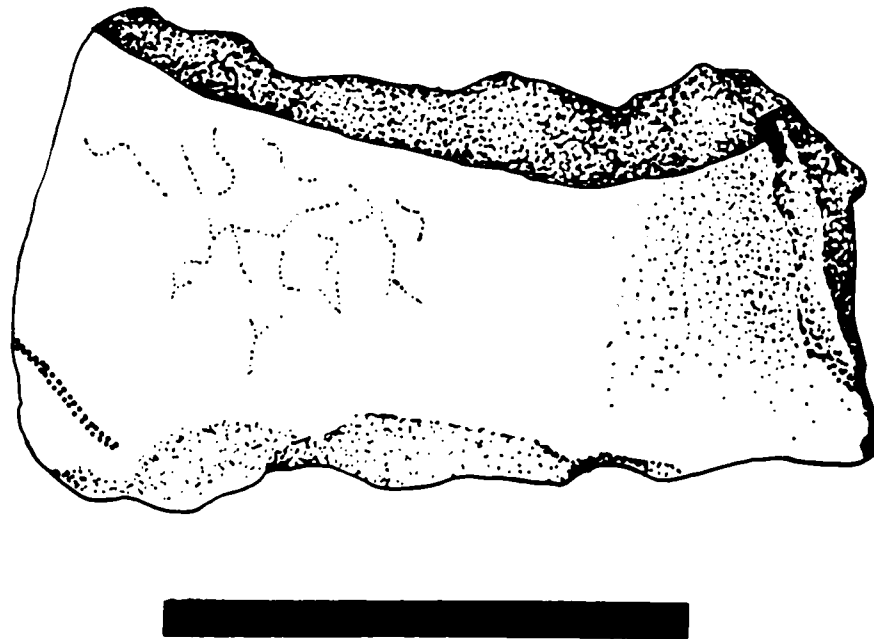
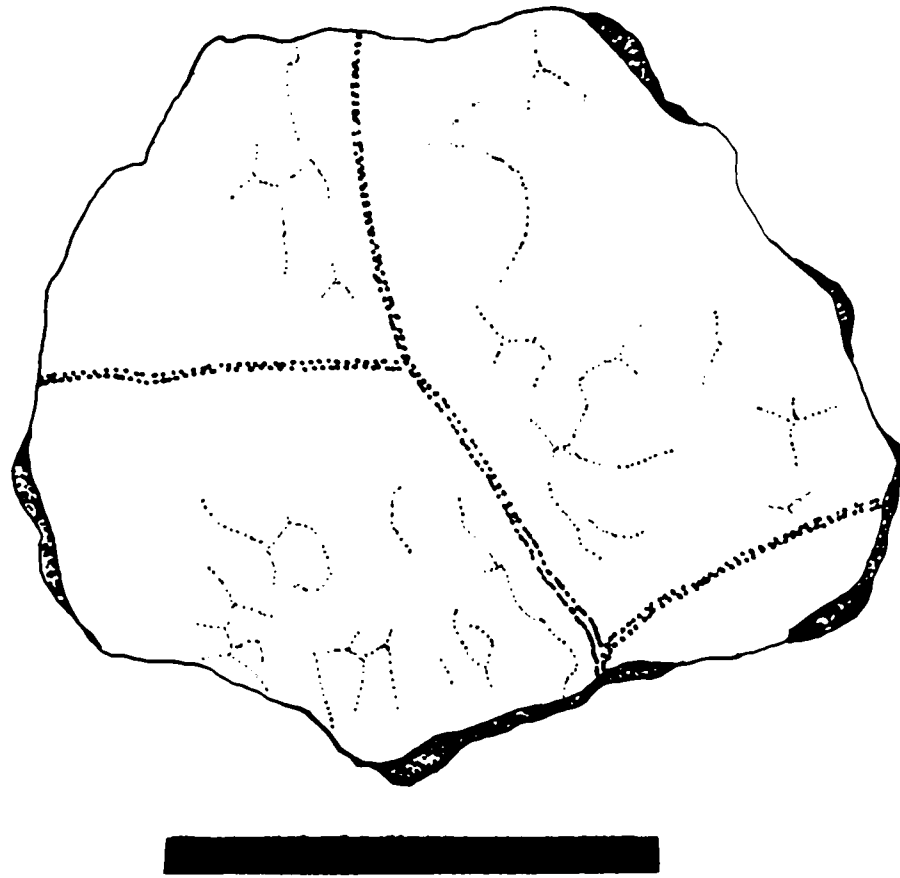


Figure 3.5. *Bothremys* sp. Top: TMM 42537-2, plastron fragment. Bottom, ST 94-9, plastron fragment. Bar scales are 5 cm.

Without a preserved skull or xiphiplastron, assigning these specimens to a genus is somewhat problematic. The distinctive, reticulate sculpturing, as stated above, has been illustrated in the literature for *Taphrosphys* and in the modern *Podocnemys*, but this same sculpturing has not been illustrated in the literature as occurring in *Bothremys*. *Taphrosphys* is a relatively rare genus, appearing in North America only in the Cretaceous sediments of New Jersey (Gaffney, 1965, 1975). Two other genera, *Bothremys* and *Podocnemys*, are reportedly very abundant in the Atlantic Coastal Plain Cretaceous nearshore and marine sediments (Gaffney, 1965; Gaffney and Zangerl, 1968). Gaffney and Zangerl (1968) have since determined, however, that all of these specimens belong in fact to *Bothremys*, and none are referable to *Podocnemys*, a living form that is present today in South America (Gaffney, 1965; Gaffney and Zangerl, 1968). It is most reasonable, therefore, that the Big Bend specimens are referable to *Bothremys* rather than *Taphrosphys*, simply on the basis of the much more abundant occurrence of *Bothremys* in correlative deposits. An examination of the anterior and posterior plastral lobes in these specimens also suggests that this is the case. In *Taphrosphys*, the pectoral/abdominal sulcus is very near the hyo-/hypoplastral suture, whereas in *Bothremys* it is proportionally not as near to that suture (Figure 3.6). In the anterior lobe containing this sulcus (TMM 43469-1), the sulcus is at one-fourth the total length. This is proportionally more distant from the hyo-/hypoplastral suture than would be expected for *Taphrosphys*, but it is approximately what is expected for *Bothremys* (Figure 3.6). In addition to this, in

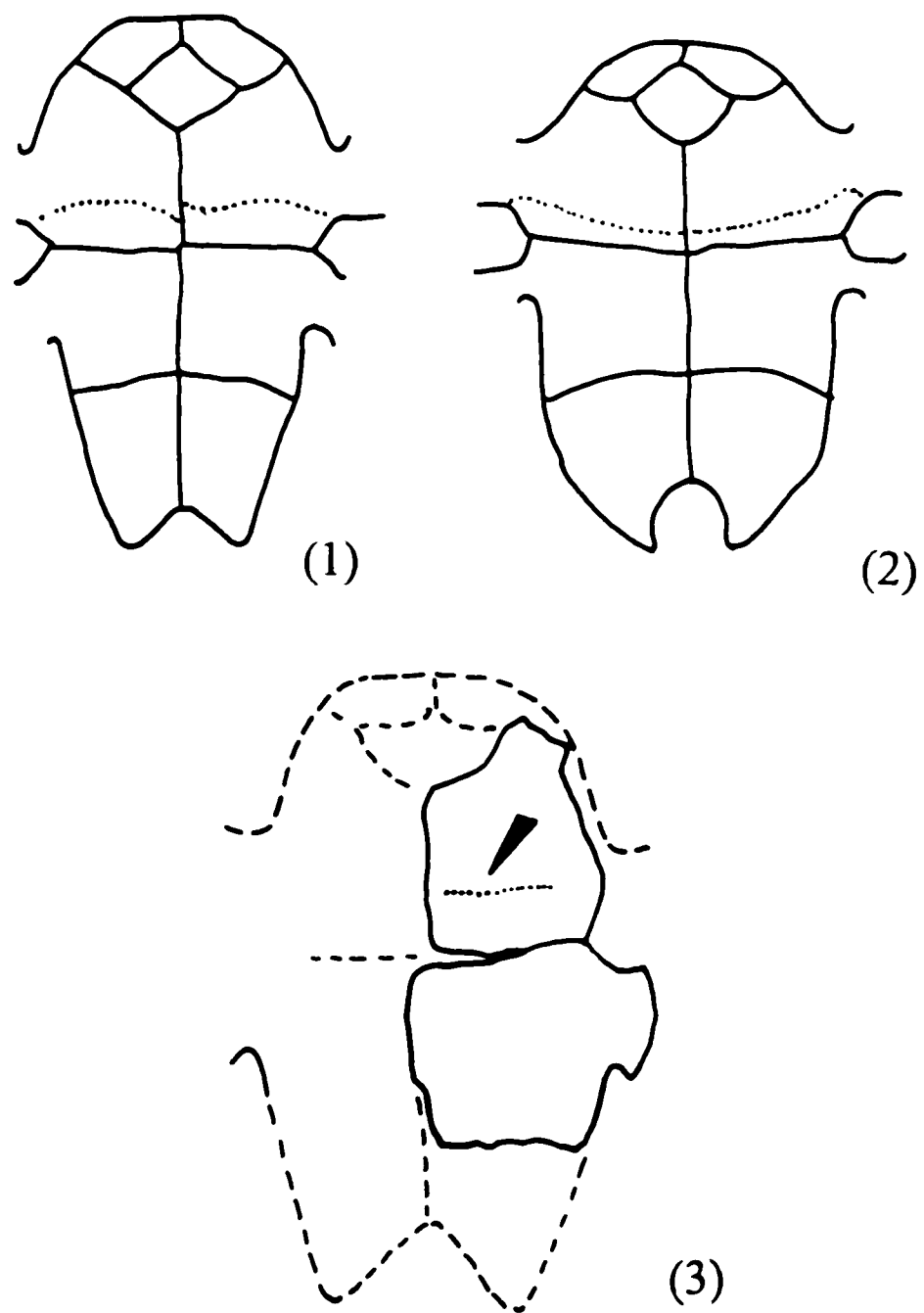


Figure 3.6. A comparison of the plastrons of *Bothremys*, *Taphrosphys*, and the Big Bend specimen. Figures (1) and (2) are from Zangerl (1948). (1) *Podocnemys* (=Bothremys; see Gaffney and Zangerl, 1968); (2) *Taphrosphys*; (3) Big Bend specimen. Arrow points to abdominal/pectoral sulcus. Plastrons are not to scale.

Taphrosphys the inguinal notch is proportionally closer to the hyo-/hypoplastral suture than it is in *Bothremys*. In TMM 43469-1-a the position of the inguinal notch position is more similar to *Bothremys* than *Taphrosphys* (Figure 3.6). The better preserved plastral lobes and first costal specimens are more readily identified as *Bothremys*. Many of the remaining fragments, however, are badly weathered and abraded, especially those that were found in coastal deposits. Most of these are unidentifiable, but some clearly exhibit the same reticulate sculpturing seen on TMM 43466-1 and TMM 43469-1. On the basis of the thickness and the sculpturing of these fragmentary specimens, they are also assigned to the genus *Bothremys*.

Suborder CRYPTODIRA Cope 1871

Superfamily BAENOIDEA (Cope 1882) Williams 1950

Family BAENIDAE Cope 1882

Subfamily BAENINAE (Cope 1882)

“Baena”

There is considerable variability in the shells of Cretaceous specimens assigned to the genus *Baena*, and few associated skulls have been described. Gaffney (1972) noted that two Eocene species, *Baena arenosa* and *Chisternon undatum*, have very different skulls, but their shell morphology is remarkably similar. Also, there is considerable morphological variation among individuals of *Baena arenosa*. Therefore it is difficult to determine which of the taxa assigned to *Baena* are actually valid species. However, as Gaffney (1972) points out, there is also a wide geographic and

geologic range, and it is unlikely that only one species exists for this genus in the Cretaceous. Therefore, Gaffney (1972) suggests considering these taxa indeterminate, and assigning them to the form-genus "*Baena*".

"Baena" cf. *B. ornata* Gilmore, 1935

Type specimen: USNM 13229 (Gilmore, 1935, p. 165, figs. 7, 8, pl. 14), carapace and plastron.

Referred specimen: LSUMG V-1136.

Localities: LSUMG V-1136 is from southwest of Sombrero Peak.

Stratigraphic Distribution: lower part of the Paleocene Black Peaks formation.

Description

LSUMG V-1136 has a sub-rounded, nearly oval carapace that is nearly as wide as it is long, and has its broadest transverse diameter at midlength, or just below midlength (Figure 3.7). The posterior end is deeply emarginated below the sulci for the fifth vertebral scute. The posterior edge is also scalloped with sharply pointed notches beginning at about the fourth peripheral, and extending to the rear emargination. A slight dorsal keel extends discontinuously along the midline the entire length of the specimen, with the most pronounced portion of the keel being near the posterior margin. The axillary and inguinal buttresses are present, and very thin-walled. The length of the bridge from axillary notch to inguinal notch is a little less than one-half the total length of the carapace. The first and second dorsal vertebrae

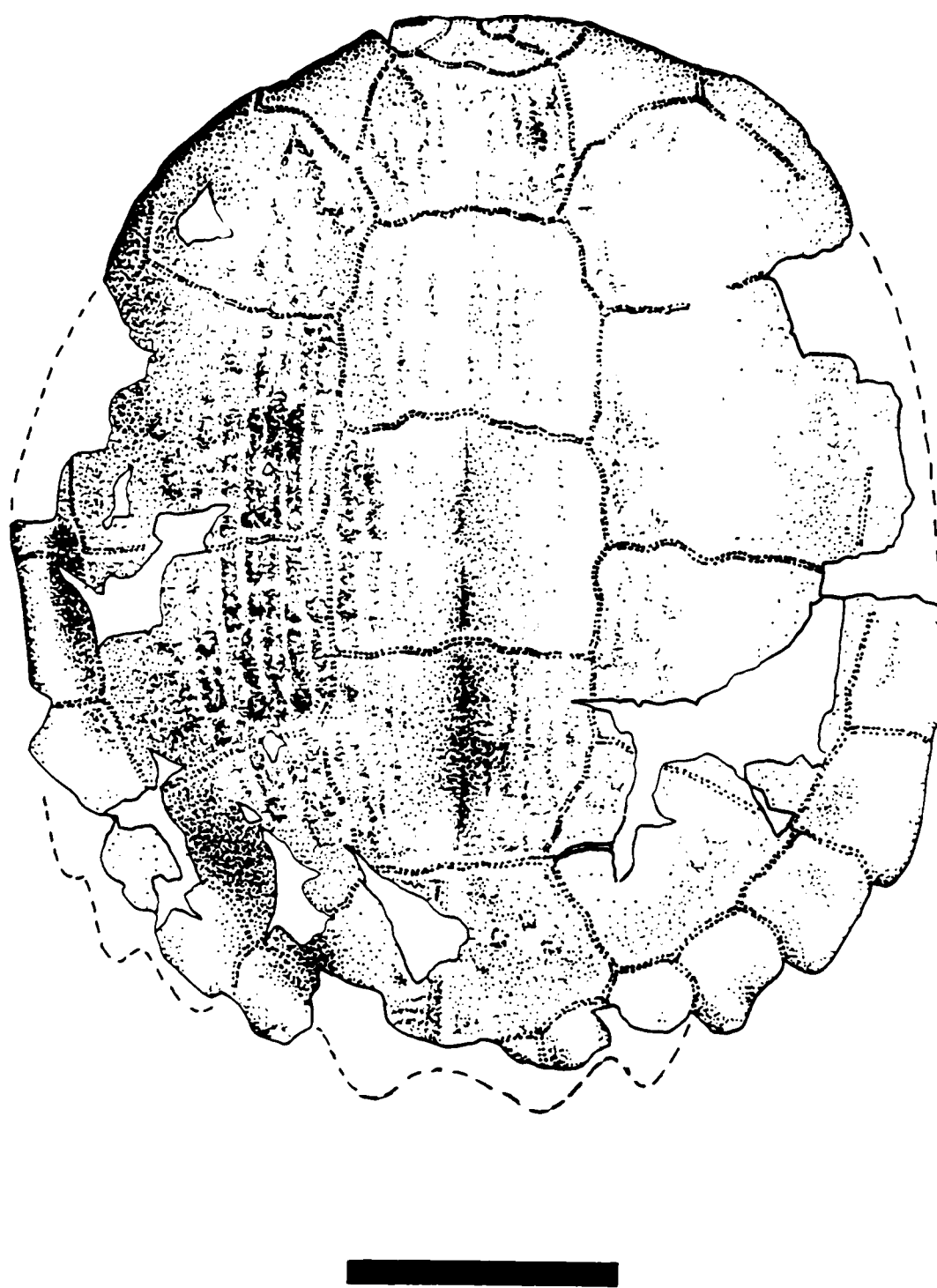


Figure 3.7. "*Baena*" cf. *Baena ornata*, LSUMG V-1136, carapace in dorsal view. Bar scale is approximately 10 cm.

are present. Strongly developed costiform processes are on the first costal bones that articulate with the first dorsal vertebra. Strongly developed costiform processes are on the eighth costal bones, for the attachment of the pedicle which articulates with the ilium.

The ornamentation consists of longitudinal ridges and distinct bumps, or nodes that cover most of the carapace surface. The ridges are concentrated near the midline, and grade into nodes toward the lateral margins. Superimposed over the large-scale ornamentation of the ridges and nodes is a finer scale surface of pinhead-sized irregular bumps, such as those seen in other baenids. Sutures are, with one exception, completely coalesced on the carapace, but are discernable in many cases through the presence of fine transverse lines. Sulci are visible, however. The specimen possesses sulci delineating a total of five vertebral scutes that are broader than long, with a rectangular first vertebral bordered by what are either paired accessory scutes or supramarginal scutes, or oddly triangular-shaped, large marginal scutes. There is no supracaudal scute; instead, the fifth vertebral simply ends at the posterior margin.

The plastron is moderately robust, with a bridge that is approximately one third the total width of the plastron (Figure 3.8). The plastron is thick, as in other baenids,

but not disproportionately so. The buttresses are thin relative to the overall thickness of the plastron. The edges are missing from the anterior and posterior plastral lobes, making their relative proportions difficult to assess. However, a rough estimate suggests that they are approximately equal in length. The anterior lobe

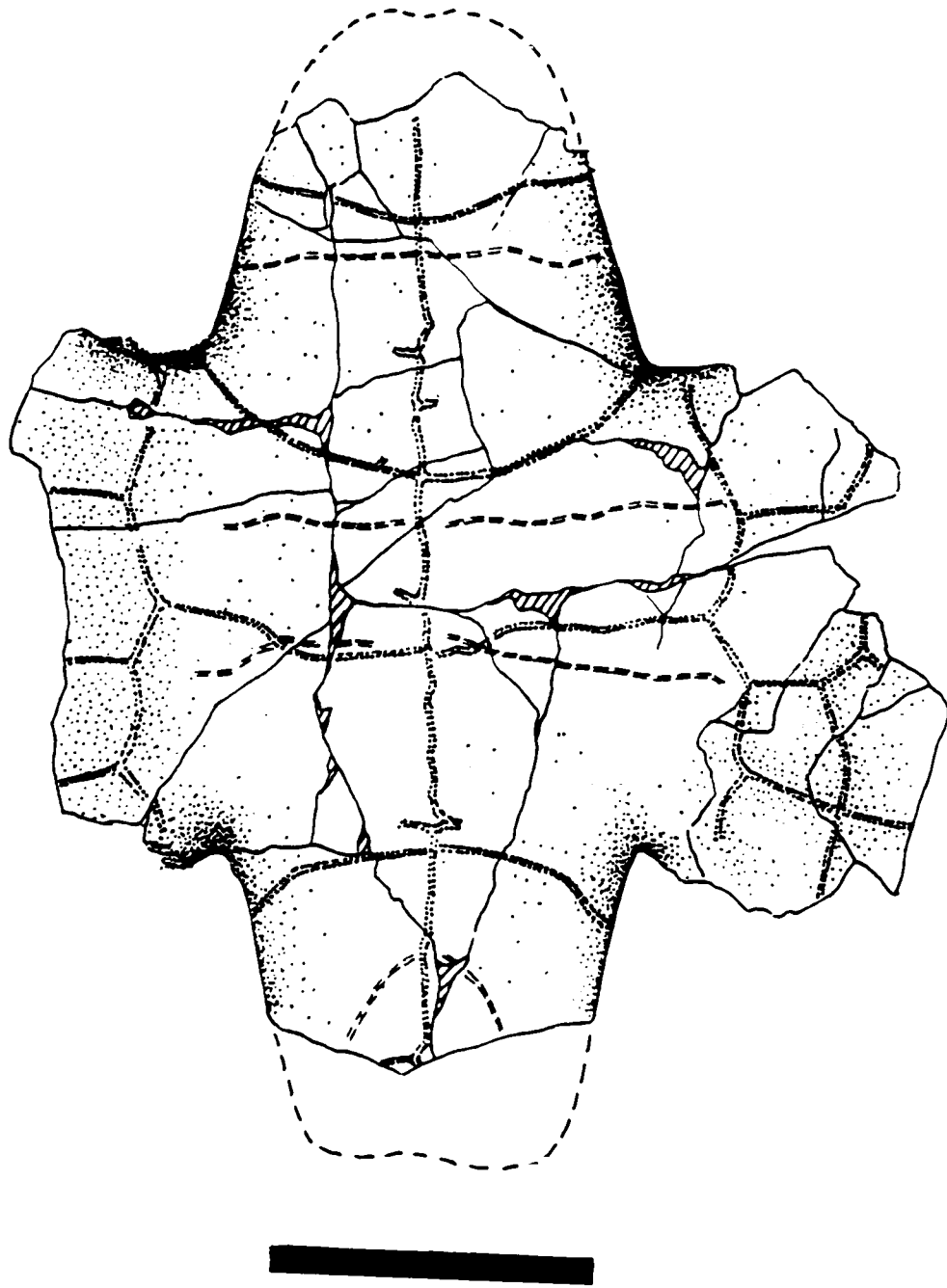


Figure 3.8. "*Baena*" cf. *Baena ornata*, LSUMG V-1136, plastron in ventral view. Bar scale is approximately 10 cm.

appears to be slightly narrower than the posterior, and tapers to a rounded point. The posterior lobe is slightly broader, and somewhat tapered. Exact configurations of the terminal margins cannot be determined. There is no apparent concavity to the ventral surface of the plastron. Sulci and sutures are both easily traced, but owing to the missing terminal margins, the gular sulci, epiplastral sutures, and part of the entoplastral sutures cannot be delineated. Heterotopic sulci are present along the midline in the form of short lateral lines in both the anterior and posterior lobes. Ornamentation on the plastron consists of small, pinhead-sized irregular bumps.

Discussion

The rugose shell ornamentation consisting of nodular bumps and ridges seen on this specimen is characteristic of only two species in the form-genus "*Baena*", "*B.*" *nodosa* and "*B.*" *ornata* (Gaffney, 1972). Gilmore (1916, 1935) suggests that these two species can be separated on the basis of shell shape, vertebral scute shape, and the presence or absence of triangular accessory scutes lateral to the first vertebral.

LSUMG V-1136 varies slightly from the diagnosis of both "*B.*" *nodosa* and "*B.*" *ornata*. In most respects LSUMG V-1136 is more like "*B.*" *ornata* than "*B.*" *nodosa*, especially in the shape of the shell. Although the shell is more rounded and quadrangular, rather than triangular, the greatest transverse width is slightly below midlength, giving it an uneven "egg" shape. Gilmore (1935) mentions one individual of "*B.*" *nodosa* which is more rounded in the anterior portion of the carapace, but no illustration is provided. Gilmore (1935) also cites Wiman's (1933) observation that

many individuals referred to "*B. nodosa*" are variable in scute pattern and shell shape. The vertebral scutes on LSUMG V-1136 are quadrangular, including the first vertebral, and have a width greater than their length. This corresponds with Gilmore's diagnosis of "*B. ornata*" (1935). However, this specimen possesses oddly shaped marginal scutes, which may or may not be triangular accessory scutes (Figure 3.7). I cannot discern any additional sulci that would separate these scutes from true marginals, therefore it appears that this is some sort of scute abnormality. This type of abnormality either represents an addition of supracostal scutes in "*B. ornata*", or the loss of one of the borders of the marginal scutes in "*B. nodosa*". The addition or loss of scutes in a particular species is not considered uncommon (Zangerl and Johnson, 1957). Therefore, little taxonomic weight can be placed on the presence of this character on this specimen. On the basis of the overall shape of the shell, the quadrangular shape of the first vertebral, and the overall shape of the vertebrae, this specimen is tentatively referred to "*Baena*" cf. "*B. ornata*".

"Baena" cf. *"B."* *nodosa* Gilmore 1916

Type specimen: USNM 8345 (Gilmore, 1916, figs. 34, pl. 76), nearly complete shell.

Referred specimens: TMM 42536-1; TMM 43251-1; TMM 42533-3.

Localities: Rattlesnake Mountain; Windy City SE locality, east of Rattlesnake Mountain.

Stratigraphic Distribution: lower and upper shale members, Aguja Formation.

Description

TMM 42536-1 is a poorly preserved, partial carapace and plastron. The shell is round, and missing the anterior and posterior one-fourth of the carapace (Figure 3.9). The surface is very friable and weathered, and the sulci and sutures cannot be located. A rough ornamentation of nodular bumps and ridges is visible.

The plastron is largely covered by matrix, but the outline of the posterior lobe is discernable, and it extends well beyond the broken edge of the carapace (Figure 3.10). It is partially broken at the posterior edge, but it appears to be narrow and tapers to a squared terminal margin. The anterior lobe is completely broken off below the inguinal notch. No sulci or sutures are visible on the plastron. Where the surface is exposed, small, irregular bumps are visible on the plastron.

TMM 43251-1 consists of fragments of badly weathered carapace and plastron (Figures. 3.11, 3.12). Breaks on the fragments appear fairly fresh, but the surfaces of

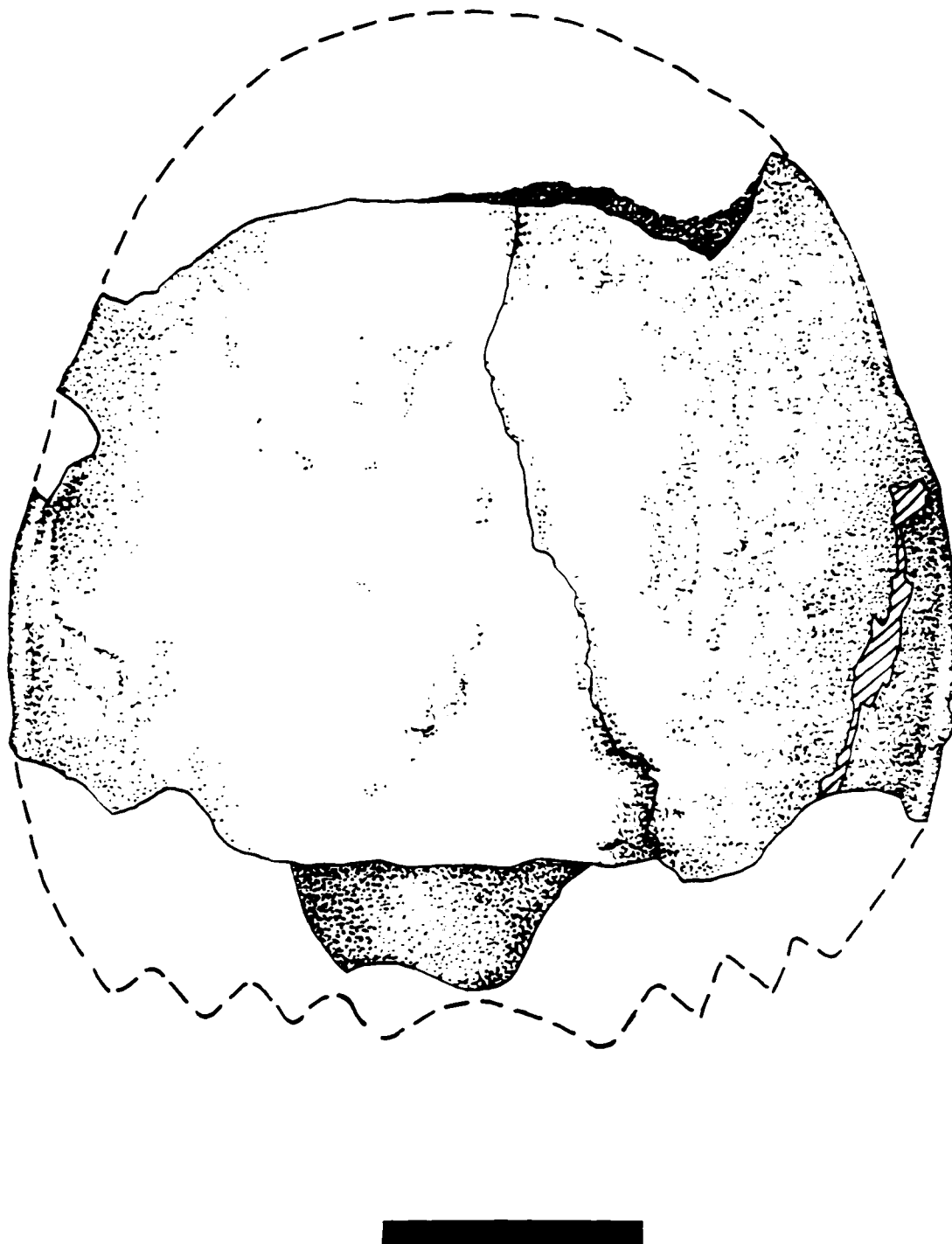


Figure 3.9. "*Baena*" cf. *B. nodosa*, TMM 42536-1, carapace in dorsal view. Bar scale is 10 cm.

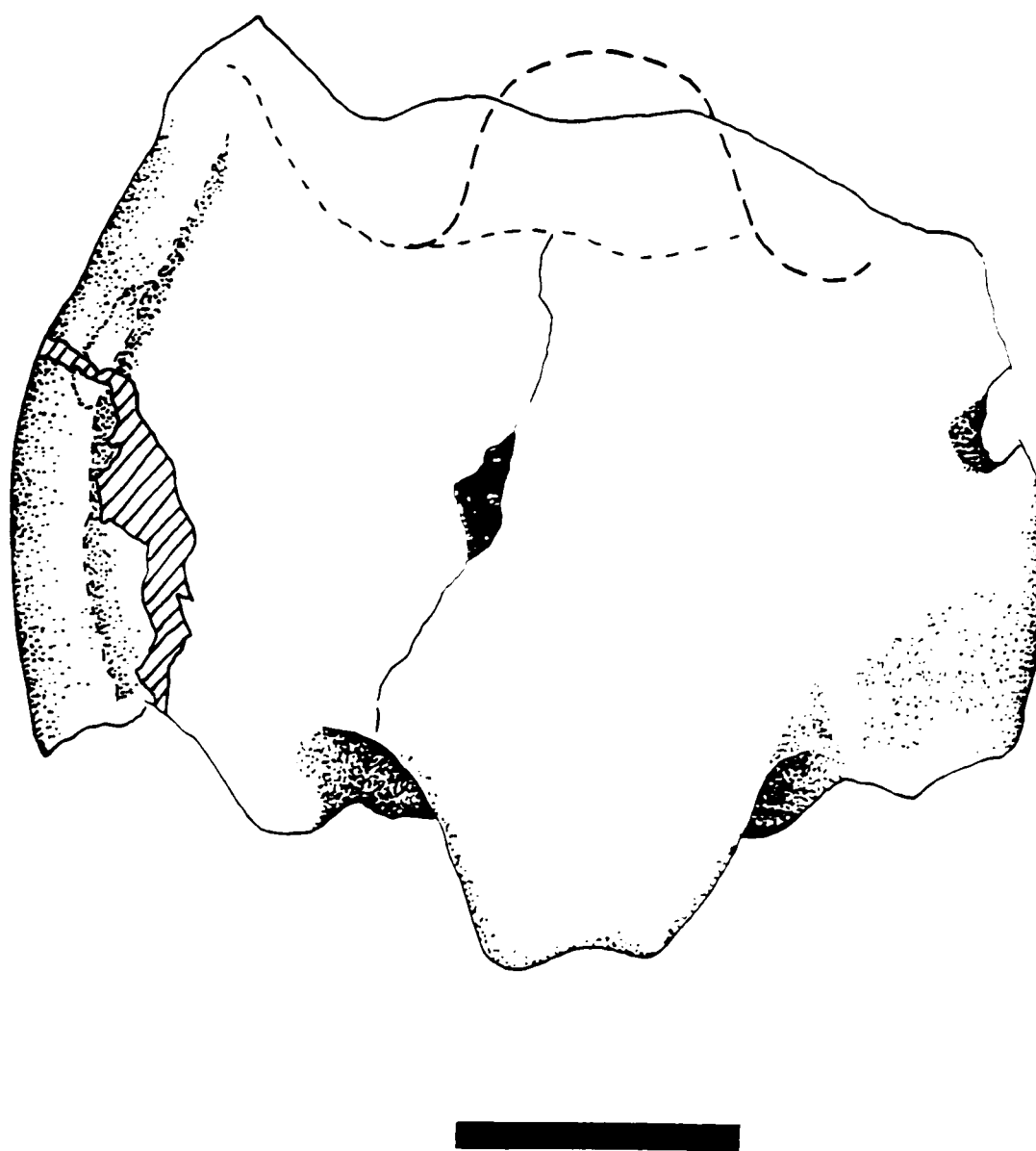


Figure 3.10. "*Baena*" cf. *B. nodosa*, TMM 42536-1, plastron in ventral view. Bar scale is 10 cm

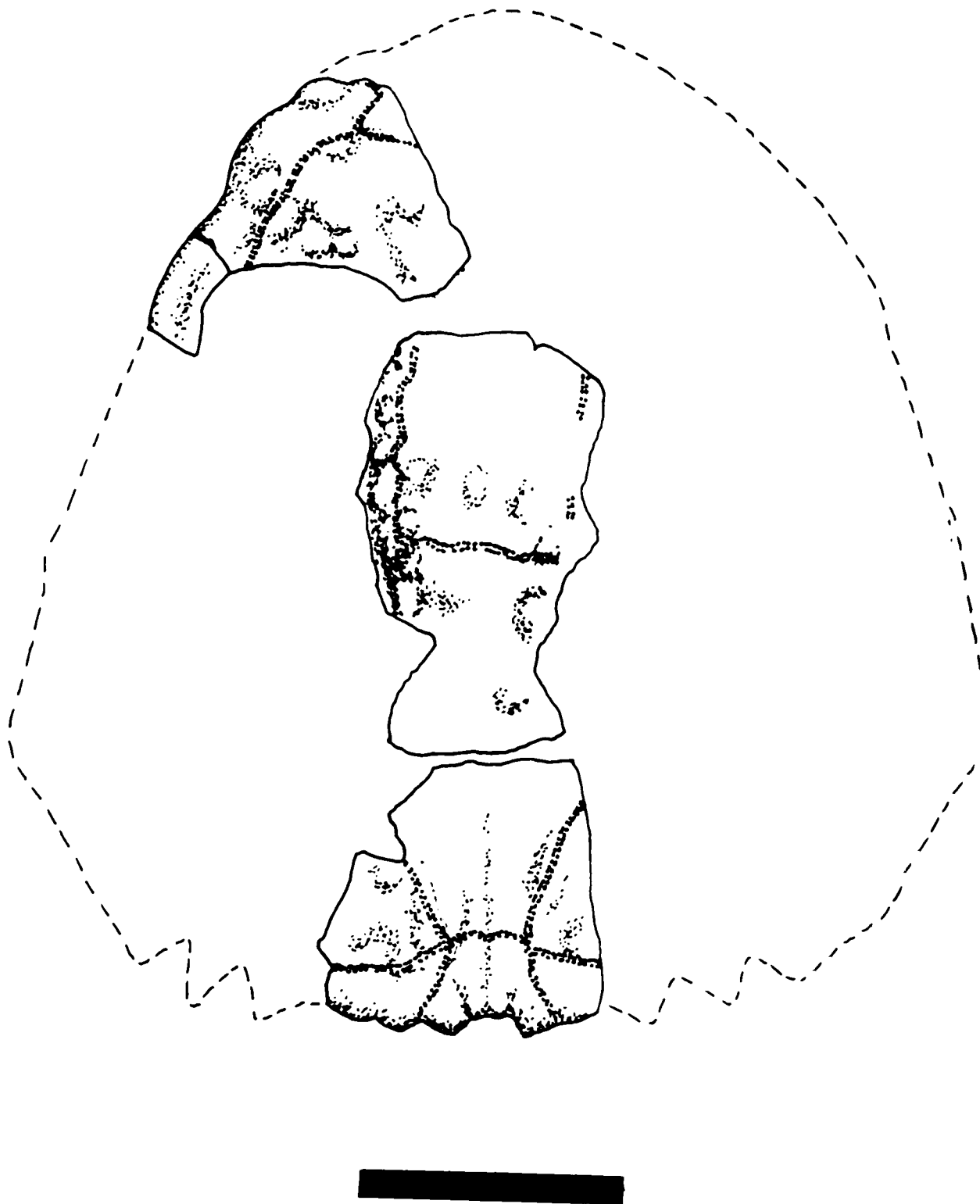


Figure 3.11. "*Baena*" cf. *B. nodosa*, TMM 43251-1, carapace fragments. Bar scale is 10 cm.

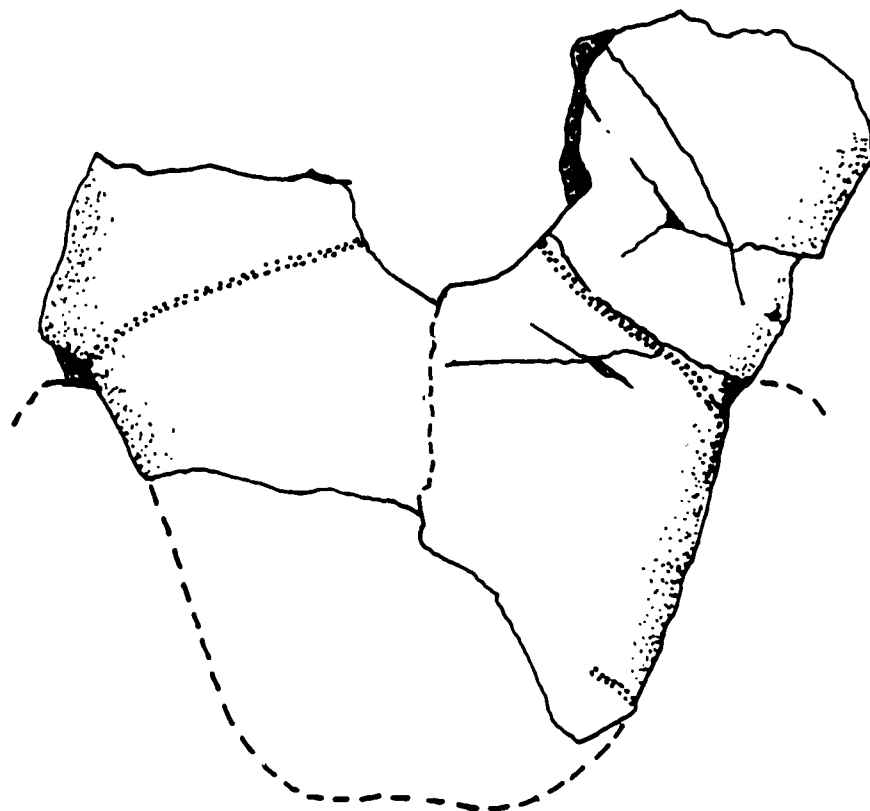


Figure 3.12. "*Baena*" cf. *B nodosa*, TMM 43251-1, plastron fragments. Bar scale is 10 cm.

both carapace and plastron fragments show considerable abrasion. The carapace fragments consist of a piece from the left lateral anterior margin, parts of the medial portion of the carapace, including the neural bones, parts of the costal bones with broken tubercles, and part of the posterior margin, including the pygal bone. The dorsal carapace surface exhibits large-scale nodular bumps and ridges. The surface is too weathered to definitively determine finer scale ornamentation. However, on the medial pieces there are some small, irregular bumps that might be remnants of the fine ornamentation. No sutures are visible. Sulci are visible on some of the fragments. Marginal and vertebral sulci are longer than they are wide.

Plastron fragments include parts of the right and left hypoplastron. Sulci are partially visible on these fragments. The right hypoplastron has part of the abdominal/femoral sulcus, and the left hypoplastron has parts of the abdominal/femoral and femoral/anal sulci (Figure 3.12). No apparent ornamentation is visible, but this might be the result of post-depositional abrasion.

Discussion

The rugose shell ornamentation consisting of nodular bumps and ridges seen on these three specimens is characteristic of only two species in the form-genus "*Baena*", "*B.*" *nodosa* and "*B.*" *ornata*. Gilmore (1916, 1935) suggests that these two species can be separated on the basis of shell shape, vertebral scute shape, and the presence or absence of triangular accessory scutes lateral to the first vertebral. Gilmore (1935) describes the carapace shape of "*B.*" *nodosa* as triangular, with the widest

transverse measurement posterior to the inguinal notches, and the shape of the carapace in "*B. ornata*" as more quadrangular, with the greatest transverse width being at midlength. In spite of having broken anterior and posterior edges, it is clear that TMM 42536-1 has a shell that is more quadrangular than triangular. However, it is unlikely that this species would extend from the early Campanian to early Paleocene. Because the sulci and suture patterns are completely obscured by the weathering of the surface and the lignite matrix, this specimen is referred to the "*Baena*" cf. "*B. nodosa*" on the basis of the shell ornamentation and stratigraphic position alone.

Unfortunately, TMM 43251-1 does not contain enough material to determine the entire shape of the shell. However, when comparing "*B. nodosa*" to "*B. ornata*", Gilmore (1935) states that the former can be distinguished from the latter by the shape of the vertebrals, and in particular, the first vertebral scute, among other things. "*B. nodosa*" is said to have vertebral scutes that are longer than wide, as opposed to "*B. ornata*", which has vertebrals that are wider than long. The first vertebral scute of "*B. nodosa*" is more triangular in shape than that of "*B. ornata*". It is also apparent from Gilmore's (1935) text and figures that "*B. nodosa*" is more likely to have intergular sulci than "*B. ornata*". On the basis of vertebrals that are longer than wide, on the triangular shape of the first vertebral scute, and the apparent intergular sulcus, TMM 43251-1 is referred to "*Baena*" cf. *B. nodosa*.

"Baena" sp.

Referred specimens: TTU 5-104-47, a partial carapace and a nearly complete plastron, TMM 42533-3, TMM 42534-3, TMM 42534-4, TMM 43380-4, TMM 43380-6, TMM 43380-7, LSUMG V-1081, LSUMG V-863, LSUMG V-1168.

Localities: TTU 5-104-47 is from Glenn Draw, 4.3 miles southeast of Glenn Springs, TMM 42533-3, TMM 42534-3 and TMM 42534-4 are from Rattlesnake Mountain; TMM 43380-4, TMM 43380-6, and TMM 43380-7 is from north Grapevine Hills; LSUMG V-1081 and V-863 are from Dawson Creek, Dogie Mountain area; LSUMG V-1168 is from Sombrero Peak.

Stratigraphic Distribution: Cretaceous Aguja Formation and early Paleocene Black Peaks Formation.

Description

The overall shell shape of TTU 5-104-47 is difficult to determine, owing to the fragmentary nature of the carapace. Some pieces have been fitted together, however, and the sulci are, in part, traceable on these larger pieces. The pieces that fit together include much of the anterior medial, as well as the right and left lateral portions of the carapace, including the axillary notches. The anteromedial portions of the carapace include the broken costal processes of the third (?) through sixth (?) costals, and parts of the third (?) through seventh (?) costals, and third (?) through seventh (?) neurals.

Part of the anterior edge of the carapace is also present, and it exhibits a strongly developed right (?) costiform process on the first costal. This piece is very distorted, and it is impossible to orient it correctly, because the matching costiform process is missing. The distortion is pronounced, and is probably due in part to post-depositional processes. However, the deformation is so great on this piece, that some of it must be pathological. The other portions that fit together also exhibit some deformation. The right lateral margin of the carapace clearly exhibits sulci for marginal scutes as well as for parts of the first two supramarginal scutes. Sulci for marginal scutes are also visible on the other edges of the carapace (Figure 3.13). The portion of the carapace with the anterior edge is unusually pointed, but some of this may be post-mortem deformation. It also exhibits what appears to be a supracostal sulcus on the first vertebral. Other visible sulci on the carapace fragments are not definitive. Sutures are completely coalesced, and owing to the poor preservation of the specimen, are not determinable by transverse lines. Ornamentation appears to consist of rough, poorly defined, longitudinal ridges, and very small, pinhead-sized irregular bumps.

The plastron is nearly complete and the sulci are clearly visible, but the sutures are not (Figure 3.14). The plastron is convex in shape on its ventral surface and very thick and robust. The anterior lobe of the plastron is shorter and narrower than the posterior, and tapers to a rounded point. The posterior lobe is wide, broadens toward the posterior margin, and is squared at the end, with no evidence of a xiphiplastral notch. The bridge is robust, and the length of the bridge is a little less than one half of

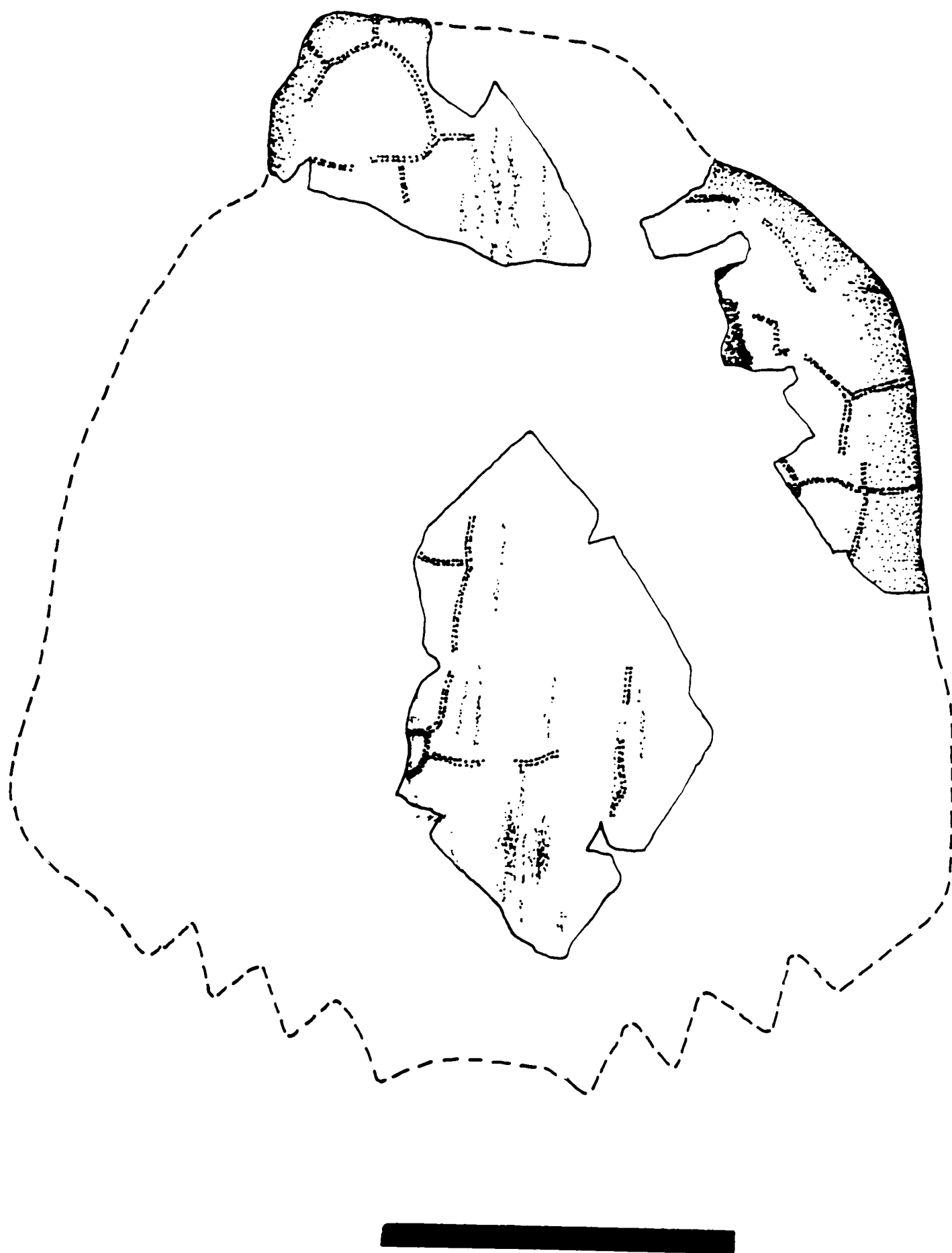


Figure 3.13. "*Baena*" sp., carapace fragments of TTU 5-104-47 in dorsal view. Bar scale is 10 cm.

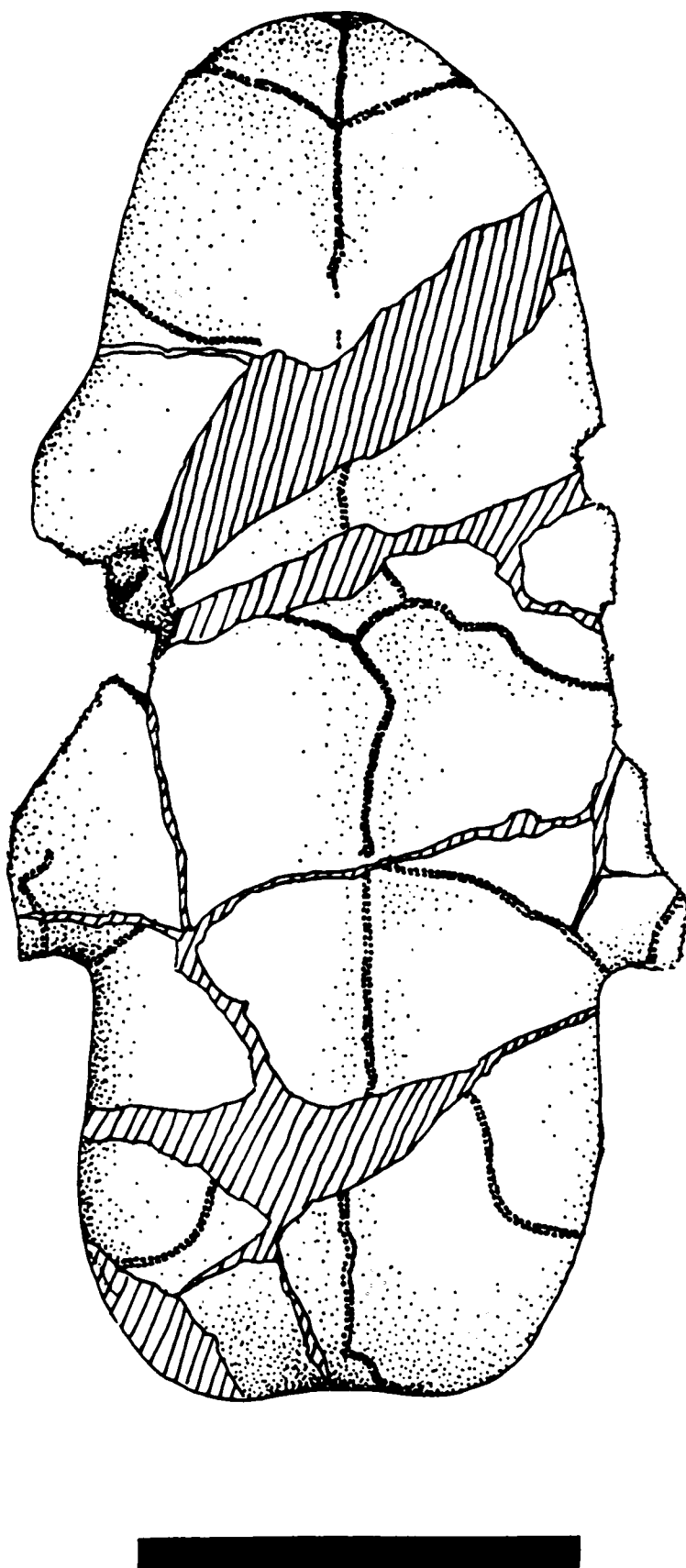


Figure 3.14. "*Baena*" sp., TTU 5-104-47, plastron in ventral view. Bar scale is 10 cm.

the total length of the plastron. The intergular and gular sulci are paired, bilaterally symmetrical, and meet at the midline. The intergulars are very small, and are only about one-eighth the size of the gulars. The anal/femoral sulcus is not visible in its entirety, but appears to be somewhat squared at the midline. Sutures are not discernible. Ornamentation consists of small pin-head-sized irregular bumps and lines.

TMM 42533-3 consists of one or more costals, probably from a single specimen. The dorsal surface exhibits large-scale nodular bumps and ridges.

TMM 42534-3 is a single specimen consisting of several broken and disarticulated carapace and plastron fragments. Many of the fragments were coated with concretion, which preserved the surface of the specimen. Other fragments are badly weathered, and surface features are gone. Carapace fragments consist mostly of parts of costals. Two pieces are from the margin. The other is a large fragment from the right edge, just below the midline, and contains both partially broken peripheral bones and costal bones. Sulci are visible on only two fragments, marginal and pleural sulci on the large fragment from the edge, and indeterminate sulci on a smaller fragment. Sutures are fully coalesced, and not discernable on the dorsal side of the carapace fragments, but are visible in some places on the ventral side. The ornamentation on the carapace fragments consists of rough, nodular bumps and ridges. There are four small fragments from the plastron, two are probably from either the hyoplastron or hypoplastron, judging from their sizes. No terminal edges, sulci, sutures, or ornamentation are present.

TMM 42534-4 is a small fragment from the medial portion of the carapace, and includes at least two, possibly three neural bones, and parts of three (?) costals. Broken costal tubercles are present on one half of the ventral side of the fragment. One tubercle is clearly visible, two more are broken off, but their positions can be extrapolated. The fragment appears to be broken down the midline of the site of attachment of the neurals to the neural arch. Sulci and sutures are not visible. Ornamentation consists of rough, nodular bumps and ridges.

TMM 43380-4 is a small fragment composed of part of a costal from the medial part of the carapace. A broken costal tubercle is present on the ventral side of the fragment. A pleural/pleural sulcus and a pleural/vertebral sulcus are visible on the dorsal side. Sutures are not present. Ornamentation consists of rough, nodular bumps and ridges.

LSUMG V-1081 is a single specimen composed of eight small fragments of carapace, and two small fragments of plastron. Two of the carapace and one of the plastron fragments contain part of a buttress. This is probably the right inguinal buttress, because parts of the abdominal/femoral and the femoral/anal sulci are visible on this fragment. It is not possible to tell which buttress is present on either of the carapace fragments. One small piece of a costal exhibits a broken costal tubercle. Ornamentation consists of large nodular bumps and ridges on the carapace fragments.

LSUMG V-863 is a single specimen, badly weathered and fragmented. This specimen consists of the first through fourth neural bones, parts of the first through fourth costal bones, and parts of two more neurals. There is also part of a vertebra

with two pairs of transverse processes, part of a neural arch (?), and other small fragments of carapace. The first costal bones exhibit well developed costiform processes for articulation with the first dorsal vertebra, as well as the broken proximal ends of the axillary buttresses. The surface is very badly weathered and all of the surface detail is gone. It is possible, however, to see the remnants of large nodular bumps on some fragments.

LSUMG V-1168 is a nearly complete plastron and fragments from the carapace. The carapace fragments are badly weathered and broken. Sulci and sutures are not visible. The carapace fragments exhibit a surface with large-scale nodular bumps and longitudinal ridges. The plastron has a complete anterior and posterior lobe, and a nearly complete right bridge (Figure 3.15). The plastron exhibits no ventral concavity. The plastron shows paired, bilaterally asymmetrical gulars meeting medially. No intergulars are present. Sutures are closed and no transverse lines are visible. The surface is mostly worn smooth, but in small areas, reticulated ridges and bumps can be seen.

TMM 43380-6 is a broken ?right hypoplastron. The abdominal/femoral sulcus is visible, and ornamentation consists of small, irregular bumps. TMM 43380-7 is part of a small plastron, probably the right hyoplastron. Two sulci are visible, and are probably the pectoral/humeral and humeral gular sulci. No ornamentation is visible.

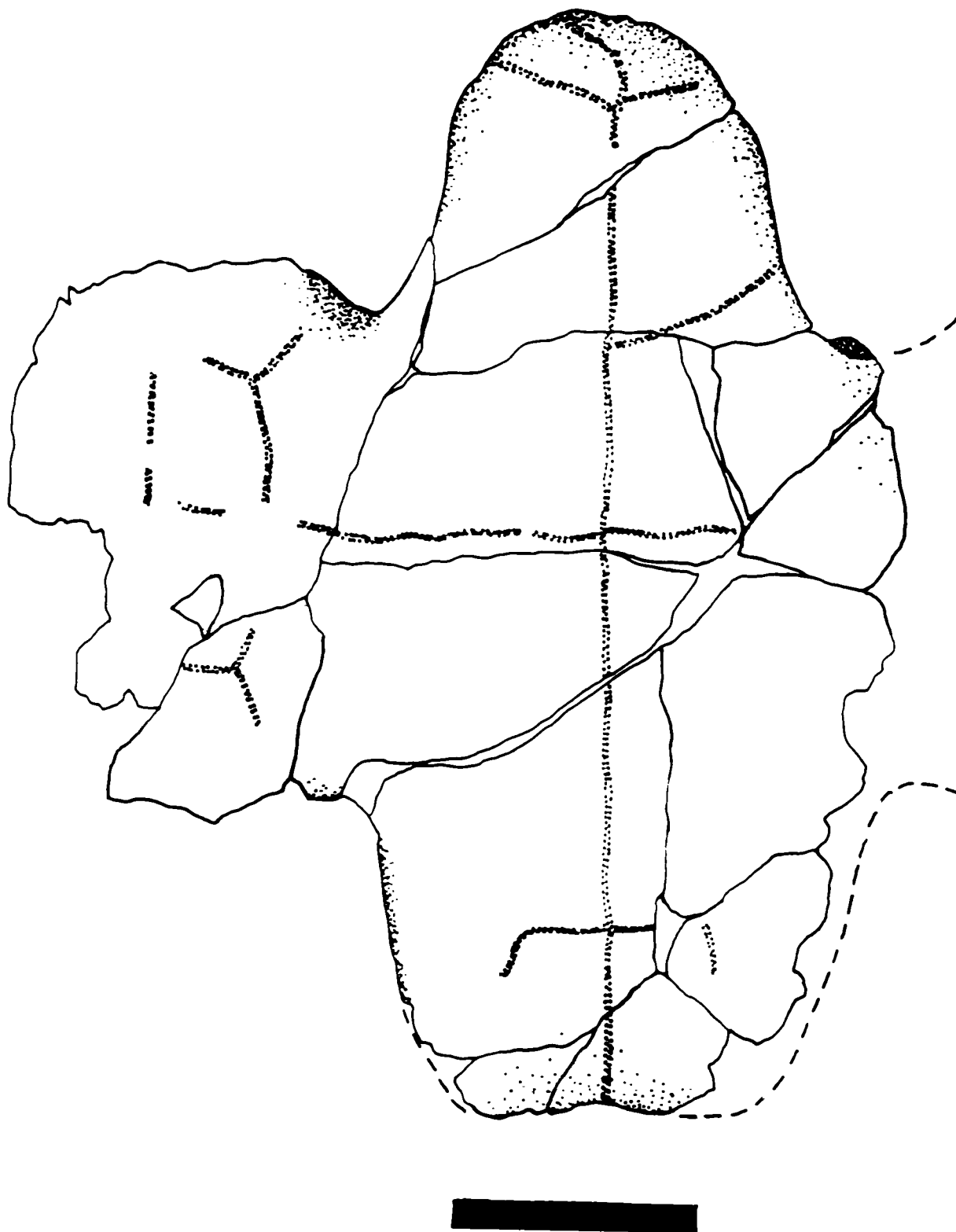


Figure 3.15. "*Baena*" sp., LSUMG V-1168, plastron in ventral view. Bar scale is 5 cm.

Discussion

The distorted nature of TTU 5-104-47 makes it very difficult to determine its identity. The most puzzling area is the anterior end of the carapace. Either the costiform processes are abnormally oriented, or the usual longitudinal ornamentation of the carapace instead runs diagonally. Neither condition would be normal. The distortions seen in the carapace cannot be fully explained by post-depositional processes, and it is apparent that this specimen has some irregularities that must be pathogenic. Therefore, other irregularities, such as supramarginal scutes and supracostal scutes, must be considered as possibly pathogenic as well, and not necessarily taxonomically diagnostic.

Lawson (1972) originally assigned this specimen to the Baenidae on the basis of the length of the bridge in proportion to the length of the anterior lobe, and the broad, non-tapered shape of the posterior lobe. Lawson (1972) identified the specimen as *Thescelus* sp. on the basis of the shape of the plastron and the very small size of the intergulars. These plastral characters superficially resemble those of *Thescelus* as described by Hay (1908). The configuration of the intergular and gulars in *Thescelus*, as well as their size, are notable. When the intergulars are present they are paired and meet each other medially, and do not meet the gulars. This condition is found in *Thescelus*, *Boremys*, "*Baena*" *marshi*, and "*Baena*" *escavada*, but according to the literature apparently not in "*Baena*" *hatcheri*, "*Baena*" *callosa*, "*Baena*" *nodosa* or "*Baena*" *ornata* (Hay, 1908; Gilmore, 1916, 1935; Gaffney, 1972). Most workers believe that the presence or absence of intergulars and the

intergular/gular relationship is a highly variable condition even within a single species (Hay, 1908; Gaffney, 1972). As such, this character is not sufficient to identify this specimen as *Thescelus*. The one indisputable character that would identify this specimen as *Thescelus* is the projection of the anterior lobe of the plastron beyond the anterior edge of the carapace. Because of the fragmentary nature of the specimen, it is impossible to determine whether this is the case.

There are two other characters that might offer clues to the identity of this specimen, the sulci for the supracostal(?) scute and the supramarginal scutes on the carapace. The odd distortion of the fragment containing sulci for this scute is discussed above. The orientation of this portion of the carapace is probably shown correctly (Figure 3.13), but owing to the reasons listed above, some doubt exists. If the orientation is correct, then this is probably a triangular supramarginal scute. Supracostal scutes may be present or absent in "*Baena*" *callosa*, "*Baena*" *nodosa*, "*Baena*" *escavada*, *Boremys*, and *Thescelus*. They are absent in all others listed previously. Again, this character seems to be variable, in particular for the form-genus "*Baena*".

The supramarginal scutes may be more diagnostic. The literature makes it clear that only four genera possess supramarginal scutes, the Triassic *Proganochelys*, Jurassic *Platycheilus*, Cretaceous *Boremys*, and present day *Macrolemmys* (Lambe, 1906; Gaffney, 1972). This would seem to indicate that the TTU specimen is *Boremys* by default. However, given the unusual condition of this specimen, the possibility of shell abnormality must be considered. Zangerl and Johnson (1957) studied scute

abnormalities and found that “abnormalities involving three or more scales in continuous aberration were the rarest of the types.” In addition, multiple abnormalities occur more frequently in larger individuals. But the addition of one or more scales is more common. Because of the manner in which the present specimen is fractured, it is difficult to tell if more than two supernumerary scutes are involved. Abnormalities occur less frequently in aquatic species than in semi-aquatic or terrestrial. Considering the observations of Zangerl and Johnson (1957), and considering that this individual has other demonstrable deformities, it is difficult to dismiss the possibility that these supramarginal scutes are abnormal.

Some parts of the carapace exhibit a subtle ornamentation of bumpy ridges. It is more subtle than the specimens identified in this report as “*Baena*” cf. *nodosa*, or “*B.*” cf. *ornata*, but nevertheless resembles that type of ornamentation. Therefore, the possibility is strong that this individual may be an abnormal representative of either “*B.*” *nodosa* or “*B.*” *ornata*.

The other specimens are all referred to the form-genus “*Baena*”, on the basis of the nodular bumps and ridges on the carapace fragments. This type of ornamentation is characteristic of both “*B.*” *nodosa* and “*B.*” *ornata*. TMM 42534-3, TMM 42534-4, and LSUMG V-1081 had previously been referred to the species “*B.*” *nodosa*, and LSUMG V-863 had previously (on the specimen labels) been referred to the species “*B.*” *ornata*. However, none of the diagnostic characters needed for the specific identification of these specimens is present. Therefore they are referred here to “*Baena*” *sp.*

Subfamily indeterminate

Compsemys victa Leidy, 1856

Compsemys parva Hay, 1910, p. 308.

Compsemys vafer Hay, 1910, p. 311.

Compsemys puercensis Gilmore, 1919, p. 19.

Compsemys torrejonensis Gilmore, 1919, p. 21.

Referred specimens: LSUMG V-1354, LSUMG V-1476, LSUMG V-5004.

Localities: LSUMG V-1354 is from “Running Lizard” locality, LSUMG V-1476 is from the “Tom’s Top” locality on Dawson Creek, and LSUMG V-5004 is from south of Dogie Mountain.

Stratigraphic Distribution: Cretaceous Aguja Formation and early Paleocene Black Peaks Formation.

Description

LSUMG V-1354, LSUMG V-1476, and LSUMG V-5004 are small costal fragments, no larger than 2 cm in width, and approximately 0.5 cm in thickness. Two partial costal processes are visible on the visceral surface of V-1354, and the dorsal surface over one of the ribs ends in an uncoalesced margin. Nearly one-half of the dorsal surface on this specimen is worn, with most of the ornamentation missing. However, all of the specimens bear a distinct ornamentation consists of small, low, densely spaced tubercles arranged in a random order.

Discussion

Gaffney (1972) places *Compsemys* in an indeterminate subfamily, and regards all named species as junior synonyms of *Compsemys victa*. This is because most of the known specimens of *Compsemys* lack any diagnostic characters that would allow diagnosis of separate species (1972). LSUMG V-1354 was identified as *Compsemys victa* by Standhardt (1986) on the basis of the ornamentation that is visible on the outer surface of the costal bone. This distinctive ornamentation is unique to the genus *Compsemys*, and sufficient to identify these fragments (Gaffney, 1972). LSUMG V-5004 is a single fragment in a much larger collection of small, badly weathered and abraded, generally indistinguishable fragments (probably pertaining to *Hoplochelys*) in the LSUMG collection marked V-5004, "Turtle".

Neurankylus Lambe, 1902

Neurankylus eximius Lambe, 1902

Charitemys captans Hay, 1908, p.98.

Neurankylus baueri Gilmore, 1916c, p.290.

Baena fluviatilis Parks, 1933, p.19.

Referred specimens: TMM 43385-1, a mostly complete carapace and plastron; TMM 43467-1, a mostly complete carapace and plastron.

Localities: TMM 43385-1 is from near the east end of the River Road; TMM 43467-1 is from the summit of Rattlesnake Mountain.

Stratigraphic Distribution: the upper shale member of the Aguja Formation.

Description

TMM 43385-1 is a mostly complete carapace and plastron (Figure 3.16). The carapace is oval with parallel sides. The shell has been partially flattened and distorted, but not severely. The carapace has a posterior margin exhibiting a slight scalloping, and an anterior margin that is rolled at the edges, forming a shallow gutter. The shell is very thin for its size, with the thickest part of the carapace at the anterior end, thinning to an acute edge at the posterior margin. A narrow keel extends from approximately the sixth neural to the second suprapygal along the midline on the posterior half of the carapace. A well-developed costiform process is present on the left first costal. Moderately developed costiform processes occur on the eighth costals. Fragments of dorsal vertebrae three through six are present.

A portion of the anterior edge of the carapace is missing, eliminating useful information about the first vertebrals of the carapace. Most of the rest of the shell is fractured, but intact. The sulci are easily traceable. The shell is completely co-ossified, as is the case with all adult baenids (Archibald, 1977). However, some of the sutures can be determined by tracing of fine transverse lines.

The nuchal scute is missing, as well as part of the first vertebral. The carapace is very fractured at the anterior end, further obscuring detail that would help to identify the second through fourth neurals, the first through third costals, and the first and second vertebral scutes. The details of nearly all the peripherals and the marginal

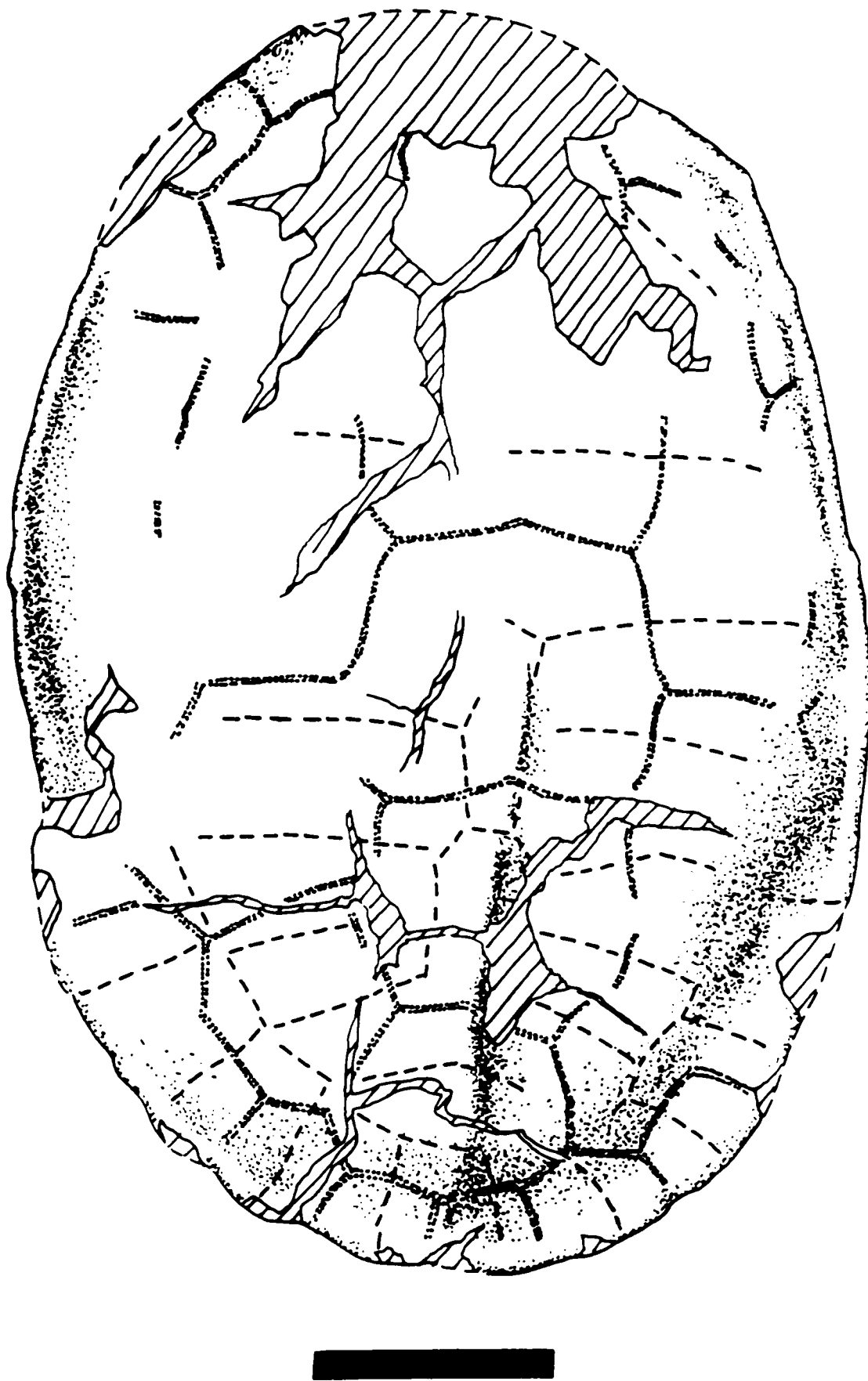


Figure 3.16. *Neurankylus eximius*, TMM 43385-1, carapace in dorsal view. Bar scale is 10 cm.

scutes have been obscured, with the exceptions of the seventh through ninth peripherals and the tenth through twelfth marginal scutes.

The anterior lobe of the plastron is partially missing, but it is evident that it was probably squared, and the posterior lobe is somewhat narrow and tapering to a rounded point (Figure 3.17). There is no xiphiplastral notch. The plastron is thin for a baenid of this size, with the thickest part being the anterior lobe, and thinning to an acute edge at the posterior margin. The anterior portion containing the gular and intergular scutes, and the entoplastron and epiplastral bones are missing, although a small portion of the right epiplastron is preserved. However, sulci for the anal, femoral, abdominal, and parts of the pectoral scutes are present and easily identifiable. Sulci for the axillary, inguinal, and marginal scutes are obscured by fractures. The sutures are not very clearly delineated, but it is possible to make out the xiphiplastral, hypoplastral, and part of the mesoplastral sutures by use of the transverse lines. The surfaces of both the carapace and plastron are relatively smooth. Ornamentation, where it exists, consists of very small, irregular bumps.

Discussion

Gaffney (1972) lists *Neurankylus* as subfamily indeterminate, and refers all described species as junior synonyms of *Neurankylus eximius*. The general shape and configuration of the shell bones and scute sulci that are identifiable agrees with the diagnosis for *Neurankylus* as given by Gilmore (1916), and Gaffney (1972): (1) the

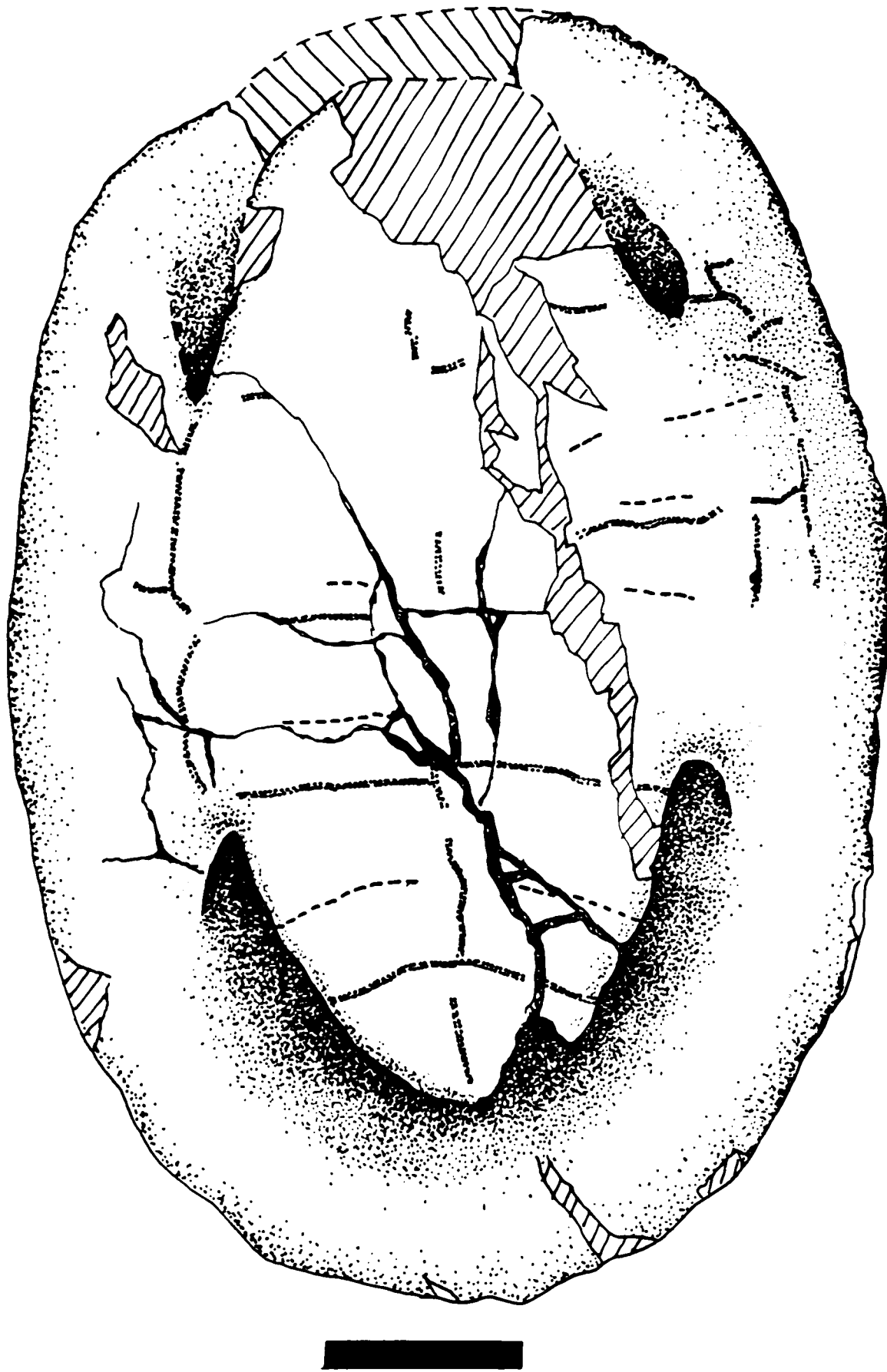


Figure 3.17. *Neurankylus eximius*, TMM 43385-1, plastron in ventral view. Bar scale is 10 cm.

vertebral scutes are wide compared to their length, with bracket-shaped sides, (2) there are no supramarginal scutes, (3) the last vertebral scute is closed posteriorly, (4) the last pair of marginal scutes meet medially behind the vertebral, (5) the last marginals are rectangular, and (6) the posterior edge of the carapace is not emarginated.

The similarities between *Neurankylus*, *Glyptops*, and *Trinitychelys* have been thoroughly examined by both Gaffney (1972) and Archibald (1977). Gaffney states that *Trinitychelys* and *Neurankylus* in particular have very similar shells, and that, although the presence or absence of a keel is variable among individuals of *Neurankylus*, this character is present in most individuals of *Neurankylus*, and may be used to separate it from *Trinitychelys*. *Neurankylus* also lacks the pronounced *Glyptops*-type ornamentation seen on the shell of *Trinitychelys*. Archibald (1977) further states that *Neurankylus* has a co-ossified shell as an adult, while *Glyptops* and *Trinitychelys* do not, and that the anterior lobe of the plastron is squared in *Neurankylus* and rounded in *Glyptops* and *Trinitychelys*. Also, the scalloping typically seen in *Neurankylus* is lacking in *Glyptops*, and it is not known whether it exists in *Trinitychelys*. On the basis of these characters, TMM 43385-1 can confidently be assigned to *Neurankylus eximius*, and TMM 43467-1 is very probably referable this species as well.

Superfamily CHELONIOIDEA Baur 1893

Family (?)CHELONIIDAE Gray 1825

New Genus, New Species

Referred specimen: TMM 43072-1

Locality: TMM 43072-1 is from near Santa Elena Canyon.

Stratigraphic Distribution: Rattlesnake Mountain Sandstone Member of the Aguja Formation.

Description

TMM 43072-1 is a large, incomplete specimen consisting of the lower mandible and hyoid bone, a portion of the margin of the carapace, a large part of the right side of the plastron and a smaller portion of the left side of the plastron, left scapula and acromial process, right and left humeri, (?) right (?) ulna, (?) right (?) radius, proximal portion of the right femur, distal portion of the (?) right femur, and assorted fragments and disarticulated elements of indeterminate nature.

The lower mandible is slender. The right ramus consists of the complete dentary, angular, splenial, surangular, and prearticular bones. The Mekelian foramen, and the adductor and glenoid fossae are well preserved. A large part of the left ramus, including all of the symphyseal region and triturating surface is present. The symphysis is completely fused, and its antero-posterior length is short (Figure 3.18). A low, serrated labial ridge is present on the triturating surface, and a subtle lingual ridge is

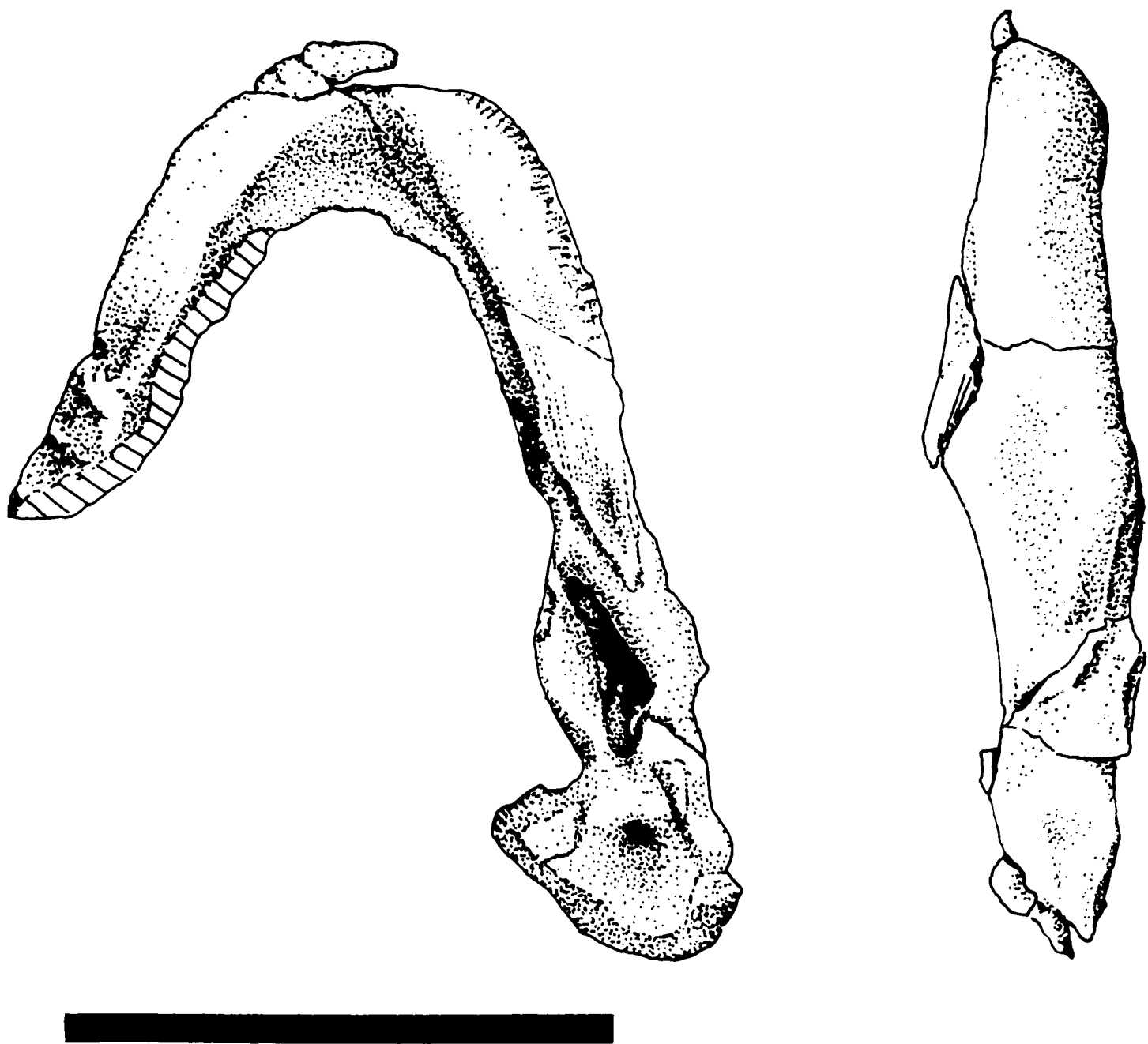


Figure 3.18. Cheloniidae, n. gen., n. sp., TMM 43072-1, lower mandible in oral and right lateral views. Bar scale is 10 cm.

present on the proximal halves of the rami. The floor of the triturating surface adjacent to the ridges is smooth. The two mandibular rami form an angle of approximately 50°.

There are two large sections of the lateral margin of the carapace (Figure 3.19). One measures 38 cm. in length and the other is 19 cm. in length. Both are relatively straight, although the larger one exhibits a subtle curve. The longer one is probably from the left margin of the carapace. The position of the smaller piece is uncertain. They are badly weathered, so surface detail is obscured.

The plastron is broken, incomplete, and weathered. It is massive, elongate, and exhibits no evidence for reduction or development of fontanelles (Figure 3.20). It appears to be slightly flattened to concave anteromedially, and somewhat less so posteromedially. The concave shape may be a postmortem feature. The right side is more complete than the left, and measures approximately 53 cm from the axillary to the inguinal notch. The axillary buttress is robust, while the inguinal buttress is slightly less robust. The plastron is thickened approximately 1.5 to 2 cm at the margins, but thins medially to a thickness of 0.5 cm in places. The left side consists primarily of the anterior third of the plastron, including the axillary notch. The plastron is completely coossified; no sutures are visible.

The left scapula and acromial process are large, and form an angle of approximately 110° to each other (Figure 3.21, 3.22). The scapula measures 28 cm from the distal end of the blade tip to a point at the base of the acromial process. The acromial process is 24.5 cm in length from the point in the center of its union with the

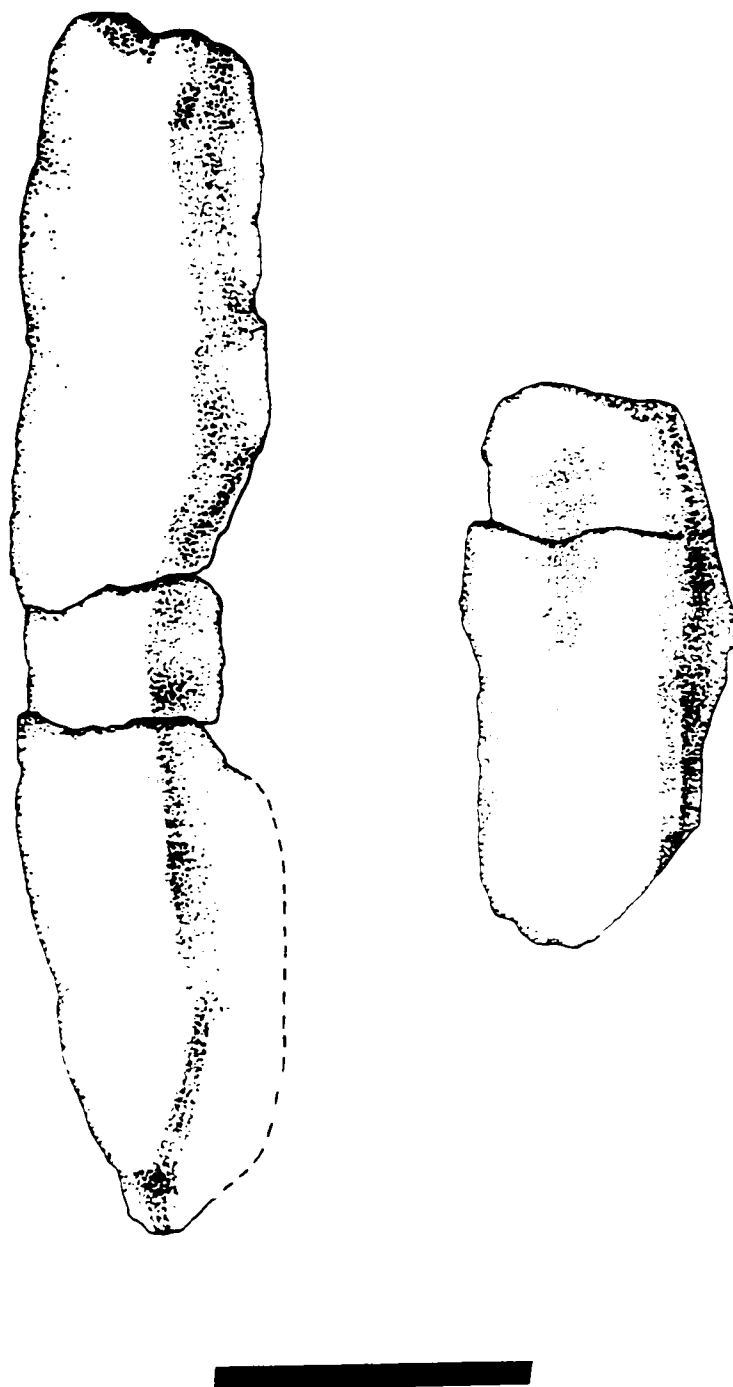


Figure 3.19. Cheloniidae, n. gen., n. sp., TMM 43072-1, carapace fragments in dorsal view. Fragments are from the lateral edge of the carapace, but exact position is unknown. Bar scale is 10 cm.

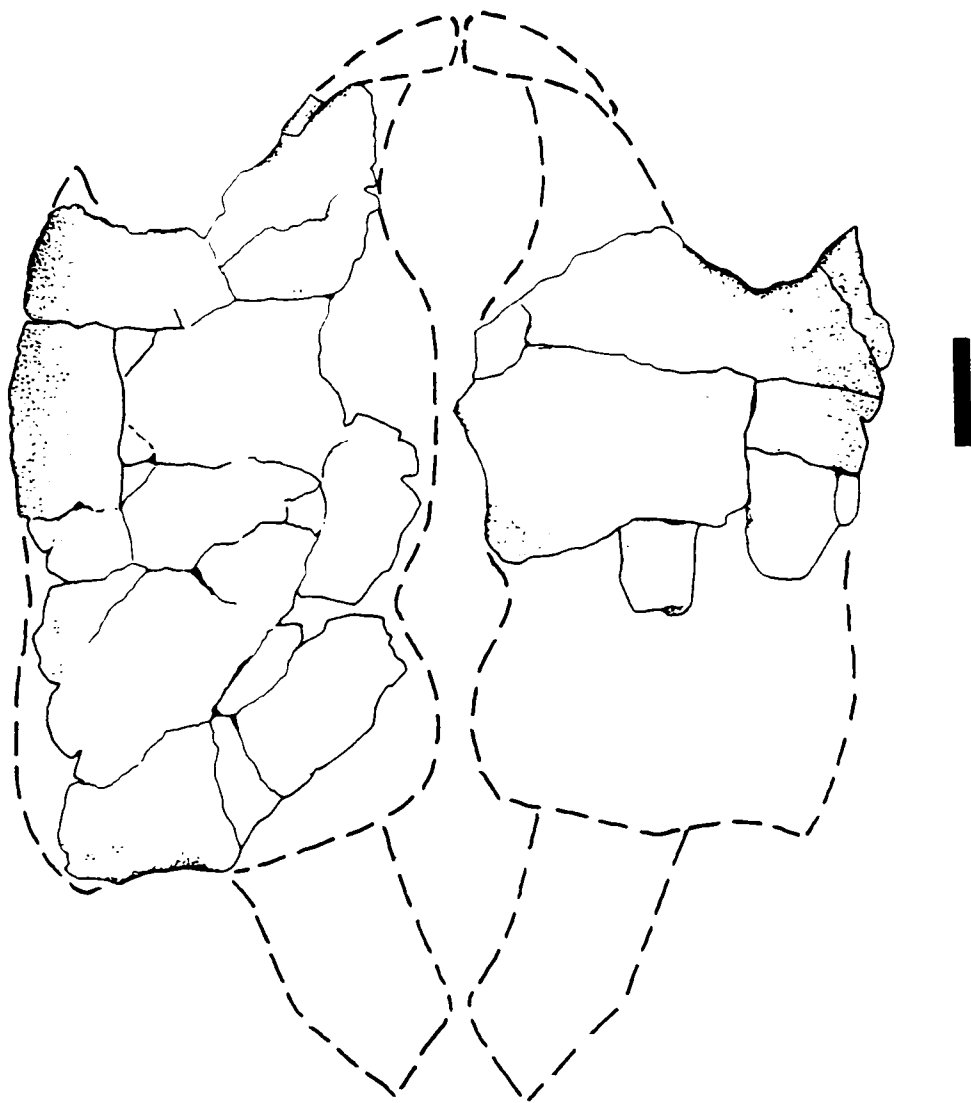


Figure 3.20. Cheloniidae, n. gen., n. sp., TMM 43072-1, plastron in ventral view. Bar scale is 10 cm.

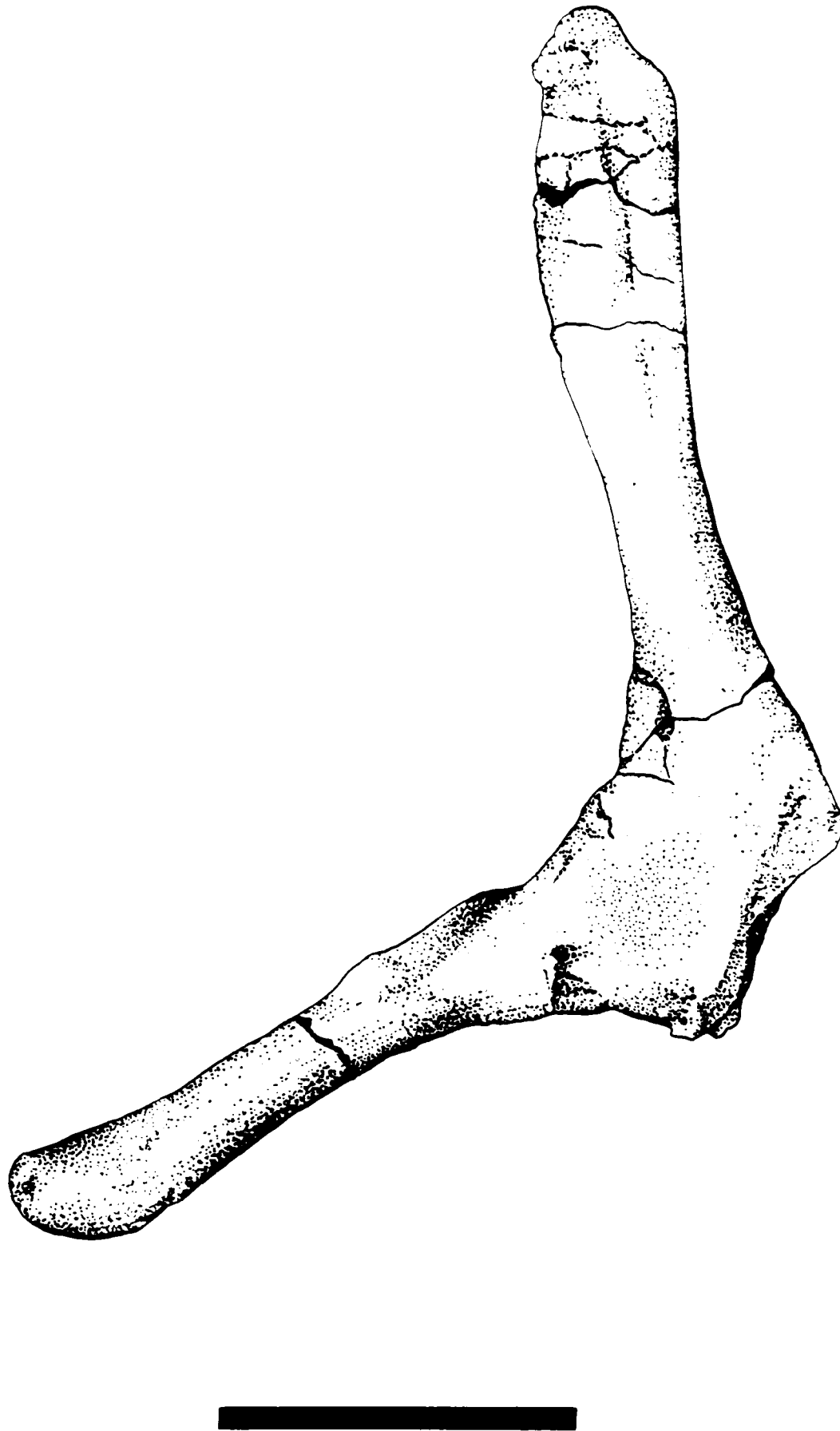


Figure 3.21. Cheloniidae, n. ge., n. sp., TMM 43072-1, left scapula, ventral view. Bar scale is 10 cm.

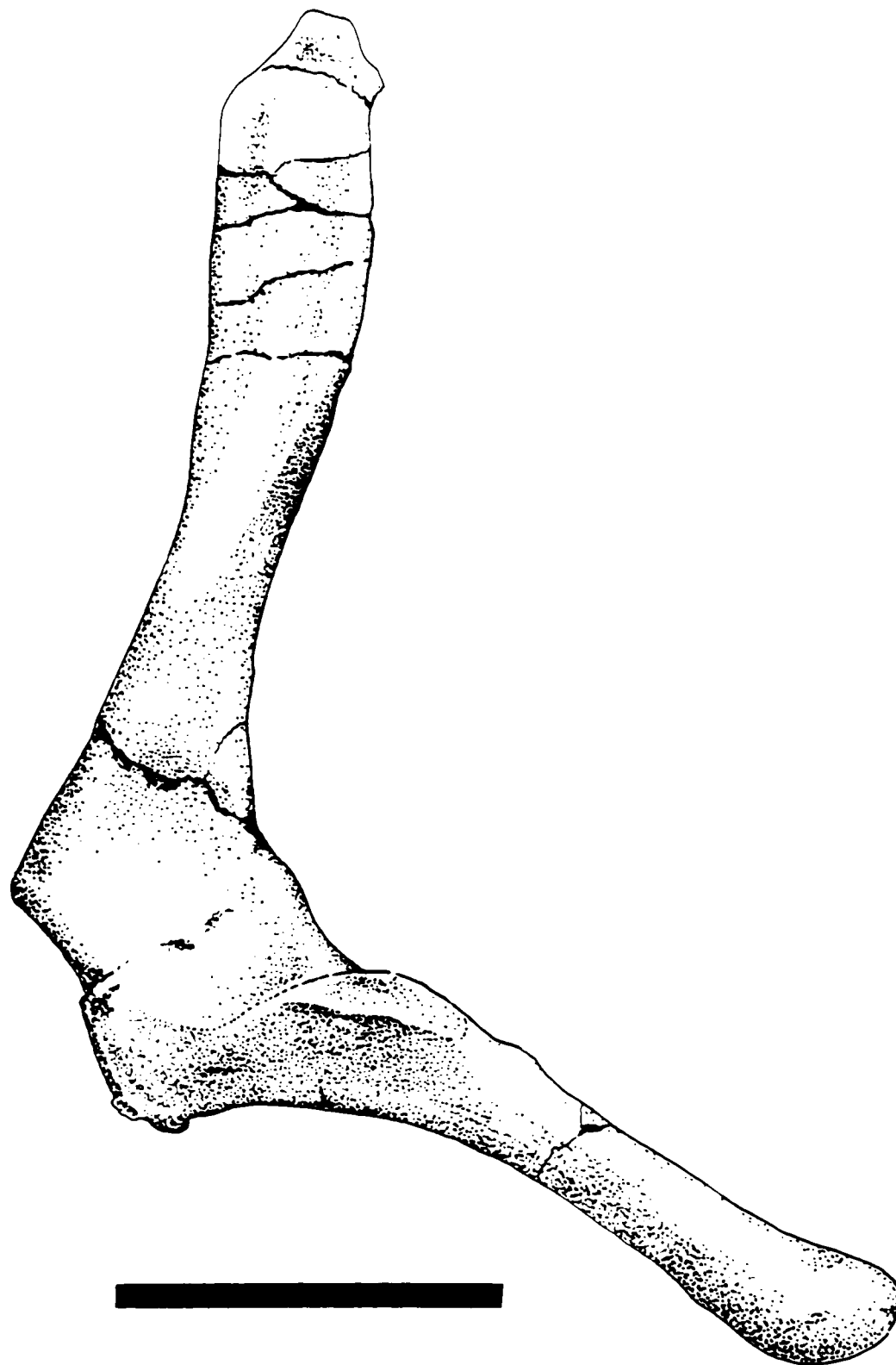


Figure 3.22. Cheloniidae, n. gen., n. sp., TMM 43072-1, left scapula, dorsal view. Bar scale is 10 cm.

scapula, to the distal tip. The scapula is distally flattened and blade-like. The acromial process is cylindrical in shape, and rounded on the distal end. There is a large, slightly flattened tubercle at the base of the acromion process. The dorsal surface of the tubercle is rough. The glenoid fossa is narrow, about 2 cm wide and approximately 8 cm long. The surfaces of the scapular and acromial shafts are striated.

The left and right humeri are large, 32 and 30 cm in length, respectively (Figure 3.23, 3.24). The shaft is slender and delicate, measuring approximately 5 cm in width at its narrowest point. The proximal end is slightly curved anterodorsally. The head is robust, and is nearly twice as large as the deltopectoral crest (= radial tuberosity). The lateral tubercle, is large and pointed, extending beyond the head a length approximately equal to the length of the head. The shaft narrows sharply below the union with the process posteroventrally. The surface of the shaft has a striated texture. The humerus is flattened on the distal end, with a robust ectepicondyle. The ectepicondylar foramen is small. The (?) right (?) ulna is robust, sub-hexagonal in cross sectional shape, and approximately 14 cm in length (Figure 3.25). It is badly weathered and abraded, and the olecranon process is missing. The distal end is flattened and flares laterally.

The (?) right (?) radius is well preserved. It is large and about 14.5 cm long (Figure 3.26). It is narrow in the middle of the shaft and flared at the distal and proximal ends. The surface is striated.

The (?) right femur is badly weathered and abraded, and consists of the proximal end, which is broken near the union of the head with the shaft at the fourth

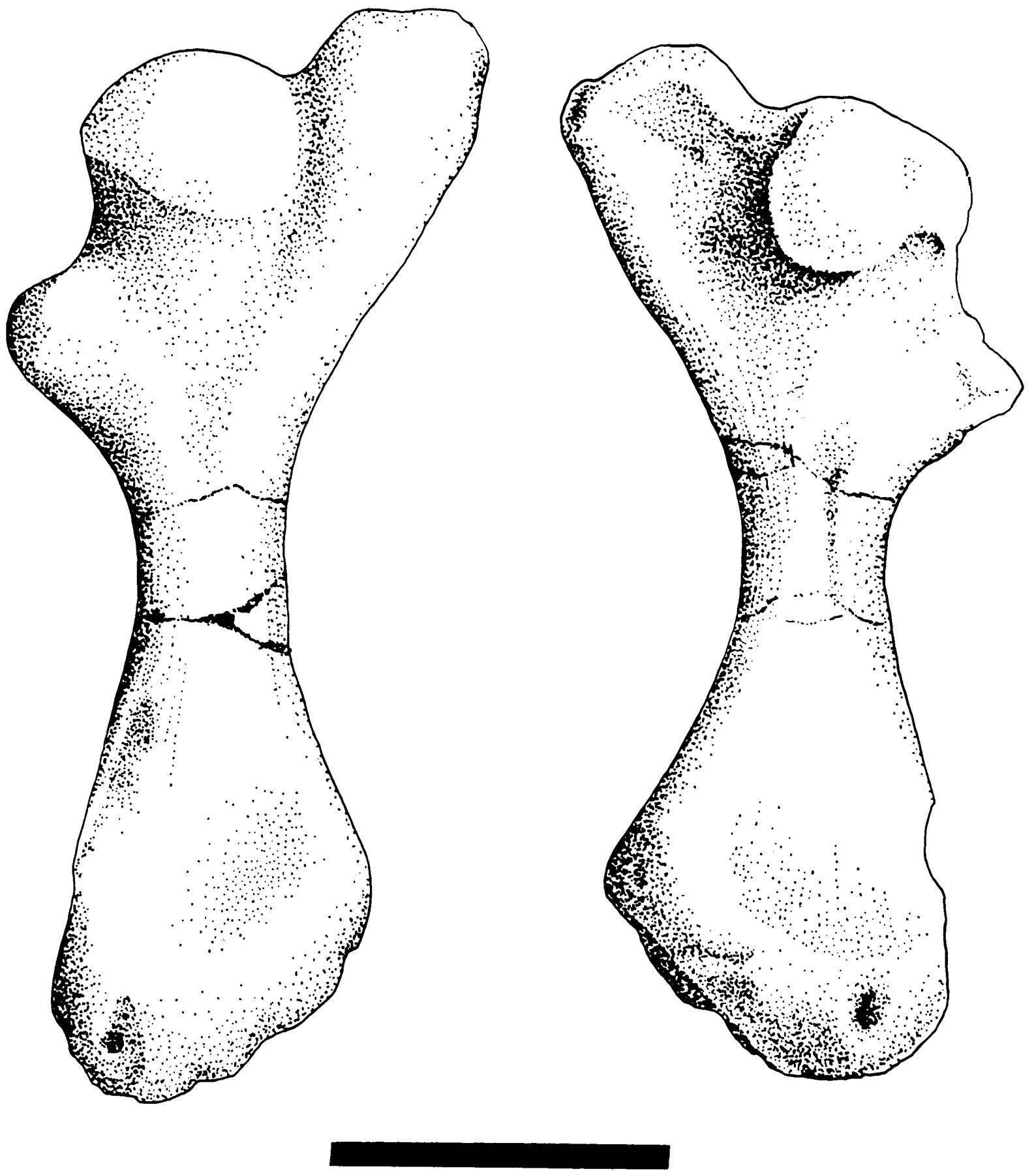


Figure 3.23. Cheloniidae, n. gen., n. sp., TMM 43072-1, left and right humeri, dorsal view. Bar scale is 10 cm.

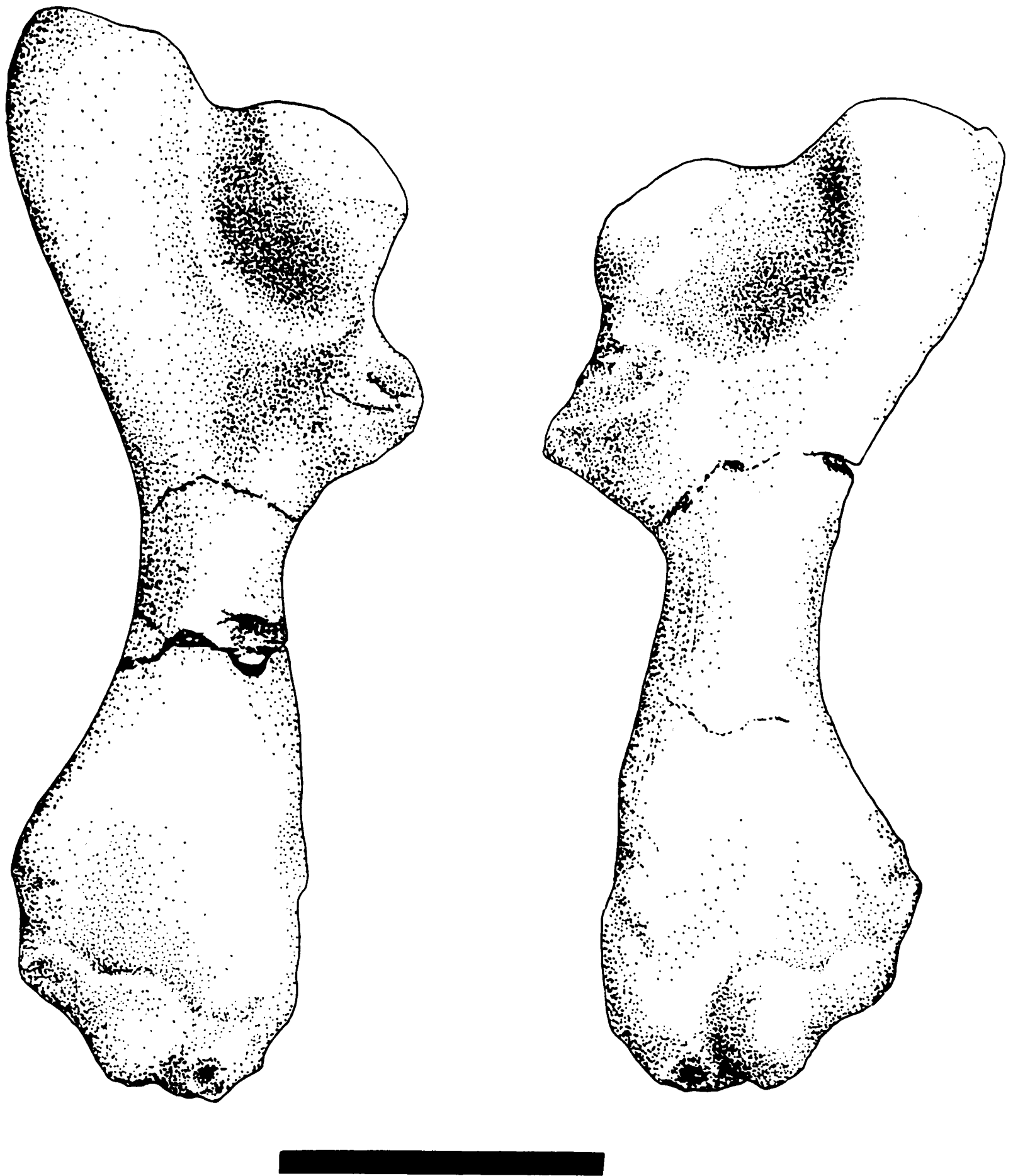


Figure 3.24. Cheloniidae, n. gen., n. sp., TMM 43072-1, left and right humeri, ventral view. Bar scale is 10 cm.

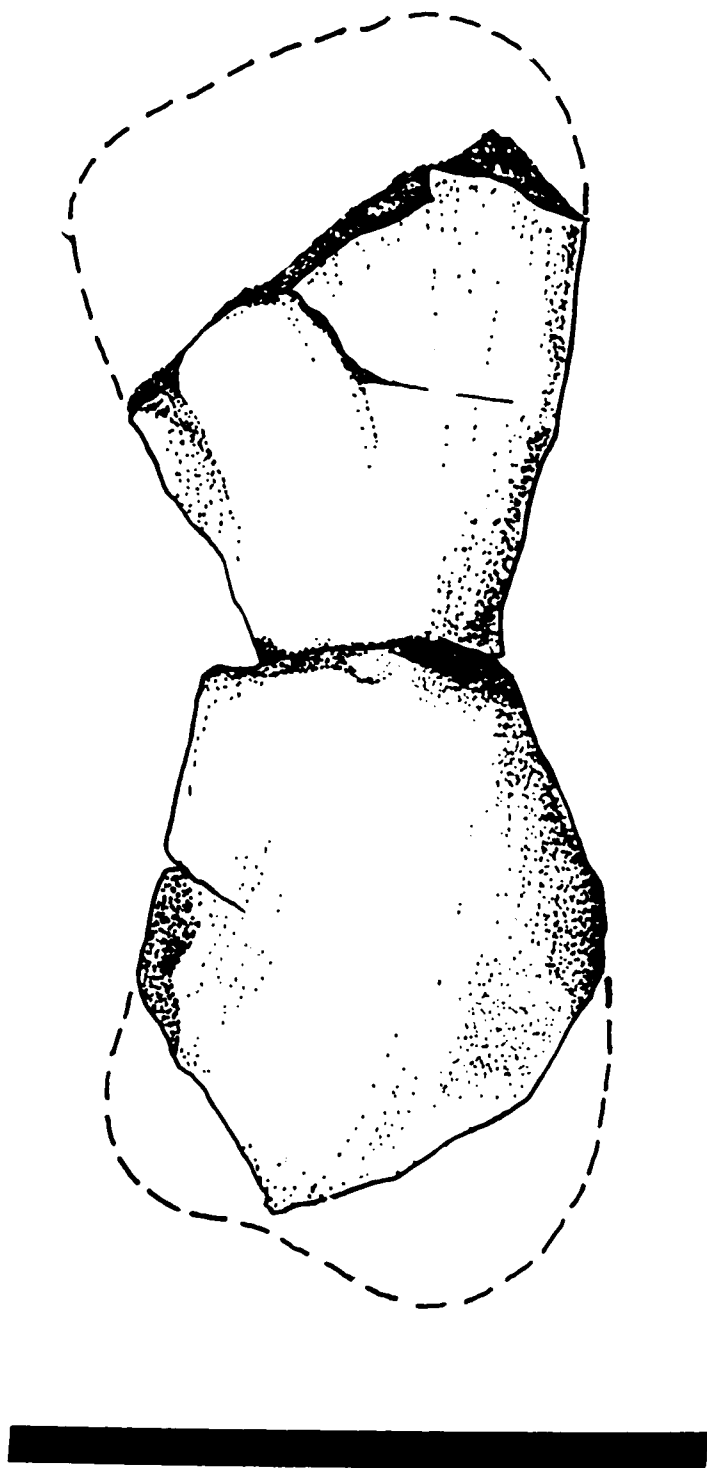


Figure 3.25. Cheloniidae, n. sp., TMM 43072-1, ?right ulna. Bar scale is 10 cm.

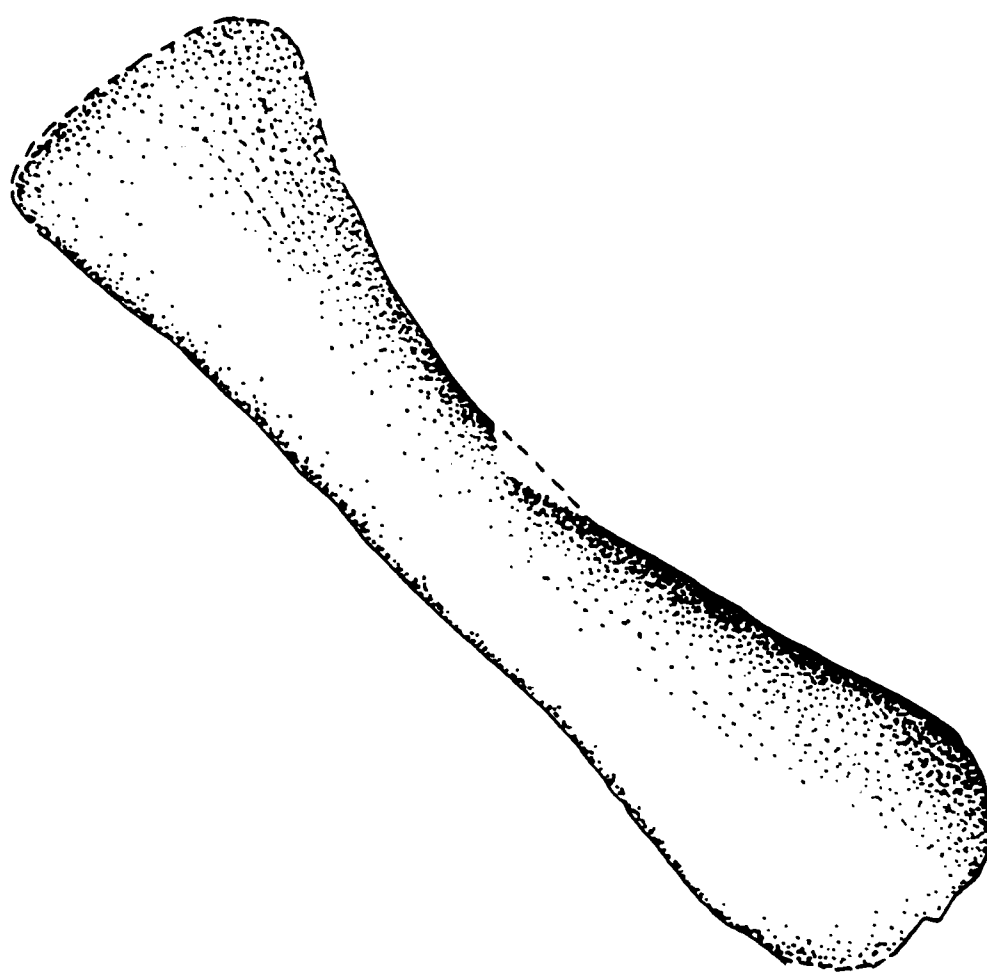


Figure 3.26. Cheloniidae, n. gen., n. sp., TMM 43072-1, right radius in lateral view.
Bar scale is 10 cm.

trochanter, and another segment of part of the shaft and the distal end of the same femur (Figure 3.27). The articular head is large, pointed, and flattened, and the intertrochantic fossa is shallow but well defined. Both branches of the ventral ridge system are broken, but it appears that the internal trochanter is slightly narrower than the proximal posterior branch. The adductor ridge appears to be worn away. The articular surfaces for the tibia and fibula are badly worn, and little can be determined about their true shape. There are a number of large, flat, and massive pieces of bone that are probably from the carapace and plastron. There are also pieces of the ends of epipodial bones, as well as smaller parts of phalanges. At this time, however, the skeletal position of each is indeterminate, in large part because of their poorly preserved condition.

Discussion

Hirayama (1994) divided the marine turtles into three families, the Cheloniidae, Protostegidae, and Dermochelyidae. The family Toxochelyidae of Zangerl (1953) has been placed within the Cheloniidae primarily on the basis of cranial features. Gaffney and Meylan (1988) have also redefined the Chelonioidea primarily, but not exclusively, on the basis of cranial morphology. Although the only cranial feature present in this specimen is the lower mandible, other skeletal characters are useful in determining the classification of this specimen, at least to the family level.

TMM 43072-1 is a very large turtle that has a number of unusual characters. The slender mandibular rami and shortened symphyseal region are similar in form to

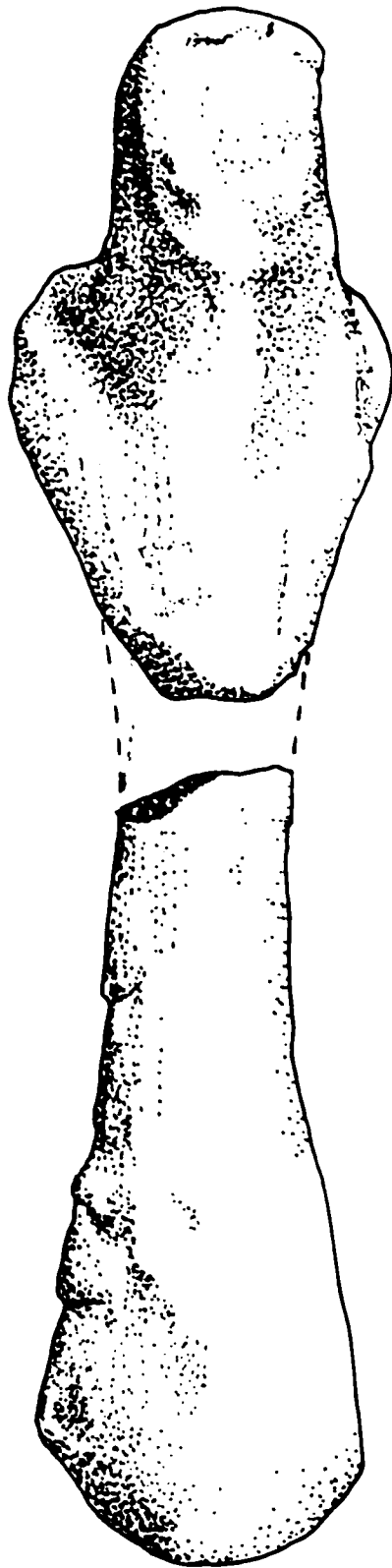


Figure 3.27. Cheloniidae, n. gen., n. sp., TMM 43072-1, right femur in medial view.
Bar scale is 10 cm.

some members of the Cheloniidae, for example, *Ctenochelys*, and *Toxochelys*. The angle of the rami, however, is narrower than that of *Toxochelys*, and the overall size of the Big Bend mandible is greater than either *Toxochelys* or *Ctenochelys*. The shortened symphysis is unlike the longer symphysis of protostegids.

The plastron is probably the most unusual feature of TMM 43072-1 because of its massive, elongate morphology. In size, it is probably closest to some of the Protostegidae, such as *Protostega*, but it lacks the radiating stellate pattern of the plates that comprise the hyo- and hypoplastron, and exhibits no evidence for development of fontanelles. Its morphology appears similar to the Australian flatbacked turtle, *Natator* (Zangerl, Hendrickson, and Hendrickson, 1988), and also to the Miocene *Syllomus* (Weems, 1974) (Figure 3.28). *Natator* and *Syllomus* are sister-taxa in the family Cheloniidae (Hirayama, 1994).

The scapula is large in TMM 43072-1, and exhibits an unusual tubercle on the acromial process. This tubercle is apparently a character that is not found in any of the late Cretaceous marine turtles. It is found, however, in the modern leatherback turtle, *Dermochelys* (Walker, 1973). Only one representative of the Dermochelyidae is known from the Cretaceous, *Protosphargis*, from Upper Cretaceous of Italy, but this turtle has a highly reduced plastron and carapace (Mlynarski, 1976).

The slender humeri have a morphology similar to *Toxochelys*, *Lophochelys*, *Osteopygis*, and *Rhinochelys* (Figure 3.29) (Hirayama, 1994; Zangerl, 1953b). They are slightly curved, rather than straight, which is a synapomorphy found in those

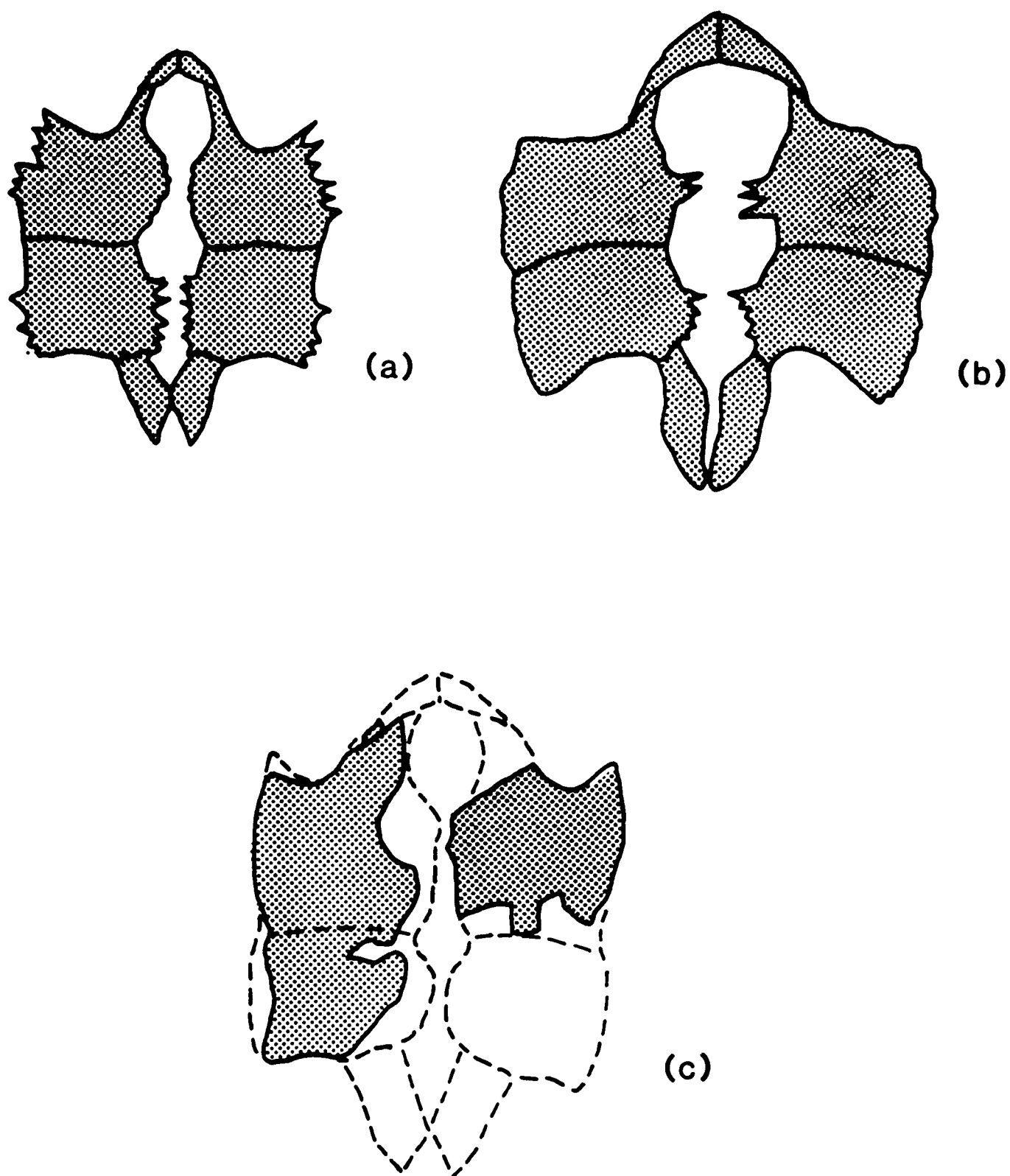


Figure 3.28. Comparison of plastrons of Chelonioida. (a) = *Syllomus aegypticus*.; (b) = *Natator depressus*; (c) = TMM 43072-1. *Syllomus* and *Natator* after Hiriyama (1994). Plastrons are not to scale.

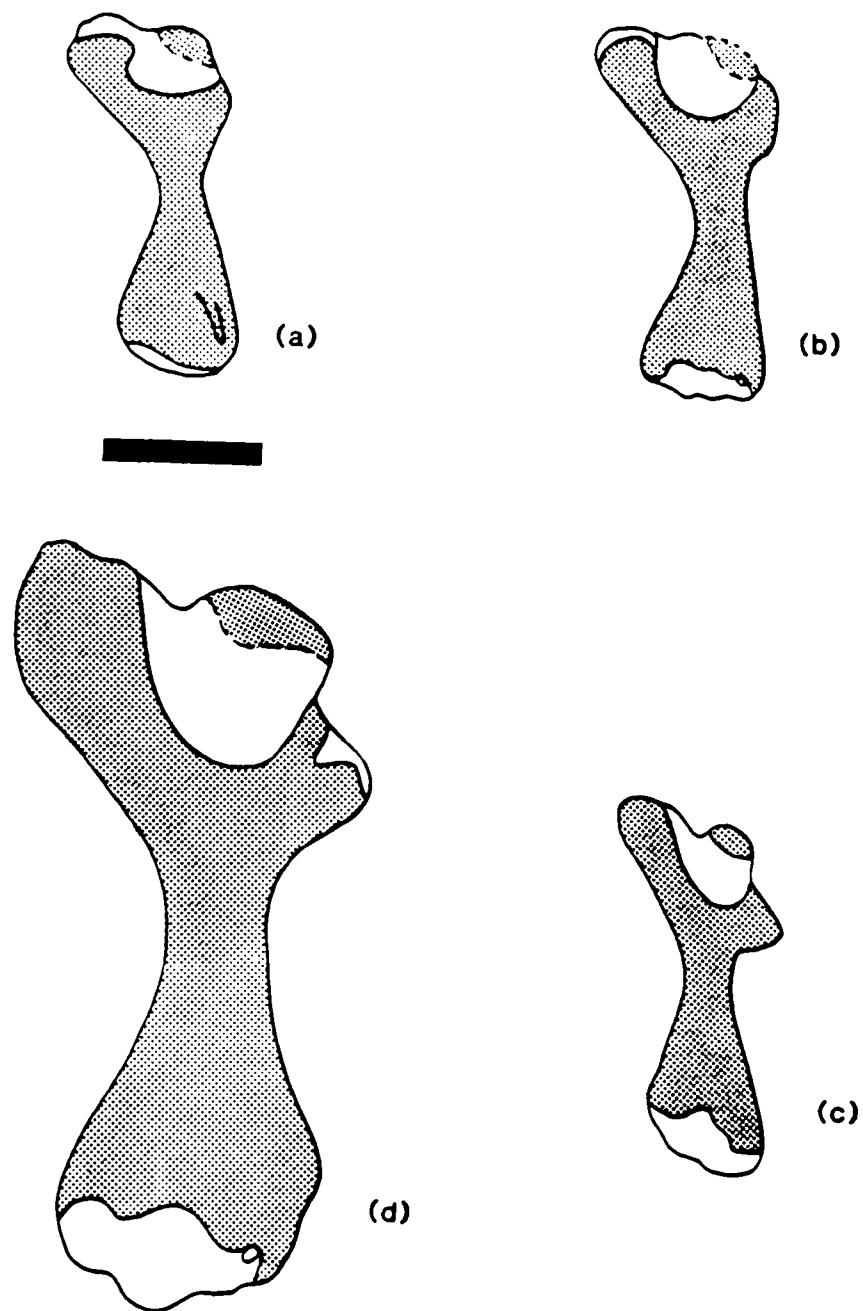


Figure 3.29. Comparison of humeri of Chelonioidea. (a) = *Toxochelys latiremus*; (b) = *Osteopygis emarginatus*; (c) = *Rhinochelys* sp.; (d) = TMM 43072-1. *Toxochelys* and *Osteopygis* after Zangerl (1953b); *Rhinochelys* after Hiriyama (1994). Bar scale is 5 cm; *Rhinochelys* not to scale.

genera, and differ from those of other chelonioids. The deltopectoral crest is most like *Rhinochelys* in its placement; it lies more distal to the head than in *Toxochelys*, *Lophochelys*, *Osteopygus*, but more proximal to the head than in other chelonioids (Zangerl, 1953a, 1953b, 1960). Zangerl (1953b) believed that the forelimb of *Toxochelys* was unusual, and is intermediate between the cheloniids and chelydrids, a view with which Gaffney and Meylan (1988) concur. It appears that TMM 43072-1 shares these characters with *Toxochelys*, *Lophochelys*, *Osteopygis*, sister-taxa in the family Cheloniidae, and *Rhinochelys*, which is in the family Protostegidae (Hiryama, 1994).

The humeral characters suggest a relationship with *Toxochelys* and other turtles included in the Toxochelyidae, and now in the Cheloniidae, and with *Rhinochelys*, which is in the family Protostegidae (Hiryama, 1994). The plastron appears similar to *Syllomus* and *Natator*, which have been placed in the family Cheloniidae, and unlike the characteristic protostegid plastron (Hiryama, 1994). These features suggest that the Big Bend marine turtle should be placed in the family Cheloniidae. The combination of characters found in this specimen is not seen in any other known Cretaceous marine turtle. Therefore, TMM 43072-1 likely represents a new genus and species.

Superfamily TRIONYCHOIDEA Gray 1873

Family ADOCIDAE Cope 1870

Discussion

Specimens from two related genera, *Adocus* and *Basilemys*, are present in the Big Bend collection. The relationship between these two genera has been controversial (Wieland, 1904; Hay, 1908; Gilmore, 1919; Hutchison and Bramble, 1981; Gaffney and Meylan, 1988; Meylan and Gaffney, 1989). All workers consider the two genera related, because among other things, they both share a unique neural formula (6>4<6>6>6>6). But while their relationship to each other is accepted, their relationship to other turtles at the family level has been debated. Most workers place them in the family Dermatemydidae (Hay, 1908; Gilmore, 1919; Hutchison and Bramble, 1989). Gaffney and Meylan (1989) revised the taxonomy of *Adocus* and *Basilemys* in a phylogenetic analysis of the superfamily Trionychoidea. In the revision, they removed *Adocus* and *Basilemys* from the family Dermatemydidae and revived the family Adocidae (first proposed by Cope, 1870). The family Adocidae is placed within the superfamily Trionychoidea, primarily on the basis of cranial and shell morphology. An evaluation of this revision is beyond the scope of this study. However, in order to be consistent with the taxonomic framework established for the Baenidae, I will use the phylogenetic hypothesis developed by Gaffney and Meylan (1988).

Genus *Adocus* Cope 1868

Adocus sp.

Referred specimens: TMM 42534-5, TMM 42537-3, TMM 41838-14, TMM 43476-1.

Localities: TMM 42534-5 is from the southwest side of Rattlesnake Mountain; TMM 42537-3 is from northwest of Grapevine Hills; TMM 41838-14 is from Sierra Aguja; TMM 43476-1 is from Paint Gap Hills.

Stratigraphic Distribution: lower part of the upper shale member, Cretaceous Aguja Formation.

Description

All of these specimens are single, small, isolated fragments. Two fragments are concave in shape, and one, TMM 4257-3 exhibits a sutural margin (Figure 3.30). Both of these are fragments of costals, and TMM 4257-3 is probably a second costal. The other fragment, TMM 43476-1 is too small to determine its position on the shell. No costal tubercles or costiform processes are present. No sulci or sutures are present. The external surface of all specimens exhibit minute tubercles that are densely patterned. The intervening pits have a subrectangular, sub-oval shape, and are aligned in linear rows. These fragments all have an ornamentation pattern characteristic for *Adocus* (Hay, 1908; Gilmore, 1919; Meylan and Gaffney, 1989). No other characters are present that would allow a species-level identification.

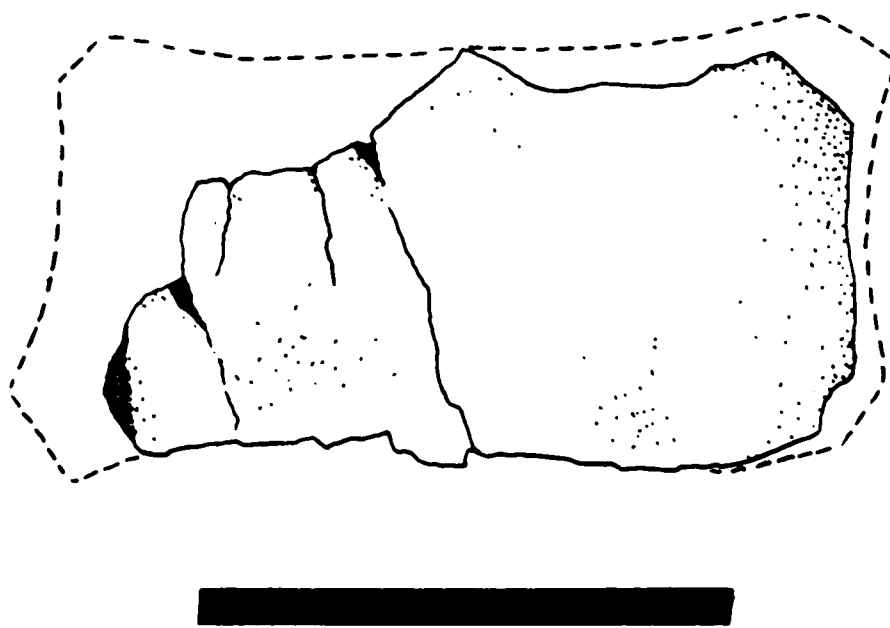
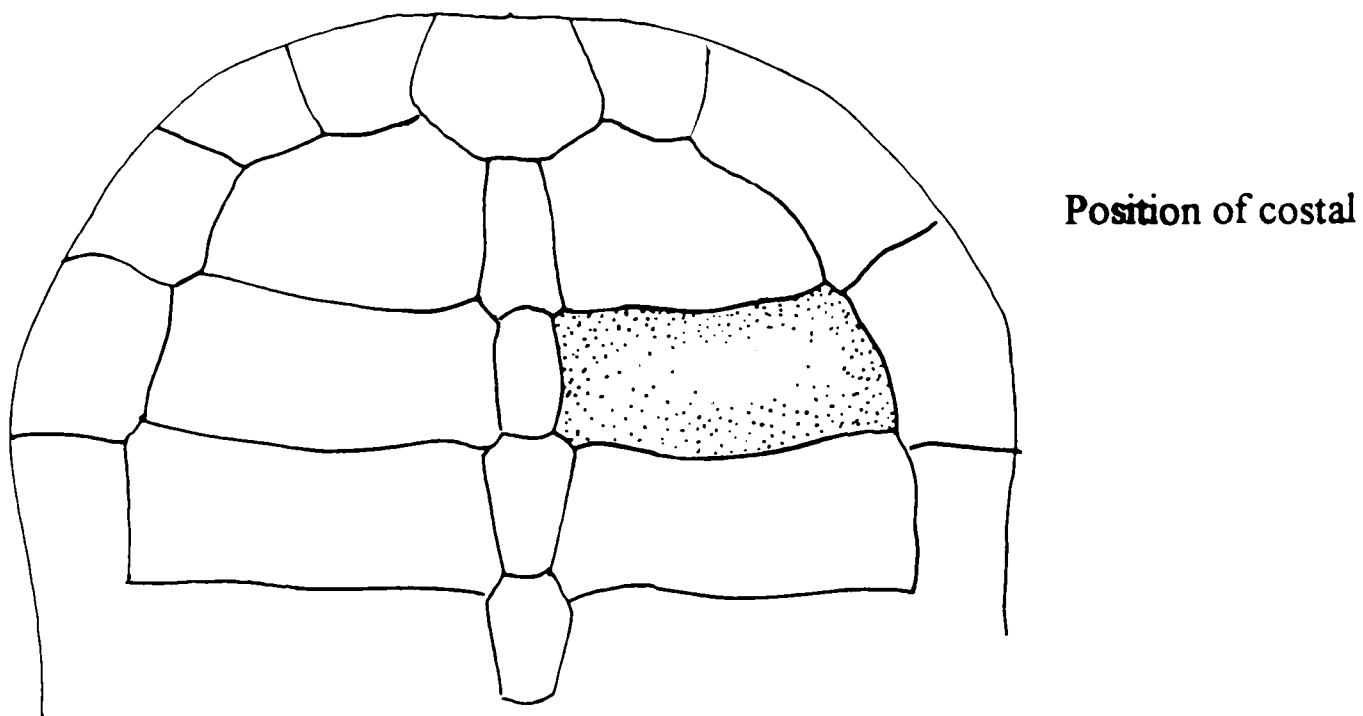


Figure 3.30. *Adocus* sp., TMM 4257-3, right second costal. Bar scale is 5 cm.

Genus *Basilemys* Hay 1902

Basilemys sp.

Referred specimens: TMM 41821-1, TMM 42876-2, TMM 42335-5.

Localities: TMM 41821-1 is from Dagger Flats; TMM 42876-2 is from Dawson Creek; TMM 42335-5 is from Dawson Creek.

Stratigraphic Distribution: upper shale member of the Aguja Formation (Cretaceous); Javelina Formation (Cretaceous).

Description

TMM 41821-1 consists of several fragments, some clearly from the carapace, others unidentifiable, and a partial limb bone. The specimen is heavily coated with calcite concretion. Two fragments are identifiable as coming from the margins of the carapace. They are very thick and roll inward, where they taper to an acute edge. All of the fragments are very thick. Only one sulcus is visible on one fragment, and it is not identifiable. No sutures are visible. The surface of the fragments have distinctive rows of pits, which are separated from one another by ridges that taper to an acute edge. The acute edges form triangular tuberosities where three ridges meet. This ornamentation is diagnostic of *Basilemys*. The partial limb bone appears to be the proximal end of the tibia, and two pieces of the shaft. The medial and lateral condyles, as well as the tibial tuberosity are present. Part of what is either the medial

or the lateral condyle is fractured. There is a foramen in the proximal end of the tibial tuberosity.

TMM 42876-2 consists of three fragments that are probably from the same specimen, and one additional fragment. One of the fragments is from the margin of the carapace. It is thick, slightly rolled, and tapers to an acute edge. The other fragments are much thinner. No sulci or sutures are visible. The surfaces of three of the fragments have the diagnostic sculpturing of *Basilemys*. The fourth fragment, has a somewhat similar sculpturing, but on a much smaller, and more subtle scale.

TMM 42335-5 consists of four fragments of the same specimen. The fragments are probably from the carapace. One of the fragments is from the margin and tapers to an acute edge, and appears to come from either the anterior or posterior margin. All of the fragments are thick. No sulci or sutures are visible.

Discussion

These specimens all possess the distinctive sculpturing and thick shell generally attributed to the genus *Basilemys* (Hay, 1908; Langston, 1956; Brinkman and Nicholls, 1993). Four species have been recognized for this genus, *Basilemys variolosa*, *B. sinuosa*, *B. nobilis*, and *B. praeclara* (Langston, 1956). None of the specimens have the diagnostic characters necessary to assign them to any species. There are no identifiable sulci or sutures, and the most complete specimen is largely covered with calcite concretion. All of this makes it difficult to identify these specimens beyond the genus level; therefore they are identified herein as *Basilemys sp.*

Family TRIONYCHIDAE Fitzinger 1826

Subfamily TRIONYCHINAE Fitzinger 1826

?*Aspideretes* spp.

?*Helopanoplia* sp.

Referred specimens: TMM 41400-5, TMM 42335-8, TMM 42534-2, TMM 42534-8, TMM 422880-6, ST 7-16b, TMM 42539-5, TMM 42874-1, TMM 43057-324, TMM 43380-5, TMM 43386-1; LSUMG V-1232.

Localities: TMM 41400-5 and TMM 42335-8 are from Dawson Creek; TMM 42534-2 and TMM 42534-8 are from Rattlesnake Mountain; TMM 42539-5 and TMM 42874-1 are from Sierra Aguja; TMM 43057-324 is from Terlingua Microsite; TMM 422880-6 is from the west fork of Alamo Creek; TMM 43379-1 is from Grapevine hills; TMM 43380-5 is from Grapevine Hills; TMM 43386-1 is from Pterosaur Ridge; and LSUMG V-1232 is from the "Gringo" locality..

Stratigraphic Distribution: Upper shale member, Aguja Formation; lowermost Javelina Formation; uppermost Javelina Formation; Black Peaks Formation.

Description

TMM 43380-5 is a partial carapace (Figure 3.31). It is fairly large, measuring approximately 34 cm from the margin of the nuchal to the broken edge of the fifth costal. It is sub-oval in shape, with a wide anterior end tapering to the posterior. The

right lateral half of the carapace is nearly intact, with a complete right half of the nuchal and partial left half of the nuchal, through a nearly complete right fifth costal. A fragmentary sixth costal, a preneural, and neurals one and two are also present, as well as parts of ribs one through five. Neural/costal sutures for costals three through five are intact, but worn. Moderately well developed first costiform processes are present on the visceral side of the carapace. All sutures are unfused. A small, suprascapular fontanelle is present. Ornamentation on the dorsal surface is very worn in places, but appears to consist of small, sub-rounded pits separated by narrow, pointed ridges. The tapered edge of the ridges gives the illusion that the pits are unusually deep in places. Ornamentation does not extend to the margins, stopping instead about 2.0 to 2.5 cm from the lateral periphery, and 3.0 to 3.5 cm from the anterior margin of the nuchal..

TMM 42335-8 is the right half of a nuchal bone (Figure 3.32). It is large, 17.5 in maximum length, 7.5 cm in maximum width, and approximately 2 cm thick. If it were complete, the whole nuchal length would be at least four times the width when measured at its widest point. It is completely coated and partially replaced by gypsum. Both the dorsal and visceral surfaces are very weathered, and it is difficult to determine much about the surface ornamentation. It is apparent, however, that the dorsal surface had pits that were fairly large, and that they had coalesced in some places. The anterior edge of the nuchal bone is slightly curved in the center of the bone, but is primarily straight, and does not exhibit a medial emargination.

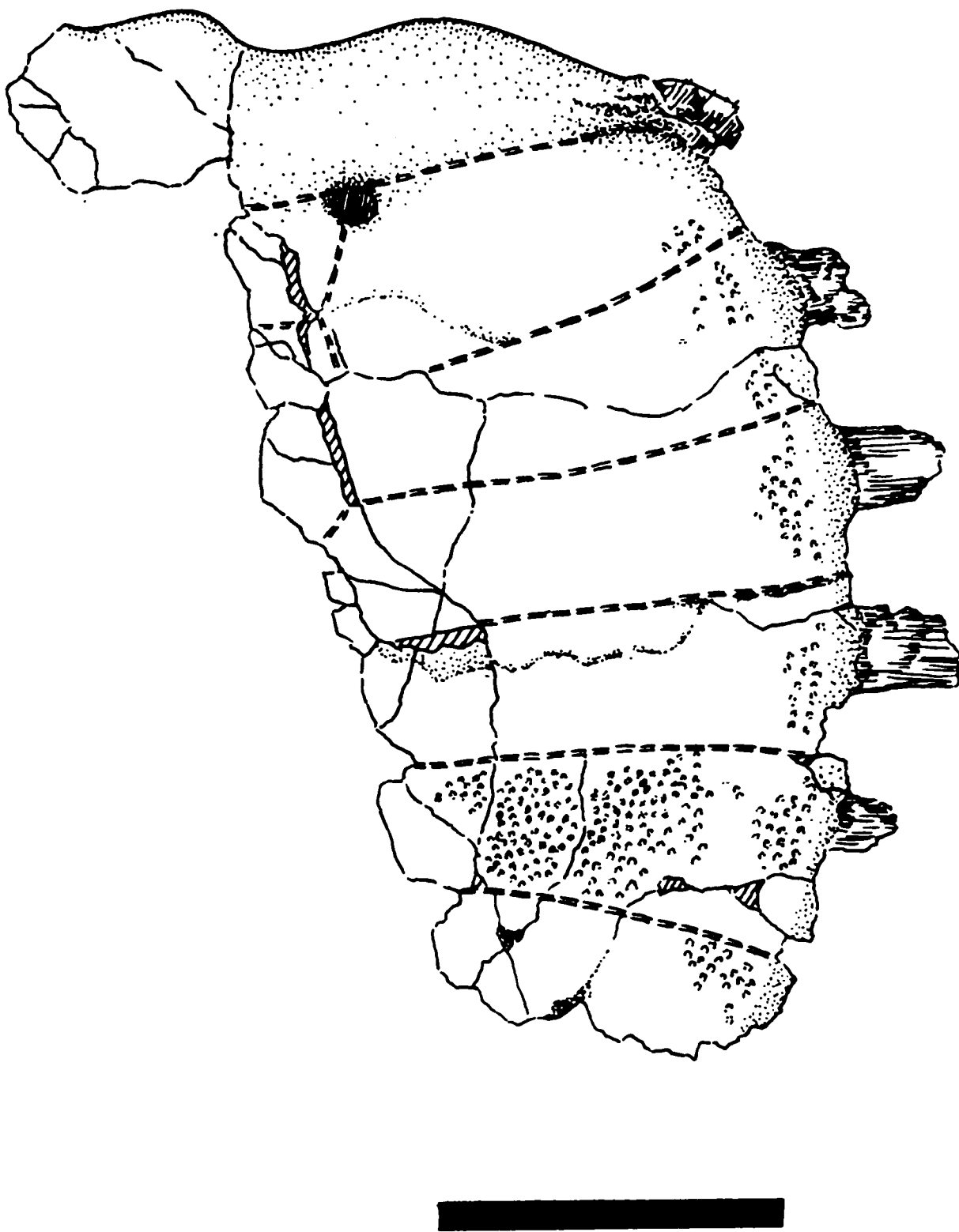


Figure 3.31. Trionychidae, TMM 43380-5, partial carapace. Bar scale is 10 cm.

Position of nuchal fragment

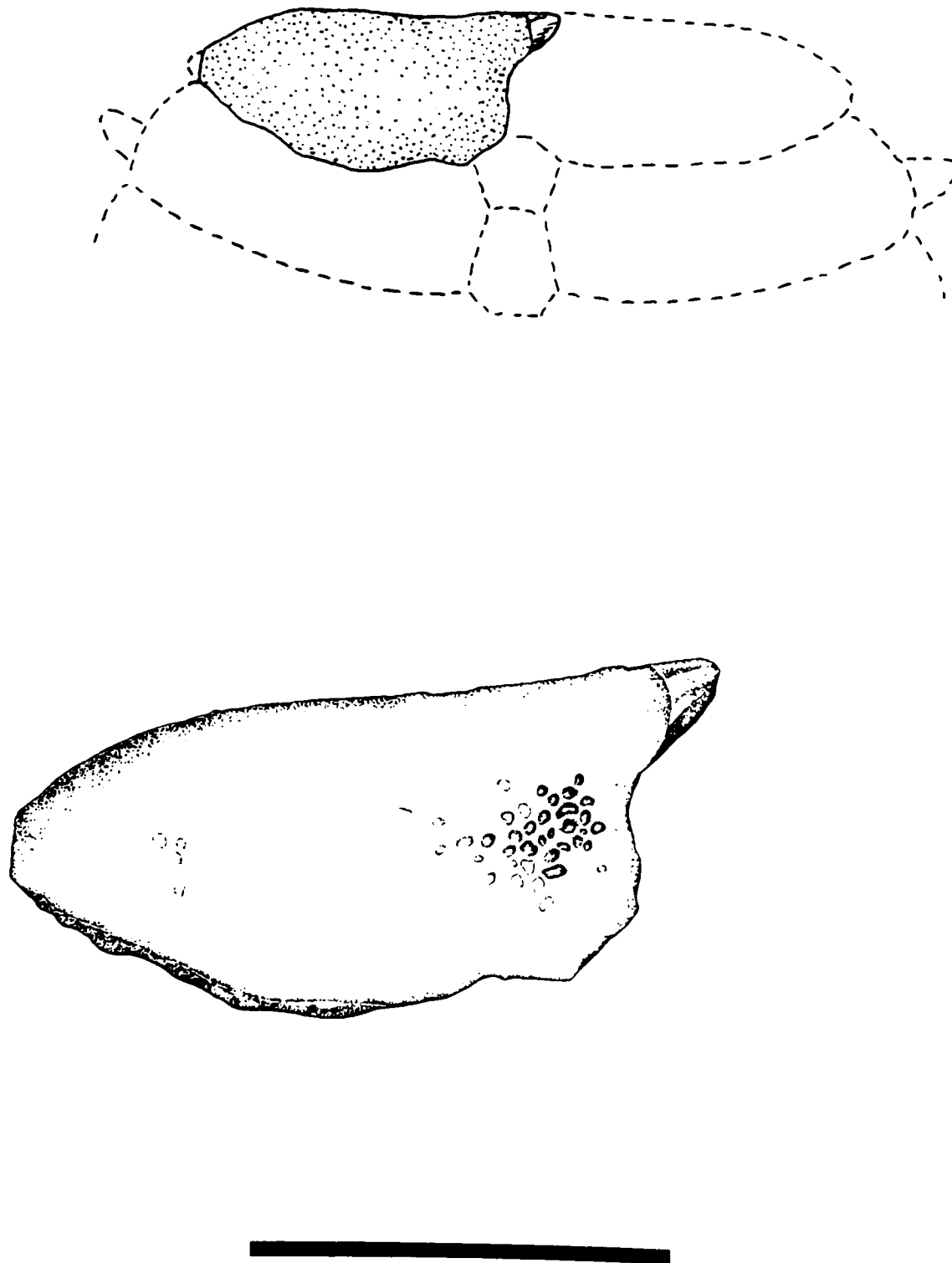


Figure 3.32. Trionychidae, TMM 42335-8, right half of a nuchal. Bar scale is 10 cm.

TMM 42534-2 is a well preserved right 5th costal (Figure 3.33). It is very large, measuring 23.5 cm in length from a point on the lateral margin midway from the anterior and posterior costal sutures to a point on the medial suture that is midway between the anterior and posterior costal sutures. Its width at the lateral margin is 14 cm, and at the midline the width is 4.5 cm from the anterior costal suture to the posterior costal suture. It is approximately 1 cm in average thickness. The costal has a pronounced curve at the 6th costal suture, and a slight curve at the 4th costal suture.

Ornamentation consists of very large round to sub-rounded, irregular pits, some of which are fully coalesced into linear furrows and ridges that extend the width of the costal. The pits extend from the medial suture to approximately 3.5 cm from the peripheral edge. The ornamentation appears worn, but does not exhibit extensive signs of weathering or post-mortem abrasion. Sutural edges are intact. The visceral surface exhibits the proximal end of a costiform process.

LSUMG V-1232 is a fragment from a costal. Ornamentation consists of tiny, reticulated, disconnected pin-sized ridges and tubercles. There are no pits.

TMM 43379-1 is an isolated fragment from a costal. Ornamentation consists of medium sized sub-rounded pits, narrowly spaced.

TMM 42534-8 is a broken, right hypoplastron (Figure 3.34). It is small, and measures 0.7 cm in width. The anterior and posterior processes appear to be equal in size. Ornamentation consists of tiny, reticulated, disconnected pin-sized ridges and tubercles. There are no pits.

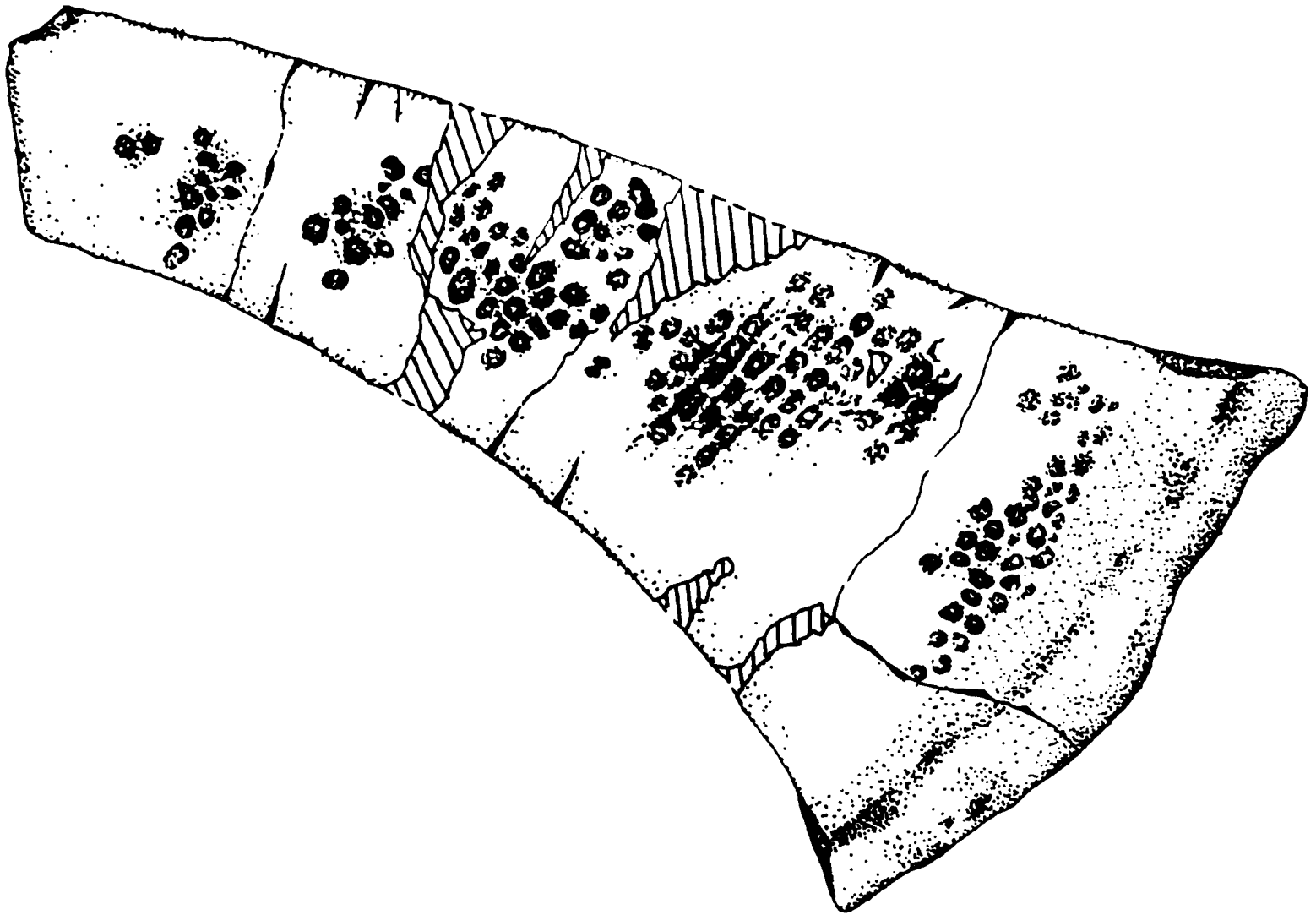


Figure 3.33. Trionychidae, TMM 43534-2, right fifth costal. Bar scale is 10 cm.

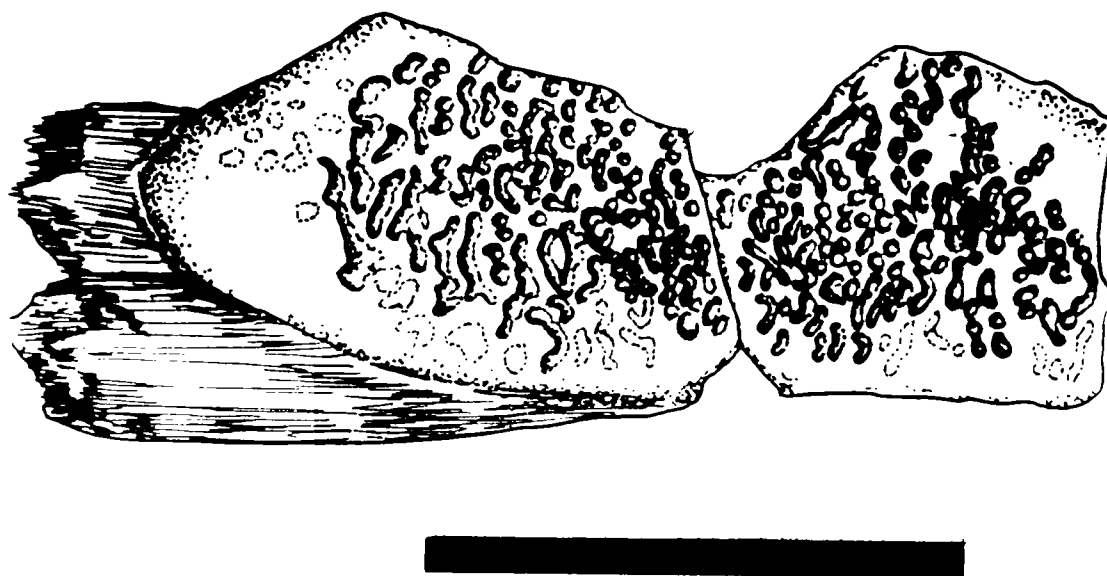


Figure 3.34. Trionychidae, TMM 43534-8, right hypoplastron. Bar scale is 3 cm.

TMM 422880-6 consists of one nearly complete, well preserved right hyoplastron, one small fragment from the lateral posterior portion of a hypoplastron, one peripheral edge of the fourth or fifth costal, and a small, unidentifiable piece of a plastral element (Figure 3.35), as well as numerous other, largely unidentifiable fragments from different individuals. The hyoplastron measures 25 cm from the medial edge to a point on the lateral edge just posterior to two lateral anterior processes. It measures 8.6 cm in maximum width, and 6 cm in minimum width. It is approximately 1 cm in thickness, excluding the thickened portion of the axillary bridge. The hyo-hypoplastral suture is intact, unfused, and exhibits no evidence of post-mortem abrasion. The plastral callosity does not extend all the way to the lateral margin of the hyoplastron. The epiplastral anterior process which would project into the median fontanelle is broken, but it was fairly substantial, straight, and would be approximately 4.5 to 5.0 cm in width. The lateral anterior processes, while wide, are thin, measuring only 0.5 to 0.7 cm in thickness. The axillary notch is moderately emarginate at a point approximately one-fourth of the total distance from the lateral margin to the medial margin. Sculpturing on the callosity consists of very reticulated pits, some of which are coalesced, and separated by narrow ridges. Sculpturing does not extend all the way to the edge of the callosity, but stops about 0.3 cm inside the edge. The right lateral, posterior fragment of hypoplastron is well preserved, with little evidence of post-mortem abrasion. Both lateral posterior processes are mostly intact. The sculpturing on the callosity consists of very reticulated sub-rounded to vermiform pits separated by thin ridges. Sculpturing does not extend to the margins of the callosity,

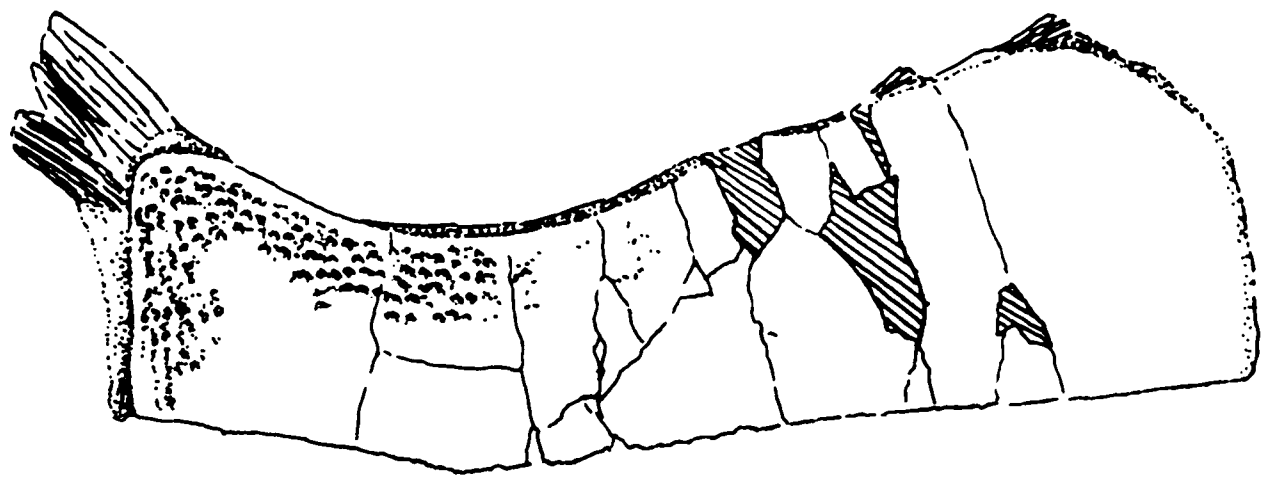


Figure 3.35. Trionychidae, TMM 422880-6, right hyoplastron. Bar scale is 10 cm.

but grades into a more or less smooth surface approximately 1.5 to 2 cm from the edge.

The well preserved costal fragment consists of the distal end of the fifth costal. The costal would have been large; the peripheral edge measures 8.5 cm in width. Both costal sutures are intact. They and the broken edge show no signs of post-mortem abrasion. Ornamentation consists of large reticulated, sub-rounded pits that do not extend all the way to the margin, instead stopping approximately 2 cm from the edge.

TMM 42539-5 consists of the distal portion of the left hypoplastron, a partial left xiphiplastral element, the distal end of the (?)right humerus, and an element that appears to be a portion of the pelvis that contained the left (?) acetabulum (Figure 3.36). The distal end of the hypoplastron is preserved, and exhibits one intact lateral process and one broken one. The digital processes are very robust, with the anterior one slightly thinner than the posterior process. The posterior and left lateral margins are intact, but the hypoplastron is broken off about midway through the inguinal notch. The broken edges do not appear to correspond to any sutures. The margin of the hypoplastron tapers to a thin edge near the inguinal notch. The anterior end of the xiphiplastron is intact and robust, measuring 10 cm in maximum length (from the left margin to the midline suture), and 1.5 cm in average thickness. The callosity of the hypoplastron and xiphiplastron is approximately 0.5 cm thick on average, and appears to run from edge to edge on all sides of both elements. The callosity would contact the right xiphiplastral element at the midline. Sculpturing of the plastral callosities consists of pits of unequal sizes separated by ridges that taper to a sharp edge.

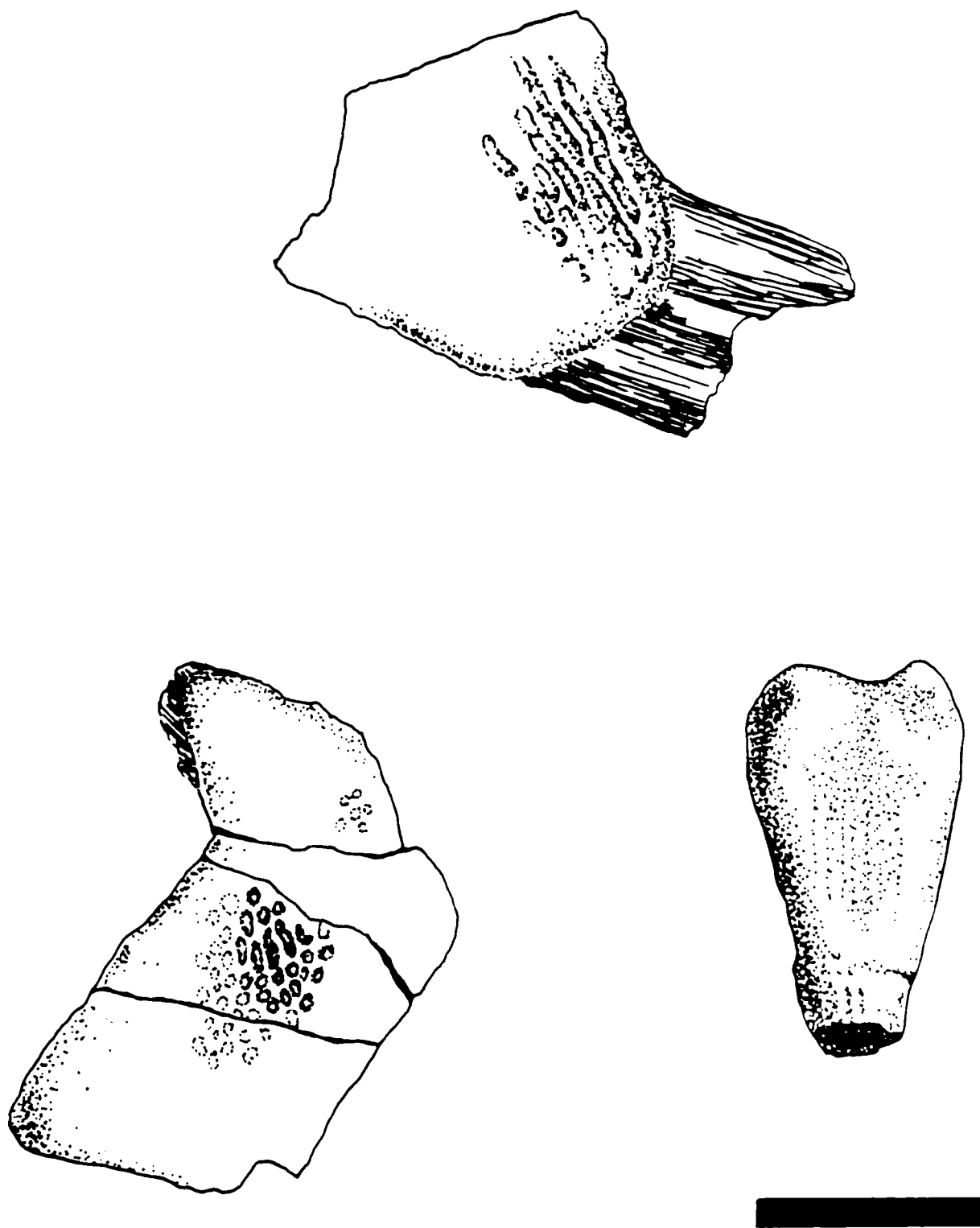


Figure 3.36. Trionychidae, TMM 42539-5, left hypoplastron, left xiphiplastron, and the distal end of a humerus. Bar scale is 5 cm.

The humerus is large, with the distal end measuring nearly 4.5 cm in width, and the shaft measuring about 1.5 cm in diameter. The humerus is broken at a point about 8 cm above the tip of the lateral condyle. The humerus is slightly curved toward the dorsal surface.

The broken portion of the pelvis containing the acetabulum is also large, measuring about 5 cm at maximum length and 4 cm at maximum width. This specimen is badly weathered and the surface is covered with a calcareous concretion. The broken surfaces of the ischium, ilium, and pubis are badly weathered and abraded, but the acetabulum is largely intact.

TMM 43057-324 is a broken but otherwise well preserved left lateral portion of a hypoplastron (Figure 3.37). It is broken toward the medial edge of the inguinal notch and near the hyo- hypoplastral suture. The inguinal notch is robust, measuring 2 cm in width on average. The lateral posterior and anterior processes are unequal in size, with the anterior lateral process more slender than the posterior process. Ornamentation of the plastral callosity consists of large coalesced pits.

TMM 42874-1 is a well preserved, partially broken right xiphiplastron (Figure 3.38). It is roughly triangular in shape, and large, measuring 11 cm from the tip of the anterior projection to the tip of the posterior medial projection. Projections are xiphiplastral callosity was probably a moderately robust portion of the plastron. The xiphiplastron is thin relative to its overall size, measuring approximately 1 cm in average thickness, including the plastral callosity. The callosity is approximately 0.4



Figure 3.37. TMM 43057-324, left hypoplastron. Bar scale is 10 cm.

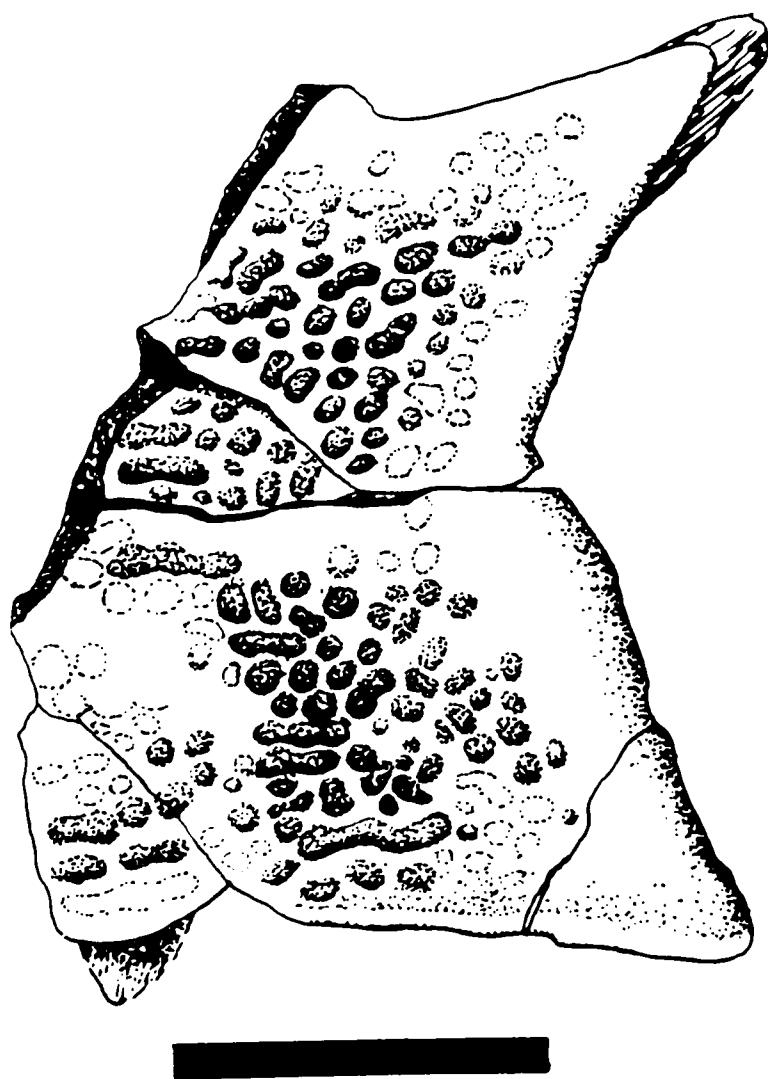


Figure 3.38. Trionychidae, TMM 42874-1, right xiphiplastron. Bar scale is 3 cm.

slender and short relative to the overall size of the callosity, indicating that the cm thick at the lateral anterior edge, and tapers to 0.2 cm at the medial edge. The callosity extends to the medial edge, but does not give any indication that it would meet the left xiphiplastral callosity across the midline. Sculpturing of the callosity consists of sub-rounded pits separated by thick ridges, which give the pits a shallow appearance. The pits are largely of similar size, but become slightly smaller toward the edges, or disappear altogether near the edge of the anterior medial projection.

TMM 41400-5 is a mostly intact, medium-sized left humerus that measures 10 cm in length (Figure 3.39). The head, proximal articulation, and internal trochanter are broken, but they appear slender and not robust. The internal fossa is shallow. The fourth trochanter is abraded, but visible. The distal end is broken just above the lateral and medial condyle, as are the articulation surfaces for the ulna and radius.

Discussion

The phylogenetic relationships of the family Trionychidae are complex, primarily because useful taxonomic criteria are still being determined (Webb, 1990). Meylan (1987) has instituted a major revision of the family using cladistic analysis in recent years, and Gardner and Russell (1994) and Gardner, Russell and Brinkman (1995) have done a great deal of work on the identification and classification of the Cretaceous trionychids, but there is still much that is unresolved, especially regarding fossil species. It is not the purpose of this study to conduct a taxonomic revision of this family; the specimens from Big Bend are not sufficient for this task. The work of

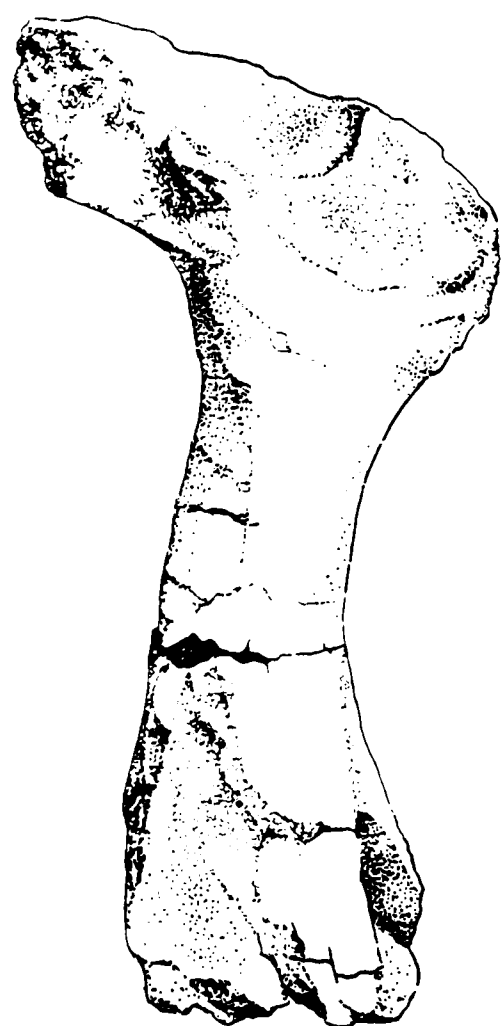
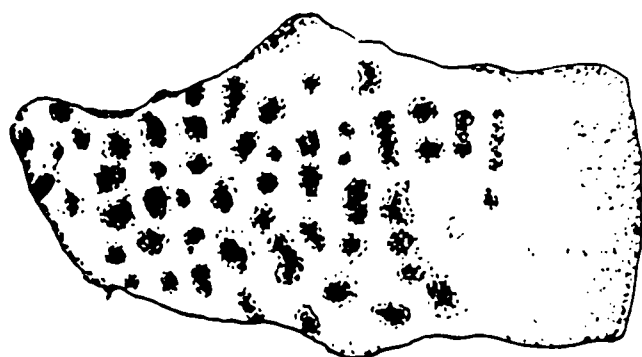


Figure 3.39. Trionychidae, TMM 41400-5, left humerus. Bar scale is 5 cm.

Gardner and Russell (1994) and Gardner et al. (1995) may ultimately prove useful in identifying the Big Bend material to a species level. Certainly there are fragments which are suggestive of *Aspideretoides foveatus*, *A. splendidus*, and *A. allani* (Gardner et al., 1995). Insufficient material exists at this time to make a diagnostic assignment concerning the specimens that resemble these species. In many instances there are noticeable differences in shell morphology in trionychids from the Aguja, Javelina, and Black Peaks Formations. While it is true that some ornamentation is related to its position on the shell, in many cases ornamentation on two separate fragments is so different as to be unlikely that the fragments came from the same species. This seems confirmed by the recent work of Gardner and Russell (1994) and Gardner et al. (1995). For the purpose of assessing the diversity of the fauna, it is useful to make a conservative estimate of the number of different species in each formation. For this reason, I will separate the trionychid fauna into forms below on the basis of ornamentation, shell thickness, and overall size. These are illustrated in Figures 3.40, 3.41, 3.42. Generic classifications are based on Hay (1908).

?*Aspideretes* sp. "A": Small with thin costal plates; ornamentation consists of very small, uniformly sized, uniformly rounded, uniformly and widely spaced pits. This ornamentation is similar to that described for *Aspideretes foveatus* by Gardner et al. (1995). Referred specimens: TMM 43473-2, Aguja Formation.

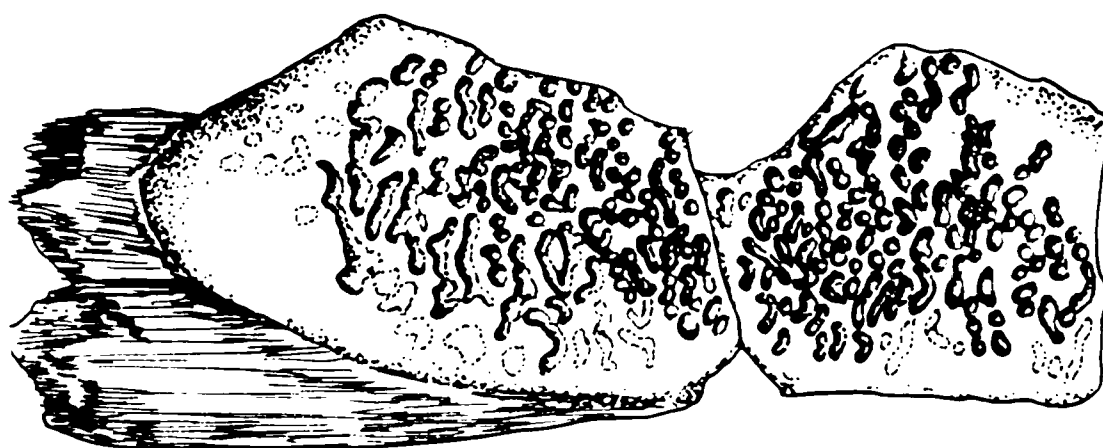
?*Aspideretes* sp. "B": Small with thin costal plates; ornamentation consists of medium sized, variably sized, rounded to sub-rounded, narrowly spaced pits. This



(1)



(2)



(3)



Figure 3.40. Representative specimens of (1) ?*Aspideretes* sp. "A", (2) ?*Aspideretes* "B", and (3) ?*Helopanopia*. Bar scales are 3 cm.

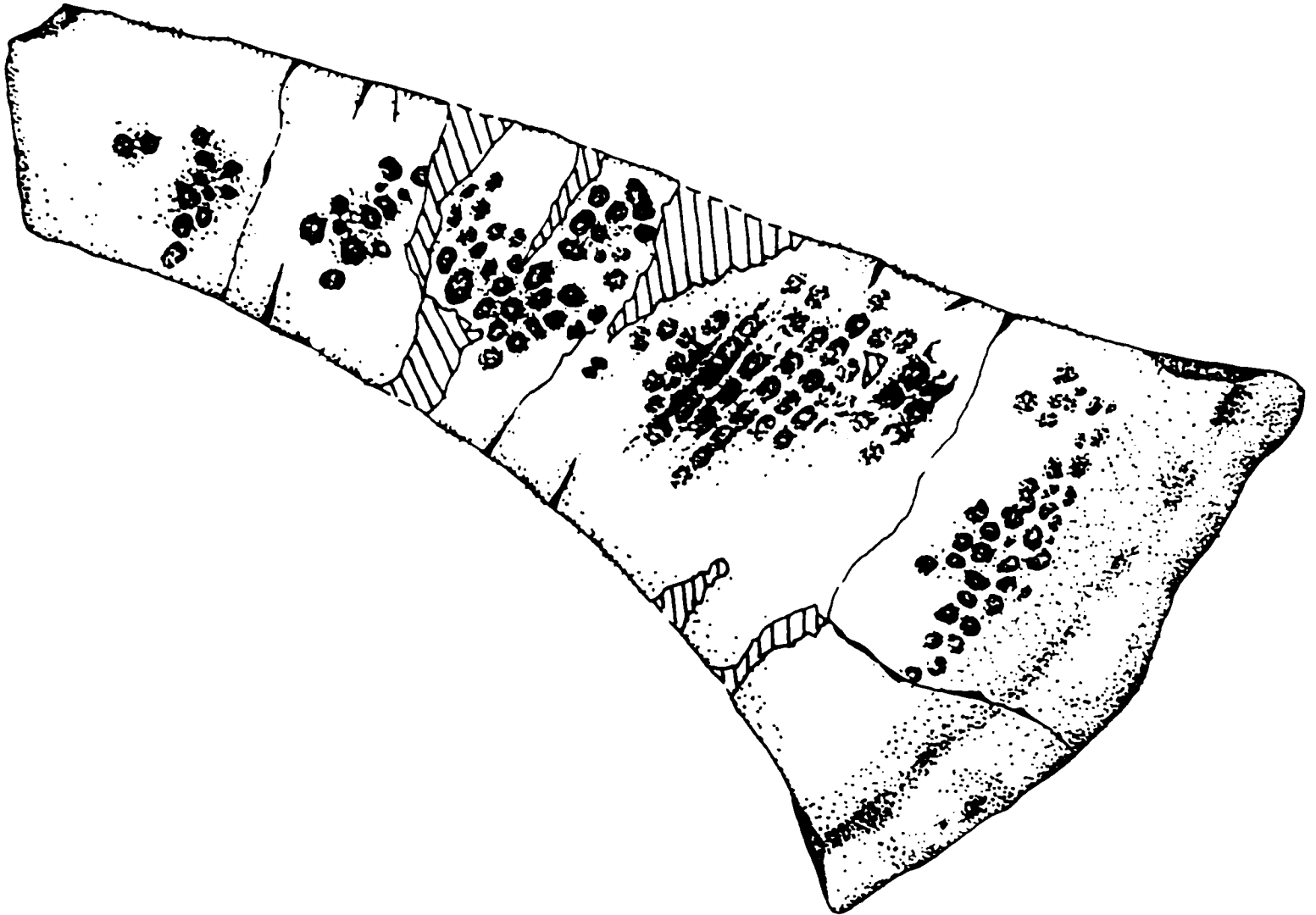


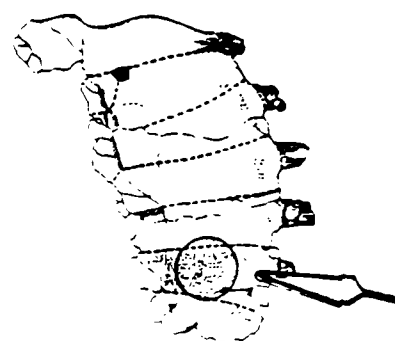
Figure 3.41. Representative of ?*Aspideretes* sp. "C". Bar scale is 10 cm.



(1)



(2)



area shown in Figure 2

Figure 3.42. Representatives of (1) ?*Aspideretes* sp. "D", and (2) ?*A.* sp. "E" (detail of carapace of TMM 43380-5, Figure 3.31). Bar scales are 3 cm.

ornamentation is similar to that described for *Aspideretes allani* (Gardner et al , 1995)

Referred specimens: TMM 42880-3, TMM 42534-6, TMM 43379-1.

?*Aspideretes* sp. "C": Large with thick costal plates and plastrons; ornamentation consists of large, variably sized, sub-rounded, variably spaced pits that are coalesced near the lateral margin. Referred specimen: TMM 42534-2. Aguja Formation.

?*Helopanopia* sp. : Small, thin hypoplastron; ornamentation consists of small, irregular, pin-head or smaller sized tubercles that sometimes coalesce to form a narrow ridge. The ornamentation is similar to that described by Hay (1908). Referred specimens: TMM 42534-8, LSUMG V-1232, Aguja Formation.

?*Aspideretes* sp. "D": Small with thin costal plates; ornamentation consists of small, uniformly sized, sub-rounded to rounded pits, spaced uniformly, at a distance that is approximately one-fourth the diameter of a pit. Referred specimen: TMM 43386-1, Javelina Formation.

?*Aspideretes* sp. "E": Large, thin carapace; ornamentation consists of large, variably sized, sub-rounded, variably spaced pits. Referred specimen: TMM 43380-5, Black Peaks Formation. This specimen strongly resembles the Paleocene species *Aspideretes puerensis* (Hay, 1908) with the sub-oval shape of the carapace (as seen in Figure 3.31). *Aspideretes puerensis* also has suprascapular fontanelles, but they are much more pronounced than the Big Bend specimen. In fact, the nuchal does not contact the first costal at all in *A. puerensis*. Other authors have noted, however, that in other specimens where a suprascapular fontanelle is present that there is significant

variation in this character among individuals (Gardner et al., 1995). Given the resemblance of the overall shape, the suprascapular fontanelles, and the equivalent stratigraphic position of *A. puerensis* and the Big Bend specimen (TMM 43380-5), it is tempting to assign the Big Bend specimen to *A. puerensis sensu* (Hay, 1908).

Family DERMATEMYDIDAE Gray 1870

Genus *Hoplochelys* Hay 1905

Hoplochelys sp.

Referred specimens: TMM 41400-19, TMM 41400-24, TMM 42957-2, LSUMG V-979, LSUMG V-1004, LSUMG V-1476, LSUMG V-1504, LSUMG 5004, LSUMG V-5005, NGH 4, NGH 1-3, TMM 43476-2, ST no number.

Localities: TMM 41400 19, 24 are from Dawson Creek; TMM 42957-2 is from the Dogie area; LSUMG V-979 is from the “Tom’s Top” locality; LSUMG V-1004 is from the “Joe’s Bonebed” locality; LSUMG V-1476 is from the “Tom’s Top” locality; LSUMG V-1504 is from the “Snail’s Place” locality; LSUMG V-5004 is from the Dogie area; LSUMG V-5005 is from the “Tom’s Top”; NGH 4 and NGH 1-3 are from north Grapevine Hills; TMM 43476-2 is from the type section for the Black Peaks Formation, and ST no number is from north Grapevine Hills.

Stratigraphic Distribution: lower part of the Paleocene Black Peaks Formation

Description

These specimens are all collections of fragments. There are several neurals, peripherals, and costals. All exhibit a characteristic fine punctate sculpturing that is visible with a handlens. The neurals are typically marked by deep sagittal sulci or deep transverse sulci which bisect dorsal carinae (Figure 3.43). Specimen collections with neurals include TMM 41400-19, LSUMG V-979, and LSUMG V-5005. There is one suprapygial bone in TMM 41400-24.

Costals also typically exhibit longitudinal carinae bisected by deep transverse sulci (Figure 3.44). Costals are found in the specimen collections of TMM 41400-19, 41400-24, LSUMG V-979, V-1004, LSUMG V-1476, and LSUMG V-5005.

Peripheral bones are thick, have either an upturned or non upturned edge, with edges that range from acute to rounded (Figure 3.45). Deep marginal sulci are often present. Peripheral fragments from TMM 41400-19 and TMM 41400-24 have a subtle wrinkling on the surface. Peripherals are found in the collections of TMM 41400-19, TMM 41400-24, TMM 42957-2, LSUMG V-979, and LSUMG V-1004.

Plastron fragments come from the hyo- and hypoplastron. They are thin compared to the carapace bones, and where present, the buttress is remarkably non-robust, given the thickness of some of the carapace fragments. Sutures and sulci are plainly visible. TMM41400-19 and LSUMG V-1476 contain fragments from the plastron.

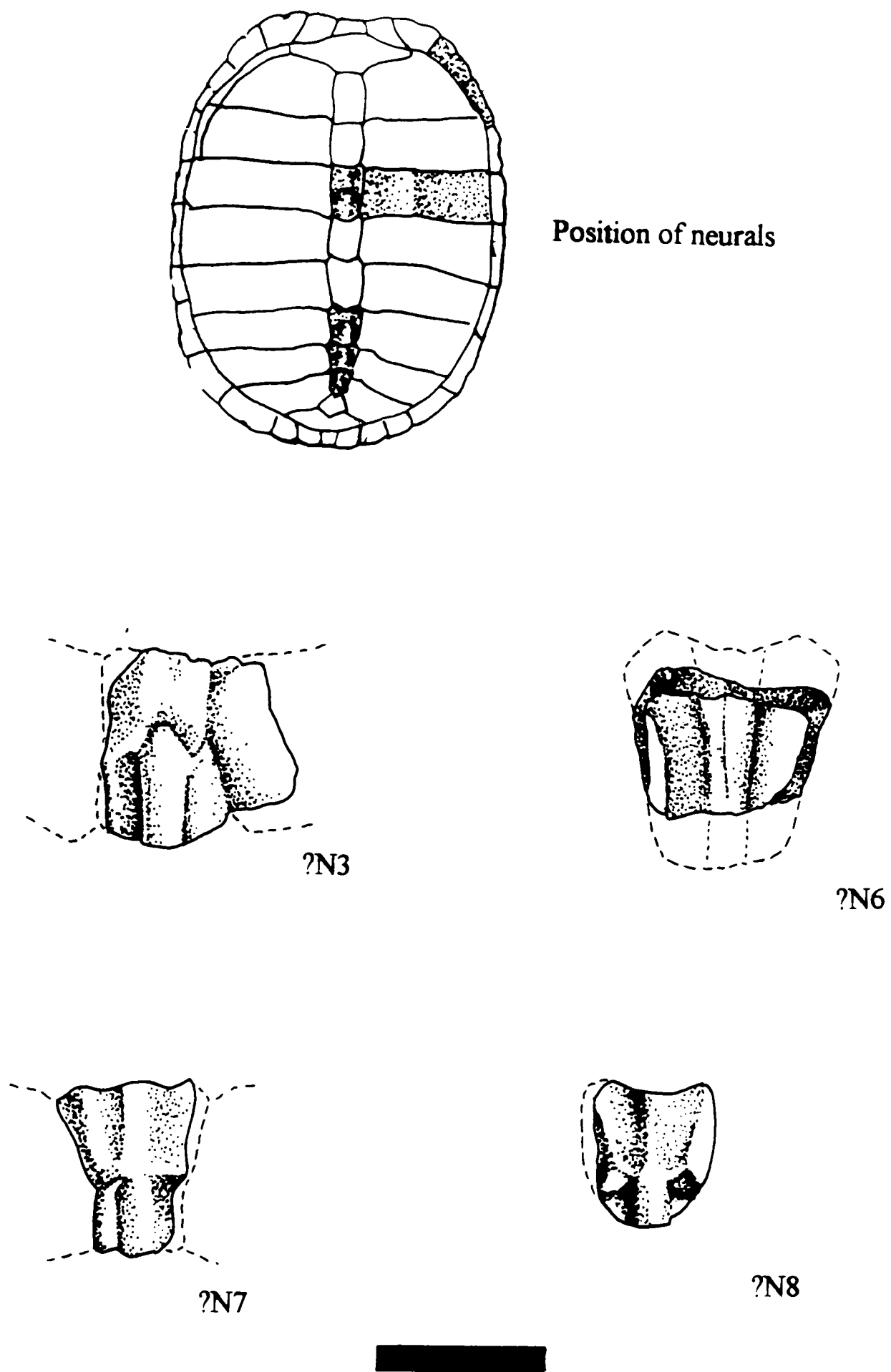
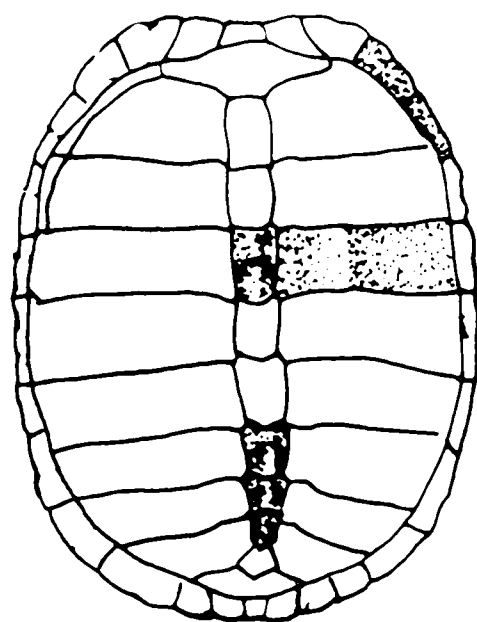
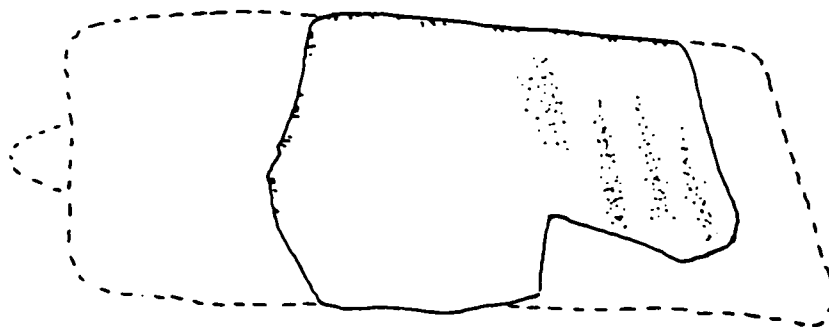


Figure 3.43. Representative neurals from *Hoplochelys* sp. specimen TMM 41400-19.
Bar scale is 3 cm.



Position of costal



?C3



Figure 3.44. Representative costal from *Hoplochelys* sp. specimen TMM 41400-19.
Bar scale is 3 cm.

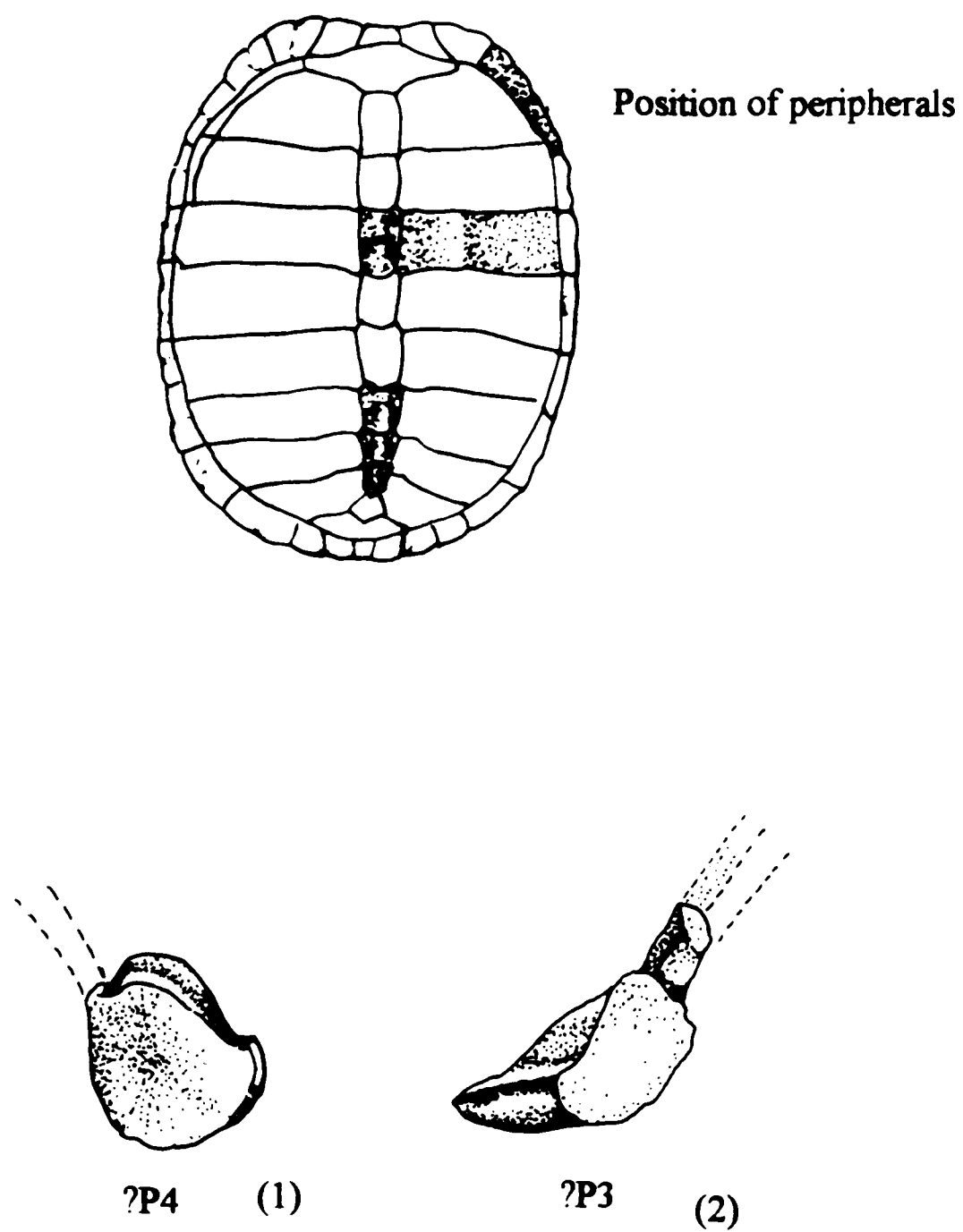


Figure 3.45. Representative peripherals from *Hoplochelys* sp. specimens (1) TMM 41400-19 and (2) LSUMG V-979. Peripherals are shown in side view. Bar scale is 3 cm.

Discussion

All of these fragmentary turtle specimens are referred to the genus *Hoplochelys*, primarily on the basis of the strongly developed dorsal carinae, the deep sulci, and the thick, rolled edges of some of the peripherals. These diagnostic characteristics match the descriptions of *Hoplochelys* found in Hay (1908) and Gilmore (1919). The distinctive punctate sculpturing is also described by Gilmore (1919), and is found on all the fragments described. Therefore, those fragments without the dorsal carina, deep sulci, and rolled edges are also assigned to this genus.

CHAPTER IV

STRATIGRAPHIC DISTRIBUTION OF TURTLES

Introduction

Fossil turtles are, in general, far more abundant in the marginal marine, brackish, and freshwater flood-plain deposits of the Aguja Formation than in other facies of the Aguja, or the fluvial flood-plain deposits of the overlying Javelina and Black Peaks Formations. A discussion of the turtles present in each formation is given below, and a listing of the turtle genera and where they occur in the stratigraphic sequence is provided (Figure 4.1). A more detailed breakdown of where each genus occurs within the Aguja Formation (Figure 4.2), and a table showing the stratigraphic distribution of each genus is also provided (Table 4.1). In some cases, as in *Bothremys*, it is easy to estimate the minimum number of individuals (MNI) because the specimens came from separate localities. But because most of the material studied is fragmentary, it is difficult to assess the MNI when many specimens are found at the same localities. Thus, the numbers shown in the figures represent, in some cases, only the occurrence of each genus at different localities, and only for the three collections studied. It is therefore probably a gross under-estimation of total number of individuals present. Additionally, the numerous fragments of trionychid shells were separated qualitatively into groups suspected of being single individuals. These fragments were used in the morphometrics study (Chapter 6).

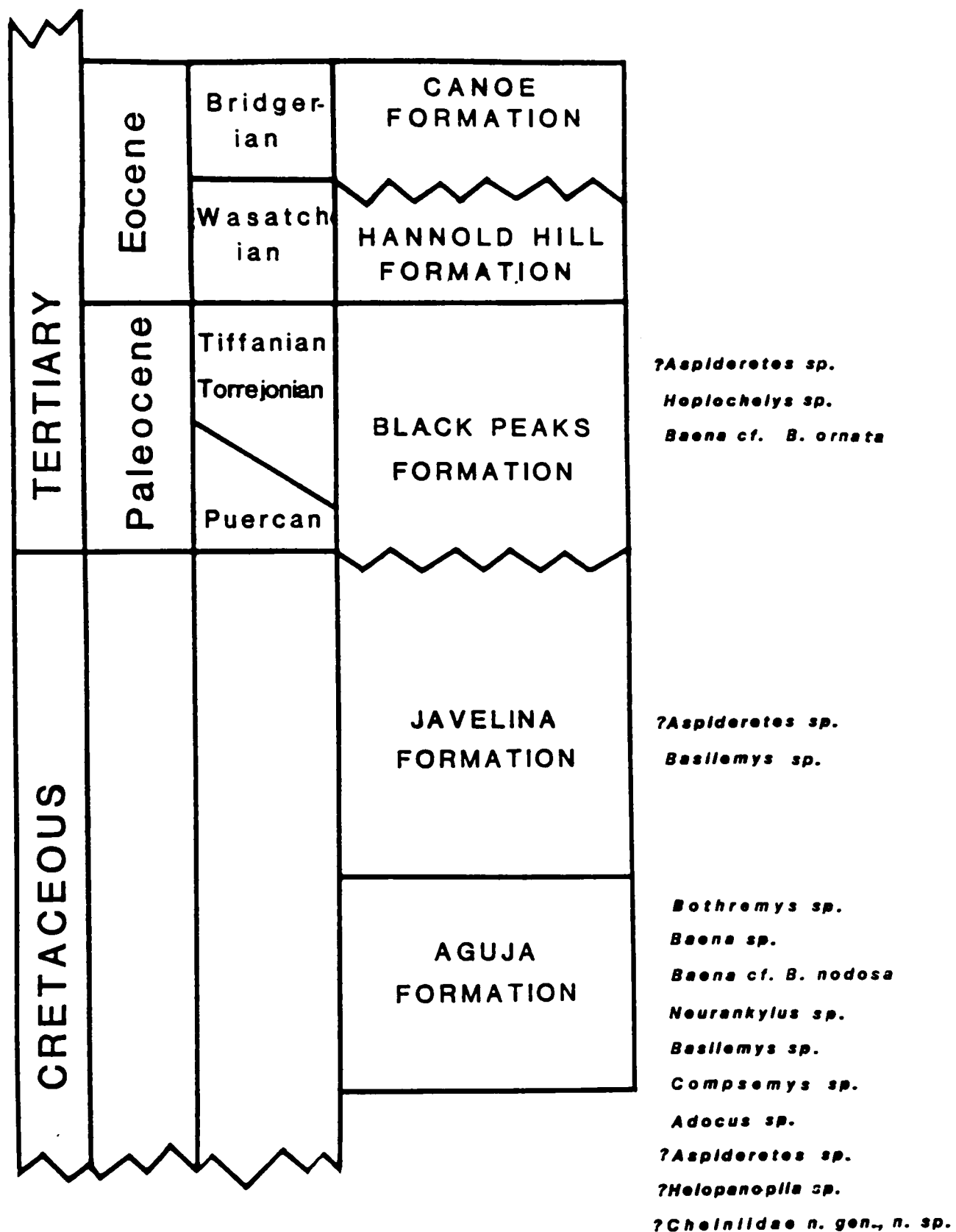


Figure 4.1. Stratigraphic distribution of turtles in the Aguja, Javelina, and Black Peaks Formations.

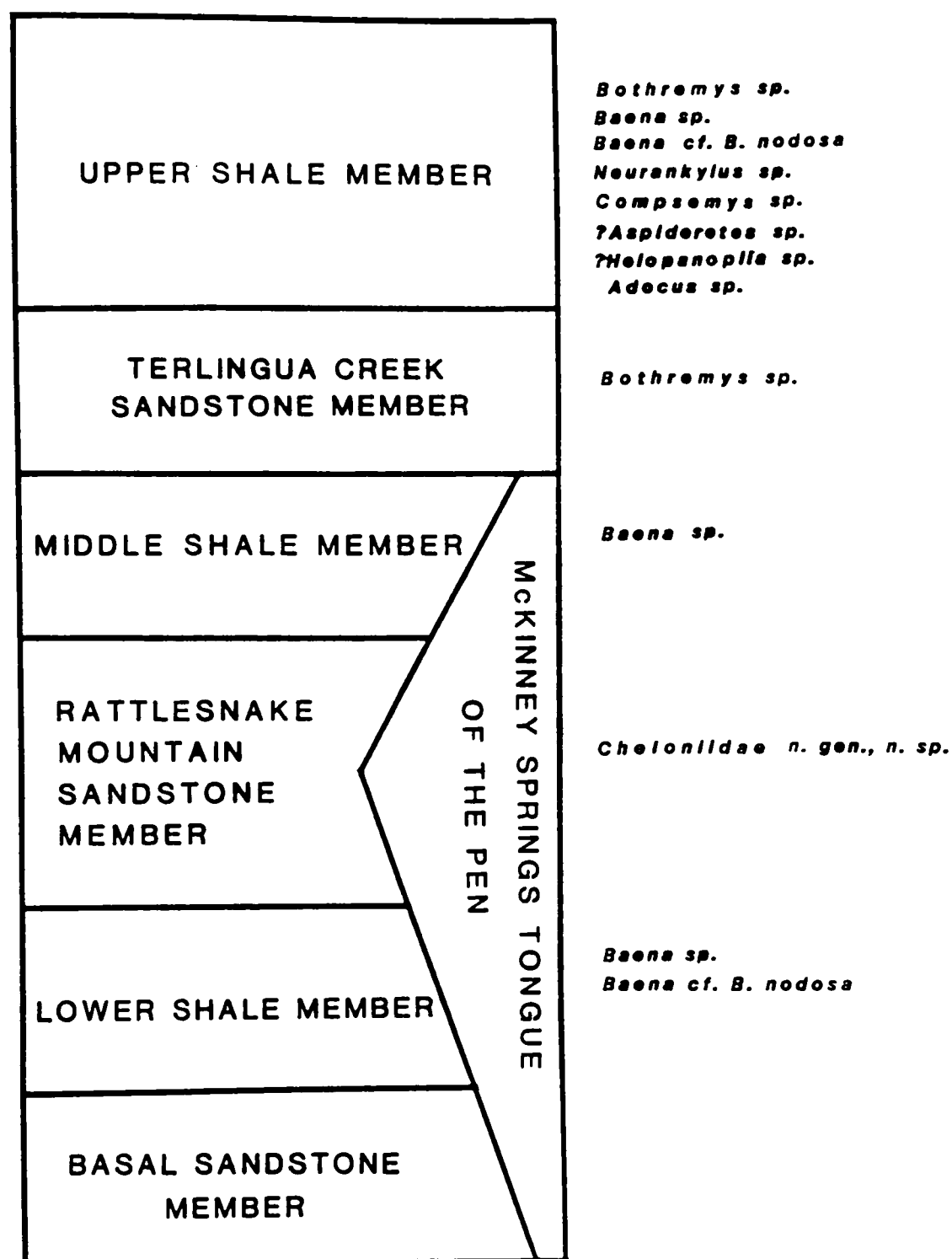


Figure 4.2. Stratigraphic distribution of turtles in the Aguja Formation.

Table 4.1. Turtles of the Aguja, Javelina and Black Peaks Formations. Numbers shown represent the Minimum Number of Individuals (MNI). Numbers are based on TMM specimens. * Includes 41 "individuals" from a single locality (TMM 42880).

| | Aguja | Javelina | B.P. |
|-----------------------------------|-------|----------|------|
| | MNI | MNI | MNI |
| <i>Bothremys</i> sp. | 5 | | |
| " <i>Baena</i> " sp. | 7 | | 6 |
| <i>Baena</i> cf. <i>B. ornata</i> | | | 1 |
| <i>Baena</i> cf. <i>B. nodosa</i> | 7 | | |
| <i>Neurankylus</i> sp. | 2 | | |
| <i>Compsemys</i> sp. | 1 | | 2 |
| <i>Basilemys</i> sp. | 2 | 1 | |
| <i>Adocus</i> sp. | 4 | | |
| ? <i>Helopanoplia</i> | 2 | | |
| ? <i>Aspideretes</i> sp. | 68* | 5 | 3 |
| <i>Hoplochelys</i> sp. | | | 14 |
| Cheloniidae, n.gen, n. sp. | 1 | | |

Distribution and Abundance of Turtle Fauna

Turtles are relatively common in the Aguja Formation, and within the Aguja they occur most commonly in the upper shale member. Of the two units in the upper shale member -- the lower, deltaic coastal plain deposits and the upper, fluvial channel and flood-plain deposits -- most of the turtle fossils are concentrated in the lower unit. Nearly all the turtles are thought to represent freshwater taxa. However, one marine turtle was collected from the Rattlesnake Mountain Sandstone Member (TMM 42880). In addition to this marine turtle there are several specimens of the pelomedusid *Bothremys* from brackish water and coastal deposits of the upper shale member. Pelomedusids have been found elsewhere in North America and the world in both brackish and marine environments. The Aguja specimens (*Bothremys*) seem to be equally distributed between the lower unit of the upper shale member, and the upper part of the underlying Terlingua Creek sandstone member.

Of the freshwater turtles, those belonging to the family Trionychidae are the most abundant, not only in the Aguja, but in all of the formations. These specimens are represented mostly by broken, and sometimes reworked carapace and plastron fragments. Most of the trionychids are probably referable to the genus *?Aspideretes*, or the poorly documented *?Helopanoplia*, but the fragmentary nature of the material makes it difficult to determine whether other genera of this family are present. Current taxonomic classification relies on skull and other shell characters besides sculpturing for diagnosis at the generic or specific level. Nevertheless, much of the shell sculpturing on the fragments collected from different localities in the Aguja are

distinctive enough to be easily grouped into patterns. It seems reasonable to surmise that at least *Aspideretes* is present, and that more than one species of this genus is present, or possibly more than one genus of Trionychidae are present in these strata. Differences in shell ornamentation patterns could be explained by other factors, of course, including the age of the individual, the original position of the fragment on the shell, or the amount of transport and weathering. The problems associated with trying to use shell sculpturing to determine the level of taxonomic diversity are discussed in the taxonomic and morphometric sections.

The second most abundant group of turtles from the Aguja Formation belongs to the family Baenidae. These are represented by "*Baena*" cf. *B. nodosa*, "*Baena*" sp., *Compsemys victa*, and *Neurankylus eximius* (Table 4.1). The baenids are also more commonly found as intact shells than any of the others. This is probably because the shells of baenids are fully coossified by the time they are adults, making the shells less likely to disarticulate after death, and more likely to be preserved intact. A nearly complete carapace and plastron of *B. nodosa* was collected from the lower shale member. A complete carapace and plastron of the baenid *Neurankylus* cf. *N. eximius* was found intact in the upper unit (fluvial flood-plain deposits) of the upper shale member of the Aguja. Another nearly complete turtle, also referable to *Neurankylus*, was found in the upper shale member. *Compsemys victa* is also present in the Aguja Formation but is very rare.

The family Adocidae is represented in the Aguja by the presence of a few isolated fragments of *Adocus* and marginal and costal fragments from *Basilemys*.

There are four fragments of *Adocus*, all from the upper shale member of the Aguja Formation. There are three specimens of *Basilemys*, two of which are from the upper shale member of the Aguja Formation.

There is a dearth of fossil turtle material from the Javelina Formation. Only *Aspideretes* and *Basilemys* appear to be present, and these are very rare. The few specimens that have been found are from fluvial flood-plain deposits.

The abundance of fossil turtle material increases in the overlying Black Peaks Formation. The most abundant form is *Hoplochelys* sp., followed by *Aspideretes* sp., and *Baena* cf. *B. ornata*.

Conclusion

The Aguja Formation contains the most diverse turtle fauna and the greatest number of specimens, probably as a result of having been deposited in a coastal plain environment. This served as an excellent preservational environment, as well as being an environment that probably hosted a large number of individuals (similar to the high level of diversity which is found in coastal environments today).

There is a notable drop in both diversity and number of individuals found in the Javelina Formation. This does not seem to be a function of taphonomic bias, because numerous other vertebrate taxa, such as *Quetzalcoatlus*, *Alamosaurus*, *Torosaurus*, and a variety of other dinosaurs, crocodilians and fish are present in moderate abundance (Lehman, 1988). Indeed, the paleoenvironment, that of inland fluvial flood-plain, would seem to be conducive to the preservation of vertebrate bones. The

paucity of turtle specimens could simply indicate that the environment was not one where turtles were living in the latest Cretaceous. The turtle fauna increases slightly in number and diversity in the Black Peaks Formation. This could be in part because the environment returned to one that was slightly more favored by turtles during Paleocene time.

CHAPTER V

ECOLOGICAL DIVERSITY OF THE BIG BEND TURTLE FAUNA

Introduction

The level of diversity of a fauna, however it is measured, is more easily ascertained in modern faunal assemblages than in vertebrate fossil assemblages. Vertebrate fossils, seldom present in the rock record in abundance, are often incompletely represented in the fossil record (and thus in museum collections) owing to numerous factors that include bias in collecting methods, bias in the preservational modes, and varied amount of exposure of the strata in question. Such factors typically result in an underestimate of the diversity of a fossil fauna relative to its living counterpart. All of these factors result in biasing the fossil turtle fauna collected from the Big Bend region compared to living faunas, thus making it difficult to determine the true level of diversity of the Big Bend turtle fauna.

A simple assessment of the relative abundance of the different taxa suggests which turtles were present in greater numbers. Knowing only the relative abundances of the taxa does not give us much useful information about the level of diversity. To determine that we must compare the Big Bend fauna both to typical modern faunas and to other turtle assemblages from equivalent strata.

Methods

To limit the impact of biasing factors on the interpretation of the diversity of the Big Bend turtle fauna, I have selected for study only the stratigraphic interval where both preservation and collection has been most thorough, the upper shale member of the Aguja Formation (see Chapter IV). Although the exposure area of the upper shale member is only a small fraction of that found in equivalent strata elsewhere in North America, it is the richest level for turtles in Big Bend. This richness is possibly a result of a good preservational environment, as well as being an environment that was originally one favored by turtles.

The upper shale member is also perhaps the most thoroughly collected stratigraphic horizon of all the intervals covered in this report. I am aware of most, if not all of the specimens collected thus far from this horizon. For the purposes of this study only specimens collected by the author and specimens in the Texas Memorial Museum collection were used. Surface collection was used by the author; all fragments of turtles found were collected, and none were culled. The TMM specimens were also surface collected, and the entire collection from this horizon was made available. Specimens from other collections involved other collection methods, such as screen washing, and were available only on a more limited basis. For these reasons they were not included as part of the diversity study.

Methods of Diversity Estimation

There are primarily three components to species diversity: species *evenness*, or how evenly the taxa are distributed in the ecosystem under study; species *richness*, or the number of species in a given area; and *heterogeneity*, which measures a combination of both richness and evenness (Magurran, 1988). This study utilized species richness to determine the level of diversity of the Big Bend fauna.

Most indices used in diversity measurement utilize the species as the operational unit. Because many of the fossil taxa are represented only by fragments in this study, and are not diagnostic at the species level, it is difficult to identify the number of species actually represented in a genus. Because of this, I compare only the genera in the different assemblages. Therefore, instead of using the term species when discussing the methods used for assessing diversity, I will hereafter use the term genus or genera.

Generic Richness

Measured generic richness is probably the simplest and most commonly used method of determining the level of diversity in an ecosystem. It is a good way to compare assemblages from different geographic localities, and as I use it in this study, potentially useful for comparing fossil assemblages to their modern counterparts.

Richness indices are based simply on the number of different taxa over a geographic area sampled (Magurran, 1988; Rosenzweig, 1995). However, the larger the area sampled, the greater the expected number of taxa represented. This has been

demonstrated to be true through empirical means, and is typically represented by a logarithmic species-area curve (Ricklefs, 1990; Rosenzweig, 1995). Therefore, samples from a large geographic area are more likely to contain a greater number of taxa. It is also true that as areal coverage increases, the expected number of taxa found in a sample approaches the number of taxa that exist in that environment. That is, new taxa will not be added when the actual limit on the number of taxa in that environment is reached. The ideal study would strike a balance between the two extremes of not sampling enough to account for all the possible taxa in an area, and a needless waste of time and resources continuing sampling when all the taxa are present and accounted for. The difficulty, obviously, lies in determining when all the taxa have probably been recorded. The sample size for the Aguja fauna is small (approximate minimum number of individuals <50 for the upper shale member), covers only one sample area (Big Bend, about 800 km² of outcrop), and contains few taxa (seven genera). The exposure area of the Big Bend strata is miniscule compared to equivalent strata elsewhere in North America (Lehman, 1996). While the approximate minimum number of individuals is known for the Big Bend fauna, that value cannot now be determined from the literature for other assemblages, modern or otherwise, in order to make meaningful comparisons in terms of minimum number of individuals.

The principle correction that must be made when comparing different modern or fossil assemblages using generic richness indices is that the sampling in each assemblage needs to be comparable in order to be meaningful (Magurran, 1988). When comparing different geographic areas, it is safest, of course, to use areas of

comparable size. All other things being equal (such as amount of time spent sampling, taphonomic biases, etc.), having comparable geographic areas somewhat ensures the probability of comparable sample size, and therefore, one sample area will not be “oversampled” or “undersampled” compared to the others. In the following sections, I have compared the Big Bend fossil turtle fauna to other faunas from both stratigraphically equivalent strata, and to a turtle fauna from an environmentally comparable modern river drainage.

Comparison of the Big Bend Fauna to a Stratigraphically Equivalent Fauna

Turtles from equivalent strata, such as the Fruitland Formation and Kirtland Shale of the San Juan Basin in northwestern New Mexico, come from much larger exposures of Upper Cretaceous strata (about 4000 km² of outcrop to about 800 km² for the Aguja, Lehman, 1996). Therefore, these strata are likely to preserve a richer fauna than that of the upper shale member of the Aguja Formation. In some cases, if the number of individuals collected from the equivalent strata is known, a technique called *rarefaction* can be used, which effectively normalizes sample sizes (Magurran, 1988). The rarefaction technique is not applicable to this study, however, because it depends on knowing the number of individuals in a sample, and this information is unavailable from the literature concerning equivalent strata of the Fruitland and Kirtland formations.

A direct comparison of the generic richness of the Big Bend fauna and the fauna from the Fruitland and Kirtland Shale formations is problematic. Nevertheless,

a genus for genus comparison with the Fruitland and Kirtland Shale fauna has been made (Table 5.1).

Comparison of the Aguja Fauna to a Modern Assemblage

Another useful measure of diversity is to compare the Aguja turtle fauna to a modern assemblage. When comparing the Big Bend fauna to modern assemblages it is again necessary to have comparable geographic areas, for the same reasons given above. In this instance, however, a rough geographic equivalence is obtained estimating the total geographic area represented by the upper shale member in both space and time, and using this to extrapolate the comparable area in a modern geographic area, i.e., to “fit” the modern assemblage to the fossil assemblage. This is achieved in the following manner.

The upper shale member does not represent only one habitat through the entire duration of its deposition, but instead represents a coastal/ marginal marine environment that eventually graded over time into an inland fluvial floodplain environment (Lehman, 1985). A comparable modern environment must also include the same diversity of habitats. The climate and geography of the Big Bend area was probably very much like the Central American peninsula (Mexico, Guatemala, Honduras, Nicaragua, Costa Rica, and Panama) during the time of Aguja deposition (Lehman, 1996), an area which includes the same coastal to inland fluvial habitats found in the Aguja. However, the information about specific drainage basins

Table 5.1, Genera of turtles represented in the modern Brazos River drainage of Texas, the Aguja fauna of Big Bend, and the Fruitland and Kirtland fauna of New Mexico.

| <u>Brazos River Drainage</u> | <u>Upper Shale Member</u> | <u>Fruitland and Kirtland Shale</u> |
|------------------------------|---------------------------|-------------------------------------|
| Caretta | ?Aspideretes | Aspideretes |
| Lepidochelys | ?Helopanopia | Baena |
| Dermochelys | Baena | Adocus |
| Trionyx | Adocus | Basilemys |
| Gopherus | Basilemys | Neurankylus |
| Geochelone | Neurankylus | Boremys |
| Trachemys | Compsemys | Plastomenus |
| Terrepene | Bothremys | Thescelus |
| Pseudemys | | |
| Malaclemmys | | |
| Graptemys | | |
| Deirochelys | | |
| Sternotherus | | |
| Kinosternon | | |
| Chelydra | | |

in Central America, and the turtles found in those basins is unavailable. The generic level of diversity for turtles in the entire Central American peninsula is easy to ascertain, however, from Ernst and Barbour (1989). There are 12 freshwater or terrestrial genera and 33 species found in Central America today. In Mexico alone there are 12 freshwater or terrestrial genera and 29 species (Ernst and Barbour, 1989). This suggests that the level of diversity for genera is relatively constant on the continental landmass. If we compare the level of turtle diversity in the state of Texas to that of Mexico, we find that there are 12 freshwater or terrestrial genera and 28 species found in Texas (Dixon, 1987), suggesting that the level of generic diversity for the two landmasses is equivalent in spite of the differences in size and climate.

Dixon (1987) provides a detailed listing of the turtles found in each county in Texas, and in this manner it is easy to determine what turtles are found along a particular drainage. Because the level of turtle diversity in Texas is comparable to that of Central America, which in turn has a comparable geography and climate to the Aguja, the Brazos River drainage in Texas, from its headwaters to the coast was chosen to represent a modern turtle habitat for comparison. But this presents a problem: the total area of the Brazos River drainage basin far exceeds that of the upper shale member, and to compare it directly to the upper shale member would incorrectly inflate the generic richness of the turtles in the Aguja fauna. That is, suppose the number of genera is the same for the Brazos River drainage and the upper shale member. Let us use an example of five taxa. Then there would be five genera per 25,280 ($632 \text{ (length)} \times 40 \text{ (width)}$) square miles for the Brazos River drainage, or

0.0002 genera per square mile, and five taxa per 1600 (40×40) square miles for the upper shale member, or 0.003 genera per square mile. This would erroneously lead us to believe that the upper shale member has a richer number of taxa per square mile.

An estimation of the position of the coastline at the beginning of deposition of the upper shale member and again at the end should provide a truer estimate of the geographic area that is being measured. That is, the length as measured from where the upper shale member is exposed today, to the approximate position of the coastline at the end of deposition of the upper shale member. This extends a length of 276 miles (Figure 5.1), should give an estimate of how far inland the outcrop area of the upper shale member was at the end of its deposition. The width is represented by the width of the exposure today, or approximately 40 miles. If the same length and width is applied to the Brazos River, measuring from the coastline to a point inland that equals the length applied to the upper shale member drainage, this yields a total area of 11,060 square miles for the area compared. It should be noted that the majority of the genera along the Brazos River drainage occur within the first two or three counties adjacent to the coast. However, to record all twelve, it is necessary to go 90 or more miles inland, a distance that is still less than half of the distance measured for the length of the Aguja drainage. This suggests that the distance measured for the Brazos River drainage is still over-inflated, and in order to compare it more accurately to the Aguja, it would be useful to know how far inland along the Aguja drainage it is necessary to go in order to have sampled all of the genera. This information is not available, therefore we will consider an area of 11,060 square miles for both drainages.

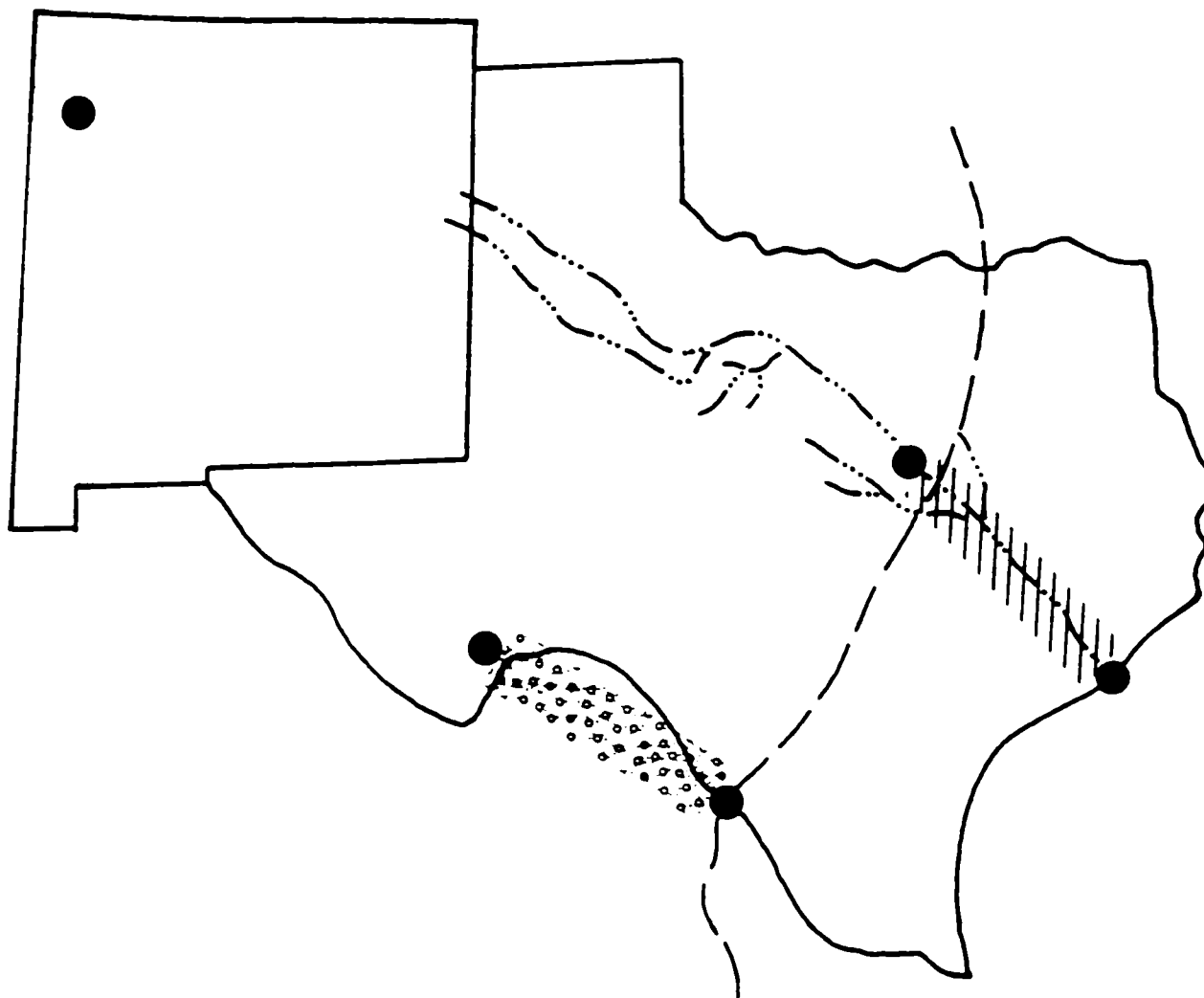


Figure 5.1. Drainage area estimated for this study. Upper shale member drainage is represented by the stippled pattern and the Brazos River drainage area is represented by the hachured lines. Paleogeographic position of the shoreline (dashed line) during the middle of the Maastrichtian is from Lehman, 1985.

The upper shale member also represents approximately two million years of geologic time, from the Late Campanian to Early Maastrichtian stage (Lehman, 1996). So a comparison to the modern fauna must also include any turtles from the last two million years (as an approximation, including the Pleistocene) of Texas. This fauna would thus include *Trachemys* (the slider turtle), *Chelydra* (the snapping turtle), and *Geochelone* (the extinct giant tortoise) (Holman, 1964, 1969). *Geochelone* is the only genus extinct today, and because relative abundance is unimportant in a taxon richness study, it is necessary only to note the occurrence of this genus.

This same technique is applied to the Fruitland/Kirtland Formations of the San Juan Basin by measuring the linear distance derived from the position of the coastline at the beginning of the Campanian, and again at the beginning of the Maastrichtian. This distance is then applied to the Brazos River (Figure 5.2). A simple comparison of generic richness between the Aguja turtle fauna and modern fauna is provided below. The total area of the Fruitland and Kirtland Formations is derived by measuring the distance between the position of the coastline of the Cretaceous Seaway during the “middle” Campanian and the position of the coastline during the Late Maastrichtian, and multiplying by the width of the Fruitland and Kirtland Formation outcrops. The total length is approximately 700 miles and the width is approximately 80 miles, making the total area 56,000 square miles. The total length of the Brazos River drainage is only roughly 600 miles, so the total area measured is $600 \times 80 = 48,000$ square miles. Although smaller, the Brazos River drainage area is roughly comparable.

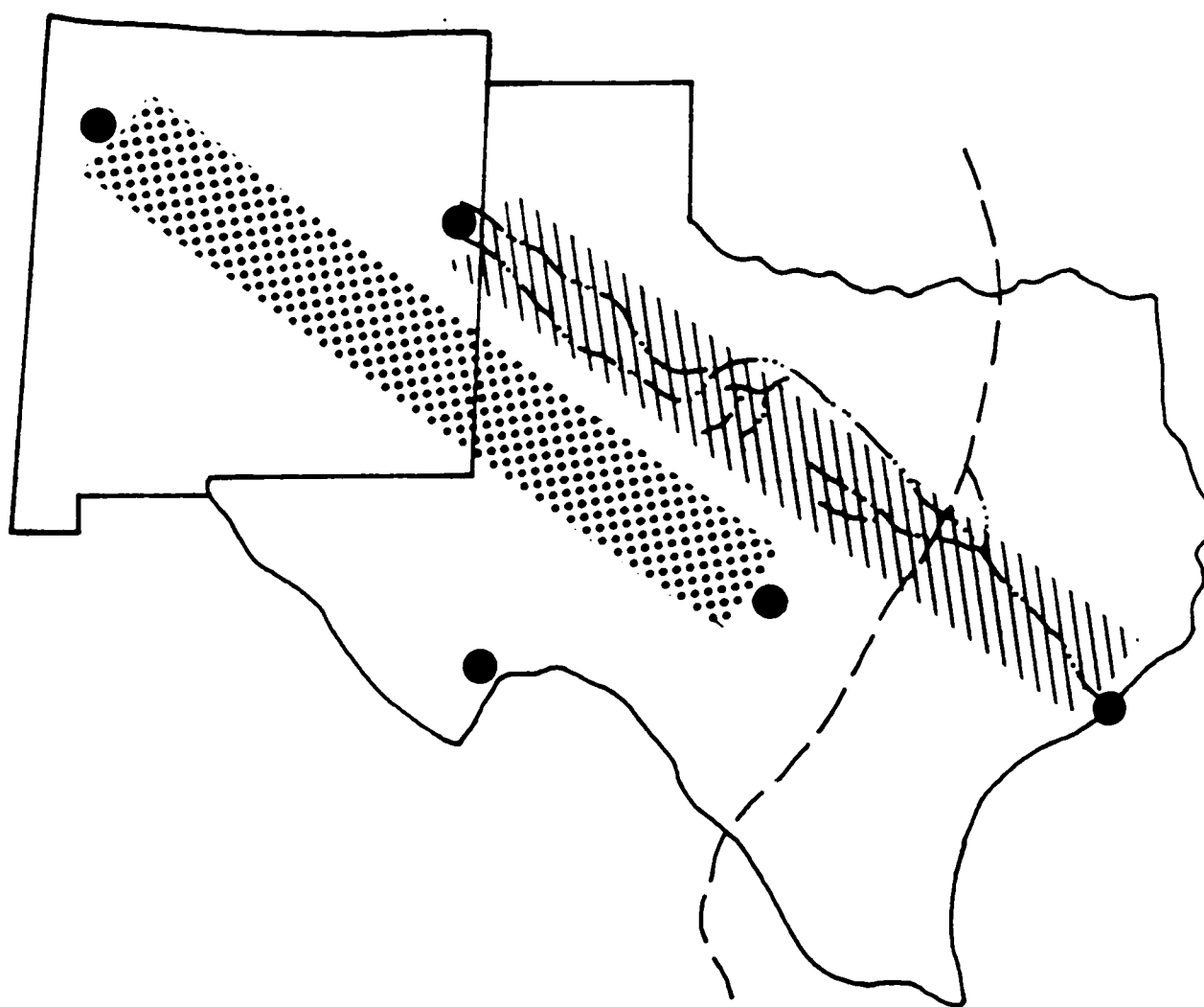


Figure 5.2. Drainage area estimated for this study. The Fruitland/Kirtland drainage is represented by the stippled pattern and the Brazos River area is represented by the hachured lines. Position of the paleoshoreline (dashed line) during the middle of the Maastrichtian is from Lehman, 1985.

Results

The generic richness for the Aguja turtle fauna is eight genera (including one marine taxon) per 11,000 square miles, while the generic richness measurement for the modern Brazos River drainage basin is a total of twelve genera (without the marine taxa) per 11,000 square miles, and fifteen genera per 11,000 square miles with marine taxa included (Dixon, 1987; Ernst, Lovich, and Barbour, 1994).

The taxon richness for the Fruitland and Kirtland Formations is eight genera for 48,000 square miles (Gilmore, 1916, 1919, 1935). The taxon richness for the Brazos River for 48,000 square miles is the same as it is for 11,000 square miles, twelve non-marine genera. The taxa known for the San Juan Basin, Big Bend, and the counties of the Brazos River drainage basin are listed in Table 5.1.

In the taxon richness comparison, the modern fauna appears to be 50 percent more diverse than the Aguja fauna, with 12 freshwater and terrestrial turtles per 11,000 square miles, and three marine turtles to the Aguja fauna's 8 freshwater turtles and one marine for the same area. A comparison of the Fruitland and Kirtland Formation's assemblage yields approximately the same levels of diversity (Table 5.1). It is interesting to note, however, that although the exposure of the Fruitland and Kirtland Formations is nearly five times that of the upper shale member (Lehman, 1996), the number of taxa represented is comparable. This implies either that the Aguja fauna is more adequately represented, in spite of its limited exposure, or that the Aguja fauna is potentially even richer than that of the Fruitland and Kirtland Formations.

Morphology as a Diversity Measure

At first glance, it is tempting to conclude that the comparable modern fauna is substantially more diverse than the Aguja fossil fauna. However, an alternative way to compare the diversity is to compare whether the diversity of the ecological niches filled is the same. Assuming that a turtle's mode of life or ecological setting is reflected in its shell morphology, a diversity assessment could be based on similar representation of turtle "morphotypes" in comparable modern and fossil faunas. In some cases, for example, in the trionychids, it is easy to see that the morphotypes are the same in both modern and fossil forms. For the other freshwater aquatic taxa, however, it is more difficult to assess whether or not they fill a comparable number of ecologic niches.

Of course, ecologic niches are complex, and include aspects that would be impossible to determine in a fossil fauna, such as whether the turtle was nocturnal or diurnal, whether it preferred burrowing in mud to swimming in clear waters, or whether it fed at the top, middle, or bottom of the water column. However, ecologists have long understood that morphology is selected by environmental pressures, and that the morphology of an organism reflects its position in the habitat (Ricklefs, 1990). An advantage in using the morphology of an organism is that morphological "measurements are independent of habitat context" (Ricklefs, 1990, p. 734). In other words, it is not necessary to know whether a fossil turtle fed from the top, middle or bottom of the water column; the organism has its own niche in morphological "space." An alternative measure of diversity, then, is whether the Aguja turtle fauna has a level

of diversity assessed in terms of morphological niche space comparable to a modern assemblage.

The part of the turtle that is most easily preserved, the shell, provides a very broadly defined niche space in the form of the morphology of the shell. In modern faunas, the largest group of freshwater turtles, the Emydidae, can be grouped into two categories according to a preference for fast or slow moving water (rivers or ponds). In general, those turtles with high-domed carapaces prefer slow moving water, such as in ponds, marshes, ditches, or in the quieter bottom water of streams. Those having a depressed carapace are more likely to be found in the fast moving water of rivers than the high-domed turtles, and they will also occur in ponds, marshes and ditches (Ernst et al., 1994). In terms of fluid mechanics, a high-domed shell has greater surface area than a depressed shell of the same circumference. Greater surface area in turn offers more resistance to stream flow owing to greater drag. To live in a fast-moving body of water then, a high-domed turtle would probably have to expend more energy. It is less clear how the overall size of the shell would determine preference for bodies of water, but as discussed below, there are some clear preferences here as well.

Because the size and shape of the shell might hold clues to the number of niche spaces available, the modern turtle fauna were divided into nine categories. The first six include the Emydidae, the largest and most diverse group. The emydids are arbitrarily divided into *small* (<17 cm), *medium* (17-40 cm), and *large* sizes (>40 cm). These size groups are in turn divided into two groups each on the basis of the ratio of total shell width (measured by holding one end of a string to the lateral edge of the

carapace at a point about midway between the anterior and posterior ends, and running the string across the dorsal portion of the carapace to the equivalent peripheral) to a straight-line measurement of width at the same point (Figure 5.3). Those turtles with a carapace height to width ratio greater than 1.5:1 are placed into the *high-domed* category, while those with a ratio of less than 1.5:1 are considered to have a *depressed* carapace. This classification of recent turtles into six categories is shown in Table 4. I was only able to directly measure shells on six genera of the modern turtles. The other turtles are placed in their categories according to measurements found in the literature, and using photographs. I was able to measure shells on all of the fossil turtle genera except *Compsemys*. The recent and fossil specimens that I measured were either specimens used in this study, or specimens from museum collections. It is important to note that fossil turtles are often found in an artificially depressed state owing to crushing from burial compaction. This must be taken into account when assessing the validity of these categorizations, and this was done qualitatively by estimation. When the emydids are classified in their appropriate morphological categories it becomes apparent that the modern turtles that prefer ponds and still waters (*Sternotherus*, *Kinosternon*, *Terrepene*) are turtles with *small, high-domed* shells. The *medium* and *large* turtles with *depressed shells* (*Pseudemys*, *Graptemys*, *Trachemys*, *Deirochelys*, *Malaclemmys*, and *Chelydra*) can be found in almost any body of water, fast or slow moving. It is interesting to note that there are no *large, high-domed* freshwater turtles. The other three groups are the marine turtles and the Trionychidae, which are more directly comparable to fossil forms than the

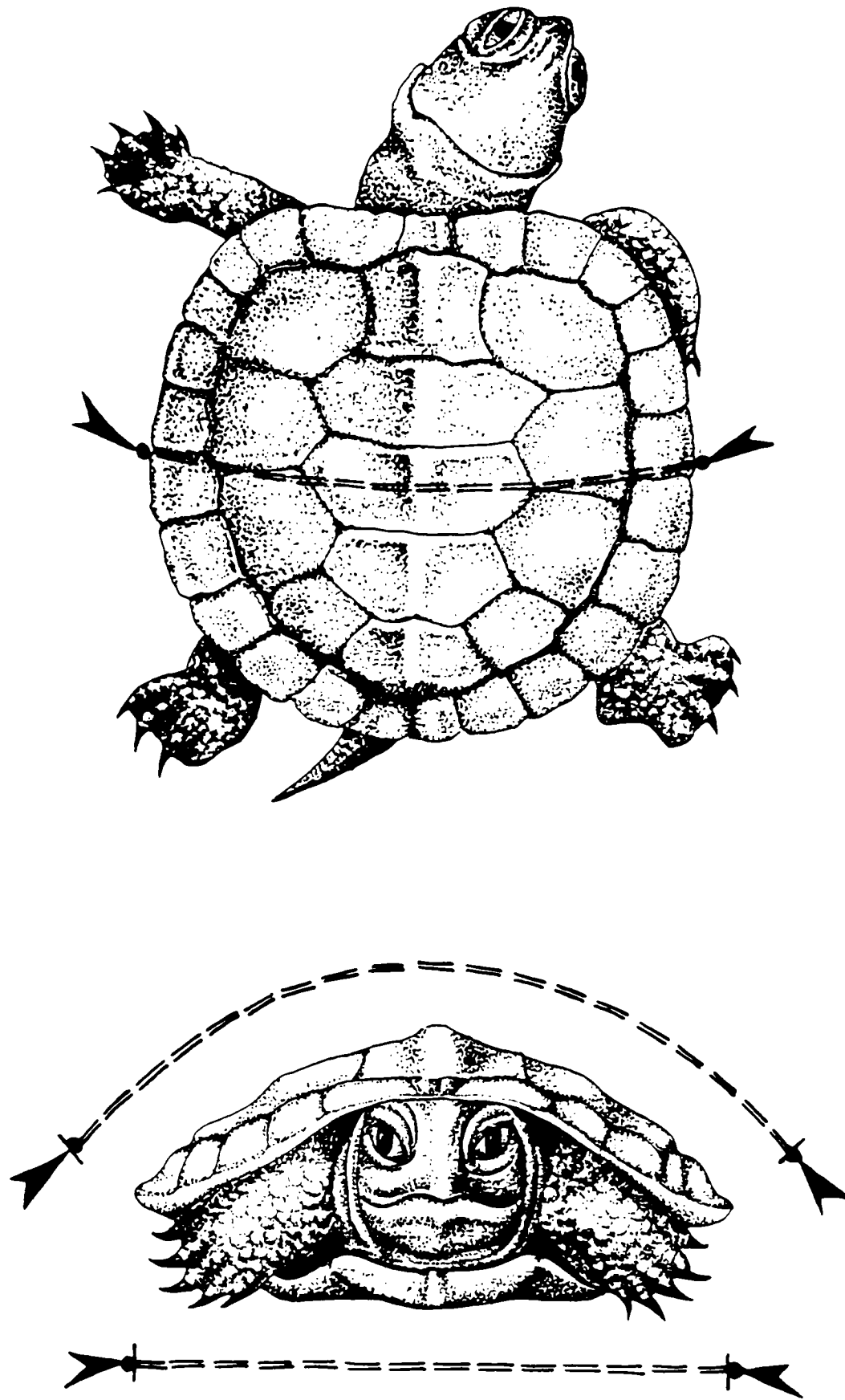


Figure 5.3. Method of measurement for morphology study. Dashed line represents measurement. Turtles are drawn in the manner of Sonrel (1857).

Emydidae are to the Aguja fauna, and the tortoises, *Geochelone* and *Gopherus*. The nine different categories are listed in Table 5.2. It is possible to compare the morphological estimates of niche space for the modern and Aguja faunas. The six categories of emydids are compared with the freshwater turtles of the Aguja fauna on the basis of the shell size and shape, and the other three categories of marine, trionychid and tortoise are also compared. Of the six emydid (or, in the case of the fossil turtles, freshwater) categories, all but the *small, depressed* and *large, high-domed* forms have representatives in both the modern and Aguja fauna. The other categories of morphological niches can be directly compared. For example, the marine turtle *Bothremys*, and the trionychids (?*Aspideretes* and ?*Helopanoplia*) each have modern counterparts or living representatives, so the presence or absence of a morphotype is easily ascertained. There is no Late Cretaceous representative for the tortoise morphotype; tortoises themselves did not appear in the fossil record until the Eocene (Hay, 1908), but the tortoise morphotype appeared in the Paleocene in the form of *Hoplochelys* (Hay, 1908).

When totaled, the modern fauna has seven morphological categories represented, and the Aguja fauna has six (Table 5.3). Where the freshwater turtles are concerned, including the Trionychidae, the modern fauna and the Aguja fauna have equal numbers of four morphological niches represented. So although there are nearly twice as many genera in the modern fauna, there are a comparable number of morphological niches (on the basis of shell size and shape) in both groups, suggesting that the Aguja fauna is probably adequately represented with respect to diversity

Table 5.2. Comparison of Brazos River drainage fauna and Aguja fauna.
Asterisks denote turtles that have not been physically measured.

| Size | Small <17cm | Small <17 cm | Medium 17-40 cm | Medium 17-40 cm | Large >40 cm | Large >40 cm |
|--------------|---------------------------|----------------------------|----------------------------|----------------------------|----------------------------|----------------------------|
| Shape | >1.5/1 Domed | <1.5/1 Flat | >1.5/1 Domed | <1.5/1 Flat | >1.5/1 Domed | <1.5/1 Flat |

| | | | | | | |
|--------|--------------|--|-------------|------------|--|--------------|
| EXTANT | Sternotherus | | Deirochelys | Pseudemys* | | Malaclemmys* |
| | Kinosternon | | | Graptemys* | | Chelydra |
| | Terrepene | | | Trachemys* | | |
| | | | | | | |
| | | | | | | |
| FOSSIL | Compsemys* | | Baena | Adocus | | Neurankylus |
| | | | | | | Basilemys |

Table 5.3. Comparison of Brazos River drainage fauna and Aguja fauna.

| General morphology | Modern | Fossil |
|--------------------|--------|--------|
| Small, high domed | x | x |
| Small, depressed | | |
| Medium, high domed | x | x |
| Medium, depressed | x | x |
| Large, high domed | | |
| Large, depressed | x | x |
| Marine | x | x |
| Trionychid | x | x |
| Tortoise | x | |

measured in morphological “space.” This is consistent with current thinking in morphological study, which holds that the number of niches in morphological space (i.e. “species packing”) is relatively constant (Ricklefs, 1990, p. 734).

Simpson’s Index of Diversity

Simpson’s Index of Diversity (SI) is a commonly used diversity index in which $D = \sum ((n_i^2 - n_i)/(N^2 - N))$, where n_i is the number of individuals in the *i*th taxon, and N equals the total number of individuals. As D increases, diversity decreases (Magurran, 1988; Pielou, 1975). The upper limit of D is set at 1.0 (Rosenzweig, 1995). Unfortunately, there are no studies of which I am aware that use Simpson’s Index on either fossil or recent turtles, so there is no D value to which I could compare the D value of the Aguja fauna. However, for any future studies that may use this index, I have calculated the SI of the fauna from the upper shale member of the Aguja Formation. For this fauna, $D = 0.3487$. A list of minimum number of individuals for this fauna is shown in Table 5.4.

Conclusions

Although a generic richness comparison of the Aguja fossil turtle fauna with a modern assemblage of turtles suggests that the Aguja fauna is only half as diverse, a comparison with equivalent strata like the Fruitland and Kirtland Formations (which have much larger area of exposure) shows a very similar level of diversity. A comparison of the Aguja fauna diversity expressed as shell morphotypes with a

Table 5.4. Taxa and number of individuals from the upper shale member of the Aguja Formation used for Simpson's Index calculations.

| Genus | Minimum Number of Individuals |
|---------------|----------------------------------|
| ?Aspideretes | 23 |
| Baena | 5 |
| Adocus | 4 |
| Bothremys | 2 |
| Basilemys | 2 |
| Neurankylus | 2 |
| ?Helopanoplia | 1 |
| Compsemys | 1 |
| Total | 40 |

modern assemblage suggests that, although not as many taxa are represented in the upper shale member, nearly as many shell forms are present in the fossil assemblage as are present in the modern assemblage. As mentioned previously, the Aguja fauna was selected for the diversity study, in part, because the collecting and preservational biases were at a minimum. Because of this, the comparison of the this fauna to both stratigraphically equivalent fauna and to a modern assemblage points to a moderate level of diversity for the Aguja fauna.

CHAPTER VI
MORPHOMETRIC ANALYSIS OF PIT VARIANCE
IN TRIONYCHID SHELLS

Introduction

Carapace and plastron fragments of turtles representing the soft-shelled family Trionychidae are abundant throughout the Late Cretaceous and early Tertiary strata of North America. Current taxonomic work on turtles relies heavily on skull characters, as well as other skeletal features, for the diagnosis of species (Gaffney 1975; Gaffney and Meylan, 1988; Meylan 1987; Meylan and Gaffney, 1989). While there is good reason for this, it is not always useful for the stratigraphic paleontologist, paleoecologist, or biostratigrapher faced with a paucity of well-preserved cranial material. In many cases, while it is evident from fragments of shells that soft-shelled turtles were abundant at some localities, without the skulls or some other diagnostic skeletal character these turtles can only be identified to the familial or generic level. This obscures a great deal of useful information that could be gleaned from the site about the level of diversity of the fauna.

For many years, patterns in the distinctive pits on the carapace or plastral callosities of soft-shelled turtles were considered to be specifically diagnostic features (Gilmore, 1919, 1946; Hay, 1908). However, this practice has fallen into disfavor (Meylan, 1984, 1989). Recent work by Gardner and others (Gardner and Russell,

1994; Gardner, Russell, and Brinkman, 1995) suggests, however, that the patterns of the pits on the shell might be of use in taxonomic diagnosis. To use the pits as a diagnostic character the assumption must be made that intraspecific variability in the patterns is low; that is, patterns are not highly variable among individuals, but are discriminatory at some taxonomically significant level, such as species or genus.

The assumption of non-discriminatory variability in pit patterns has never been assessed quantitatively. If it could be found that characteristic pit patterns, however subtle, can be identified for distinct groups (perhaps reflecting different genera or species), the potential for identifying fragments as belonging to different species of turtles increases, as does the potential for using these fragments in ecological or stratigraphic studies.

A number of factors must be considered before attempting to quantify pit variability. Variability in patterns may be related to (1) where the pits are located on the shell, or to (2) sexually dimorphic, (3) ontogenetic, or (4) taphonomic processes. Before any study like this can be interpreted with confidence, such “noise” factors must be identified and partitioned or filtered out. As a first step a model should be developed which would assess whether any patterns of a discriminating nature at all are distinguishable. If no such patterns are found then the assumption of a discriminatory variability is shown to be false, and no further testing would be necessary. If a discriminatory pattern is found, however, then further testing is desired on a larger data set in order to determine whether it is possible to filter out the noise factors, and if so, whether it is then possible to use this method for taxonomic

purposes. Furthermore, if a pattern is shown to exist, it is important to determine whether the pattern or patterns that are discerned are simply an artifact of the statistical analysis or something with a biological basis. This can be done by generating random numbers that are similar in character to the numbers used to describe the pits.

Morphometric studies are multivariate analyses used to describe biological forms, as well as to discriminate among biological forms (Bookstein, Chernoff, Elder, Humphries, Smith, and Strauss, 1985; Pimentel, 1979). One of the methods long used by biologists to compare forms is to place them into morphological space, or “morphospace” (Bookstein et al., 1985). This idea, used by Raup in a landmark study on the coiling of molluscs (1966), takes natural forms and compares them to imagined or unobserved forms by placing them into a multi-dimensional space that geometrically describes the forms. The pits on trionychid turtle shells are forms that will fit somewhere in morphospace. Ideally, the differences in the shapes, sizes, and spacing of the pits on the shells, will fit in different places in this multi-dimensional morphospace. Then, if the variability is discriminatory (i.e., if there is a discernable pattern for a given taxonomic level, like species or genus), the differences in patterns will show up as different places in morphospace. If this should be the case, we might be able to verify, at the very least, the presence of more than one taxonomic group in a fauna, even if their actual identities are unknown.

The following is a preliminary study utilizing some fundamental morphometric techniques to determine whether any discriminatory patterns in the pits of trionychid shells can be identified. If the results indicate that patterns are discernable in the pits,

then further studies will be conducted at a later date in order to determine what these patterns represent, and whether they will be of any biostratigraphic or paleoecological use determining stratigraphic correlations or levels of diversity in a turtle fauna.

Methods

Morphometric measurements were made on fragments of Late Cretaceous and early Tertiary turtle shells collected from Big Bend, using Image--pro Plus Image Processing System software (Media Cybernetics, 1992). A digitized measurement of the total area and perimeter was made first for each fragment. Then each individual pit was measured, taking the outside perimeter measurement and deriving the area from that. Where two or more pits had apparently grown together (coalescing to form one pit), the original individual pits were measured first separately, and then the coalesced measurement was taken. The coalesced measurements were kept in a separate data set in order to determine the effect they might have on principle components.

Of the available fragments, 24 were from the same locality (TMM 42880) in coastal floodplain facies of the upper shale member of the Aguja Formation. These fragments, although from the same locality, are not all from the same individual. This assumption is based on a taphonomic assessment of where the fragments were located at the site, a qualitative assessment of pit patterns and appearances, and a distinct difference in the preservational appearance of the fragments. However, a minimum number of individuals is not determinable. Standards for comparison were chosen from two other localities; these included 3 additional trionychid shell fragments, 2 from a

locality within the Javelina Formation, and 1 from a Paleocene locality within the overlying Black Peaks Formation. A fourth standard was chosen from the Javelina Formation from a specimen representing the family Dermatemydidae, and the genus *Basilemys*.

Principle components analysis (PCA) was chosen as a method of measuring variance/covariance of the variables in the data set. PCA is often used as a starting point in any analysis of biometric data, partly because the interpretation of the data is often straightforward and uncomplicated (Davis, 1986). In principle components analysis selected variables (characters that are being measured) and their covariances are plotted on a matrix. For example, the total area and perimeter of a section on the shell containing a collection of pits would be two variables (or *components*). The covariance between these two measurements is then calculated. The variance-covariance matrix can then be interpreted geometrically, and the principle components analysis measures the axes and their magnitudes on an x/y plot. In a multivariate data matrix PCA isolates the *principle components*, and plots them in multidimensional space in a series of x/y plots.

The primary value in PCA lies in being able to isolate those variables that are most (and least) significant. In PCA the components are weighted factors, with each factor comprising a percentage of the total variance (Kachigan, 1991). For example, principle component 1 (PC1) might account for 80% of the total variance. This identifies PC1 as the single most important variable measured. PCA can thus be used to identify the most (and least) important variables being measured.

The computed scores of the eigenvectors are called “loadings”, and are the coefficients of the linear equation which defines the eigenvector (Davis, 1986). A high negative or positive loading for a variable indicates that it is highly correlated with the principle component. A component having both negative and positive loadings is considered bipolar, while one with a single sign is a general size factor (Bookstein et al, 1985). A bipolar component is usually a character that is not related to overall size (e.g., simply measuring the difference between a large and small specimen of the same organism), but measures the relationship between other variables, such as size and shape.

One advantage of using PCA in this application is to identify the most important contributions to size/shape variance among the pits on trionychid shells. Also, because it is not known how many groups are actually present in the data set, PCA can also be used to see whether there is a pattern to the distribution that suggests when more than one group is present.

Data Analysis of Big Bend Trionychid Shell Fragments

Principle components analysis was applied to the data set using nine variables. These variables were chosen to describe the morphology of the pits by measuring size of the individual pits, complexity of shape, and distance between individual pits. The nine variables included: total fragment area (TOTAREA), total fragment perimeter (TOTPERIM), mean areas (M_AREA) and perimeters (M_PERIM) of individual pits within the total area measured, standard deviations of the areas (S_AREA) and

(S_PERIM) perimeters of the individual pits within the total measured area, sums of the areas of the individual pits subtracted from the total measured area (SPACE), and the covariance between area and perimeter of the individual pits (SQCOV) (Table 6.1). All variables were transformed to natural logarithms. Complexity of form is assessed by comparison of the standard deviation of pit perimeter to area of the pit measured. Variability in the size of pits is measured by comparison of the standard deviation in area of pits measured to the mean size of the pits in the area measured. Distance between pits is measured by subtracting the sum of the area of the pits on a specimen from the total area measured on the specimen. The program was written in the SAS programming language. This program is provided in the Appendix and is called "Totturt.SAS". The results are discussed in the Results section below.

Randomized Data Analysis

The purpose for generating random data is to determine whether the patterns seen in the PCA are biological or geometrical in origin. In Raup's (1966) study with the coiling of mollusc shells he was able to demonstrate that one could predict where a biological form would plot in morphospace by plotting geometric forms. Real data from a real form would then hypothetically plot somewhere within that space defined by geometrically generated data. If data were genuinely random in nature, and the real data being tested were not random in origin, but had biological constraints, then the two data sets should plot differently. The ideal study would first try to generate random data, within a range similar to the real data, to determine whether the two sets

Table 6.1. Variables used in morphometric study.

| | |
|--|----------|
| Total area | TOTAREA |
| Total perimeter | TOTPERIM |
| Mean, area of individual pits | M_AREA |
| Mean, perimeter of individual pits | M_PERIM |
| Standard deviation, area of individual pits | S_AREA |
| Standard deviation, perimeter of individual pits | S_PERIM |
| Space between individual pits | SPACE |
| Covariance between pit area and perimeter | SQCOV |

of data plot similarly. If they do not, then this would suggest that the real data are measuring variables that are somehow constrained biologically. That is to say, random forms represent the null hypothesis of non-discriminating variation.

Two SAS programs were written to compare the observed data to randomly generated data. In the first of these, a random set of data was generated for comparison to the real data in order to determine whether any patterns that arose from the data were statistical or biological in nature. In the second program, random data and real data were merged in order to isolate any biological constraints that would determine where the real data would plot in morphologic space. These programs are provided in the Appendix and are called “RandturtNC.SAS” and “Alldata.SAS” respectively. The results are provided in the results section below.

In the program to generate representative random data the following constraints were placed on the data: pit perimeter and area had to be of a comparable size to the real data; pit number per specimen had to be of comparable size and vary in number from 4-10; random numbers generated for the perimeter have a normal distribution; perimeter/area is variable. Fifty “specimens” were generated for a total of 259 observations. This program provided in the Appendix and is called “Randturtnc.SAS”.

The second program merged random data with the real data. In this program constraints were placed on the random data. Because results from real data suggest that the variance in the shape and size of the pit is inversely proportional to the size of the pit, this was included as a constraint on both the area and perimeter of each pit. An

additional constraint factor was added for the perimeter in order to limit the variance in the complexity of the shape. These data were then merged with real data to compare the results in PCA loadings and plots. This program is included in the Appendix and is called "Alldata.SAS".

Results

Data Analysis of Big Bend Trionychid Shell Fragments

Two initial sets of analyses were run on the SAS program, one to account for the coalescence of pits, the other to remove the coalescence factor. No differences in results were observed. The first principle component (PC1) reflects ~50% of the total variance among the pits (Table 6.2). This axis is a bipolar axis with strong positive loadings for the standard deviations of the areas and perimeters of the pits, and strong negative loadings for the means of the areas and perimeters of the pits, suggesting that it measures variability in the size of the pits within the area measured.

PC2 reflects ~32% of the total variance. This axis exhibits all positive loadings, and is therefore a general size component. PC3 accounts for ~16% of the total variance, and is a bipolar axis. A very strong positive loading, with a value near 1.0, is registered for the space factor. This component, then, measures the distance of the space between the pits. Principle components 4 through 7 accounts for less than 3% of the total variance, and are therefore considered to have little influence on the total variance. The plots of PC1 versus PC2, and PC2 versus PC3 are shown in Figures 6.1 and 6.2, respectively.

Table 6.2. TOTTUR Data.

| | M_AREA | S_AREA | M_PERIM |
|------|--------|--------|---------|
| Mean | 0.8431 | 0.2567 | 2.268 |
| StD | 0.2610 | 0.1006 | 0.2673 |

| | S_PERIM | SPACE | SQCOV |
|------|---------|-------|--------|
| Mean | 0.2881 | 59.18 | 0.2678 |
| StD | 0.1310 | 28.36 | 0.1088 |

Correlation Matrix

| | M_AREA | S_AREA | M_PERIM | |
|---------|--------|--------|---------|-------------------------------|
| M_AREA | 1.000 | -.1869 | 0.9909 | the mean, AREA |
| S_AREA | -.1869 | 1.000 | -.1882 | the standard deviation, AREA |
| M_PERIM | 0.9909 | -.1882 | 1.000 | the mean, PERIM |
| S_PERIM | -.0956 | 0.9220 | -.0937 | the standard deviation, PERIM |
| SPACE | 0.2129 | 0.1137 | 0.1553 | |
| SQCOV | -.1578 | 0.9857 | -.1539 | |

| | S_PERIM | SPACE | SQCOV | |
|---------|---------|--------|--------|-------------------------------|
| M_AREA | -.0956 | 0.2129 | -.1578 | the mean, AREA |
| S_AREA | 0.9220 | 0.1137 | 0.9857 | the standard deviation, AREA |
| M_PERIM | -.0937 | 0.1553 | -.1539 | the mean, PERIM |
| S_PERIM | 1.0000 | -.0502 | 0.9711 | the standard deviation, PERIM |
| SPACE | -.0502 | 1.0000 | 0.0362 | |
| SQCOV | 0.9711 | 0.0362 | 1.0000 | |

Eigenvalues of the Correlation Matrix

| | Eigenvalue | Difference | Proportion | Cumulative |
|-------|------------|------------|------------|------------|
| PRIN1 | 3.042 | 1.097 | 0.5070 | 0.5070 |
| PRIN2 | 1.9450 | 0.9970 | 0.3242 | 0.8312 |
| PRIN3 | 0.9479 | 0.8914 | 0.1580 | 0.9892 |
| PRIN4 | 0.05651 | 0.04895 | 0.009418 | 0.9986 |
| PRIN5 | 0.00756 | 0.0066 | 0.0013 | 0.9998 |

Table 6.2 Continued. TOTURT Data

Eigenvectors

| | PRIN1 | PRIN2 | PRIN3 | |
|---------|---------|---------|---------|-------------------------------|
| M_AREA | -.2312 | 0.6467 | -.1468 | the mean, AREA |
| S_AREA | 0.5496 | 0.1656 | 0.0629 | the standard deviation, AREA |
| M_PERIM | -.2301 | 0.6393 | -.2057 | the mean, PERIM |
| S_PERIM | 0.5333 | 0.2047 | -.1539 | the standard deviation, PERIM |
| SPACE | -.01429 | 0.2668 | 0.9525 | |
| SQCOV | 0.5539 | 0.1812 | -.03647 | |
| | PRIN4 | PRIN5 | | |
| M_AREA | 0.0159 | -.68320 | | the mean, AREA |
| S_AREA | -.6413 | -.19390 | | the standard deviation, AREA |
| M_PERIM | -.1117 | 0.66730 | | the mean, PERIM |
| S_PERIM | 0.7386 | -.03060 | | the standard deviation, PERIM |
| SPACE | 0.1357 | 0.05490 | | |
| SQCOV | -.1109 | 0.21530 | | |

Figure 6.1. Plot of PRIN2*PRIN1, TOTTUR Data. Bold, underlined characters are standards used, which include *Basilemys* sp. TMM 42335-5 (**z**), *Aspideretes* sp., Javelina Formation TMM42874-1(**A**), Trionychidae(a) TMM 42876-1 (**B**), and Trionychidae(b) TMM 42876-1 (**C**). PRIN1 represents variability in pit size; PRIN2 represents overall size of pit.

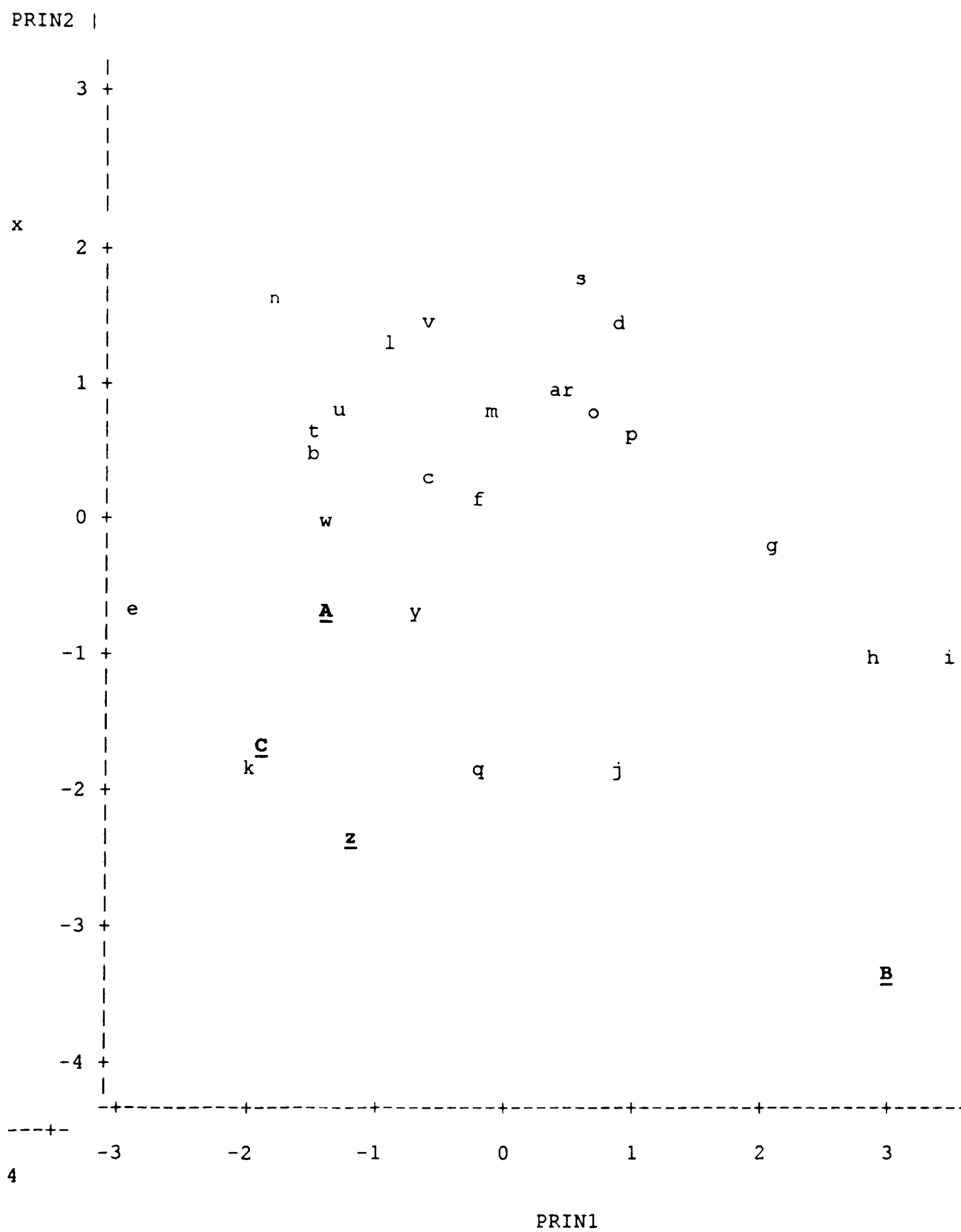
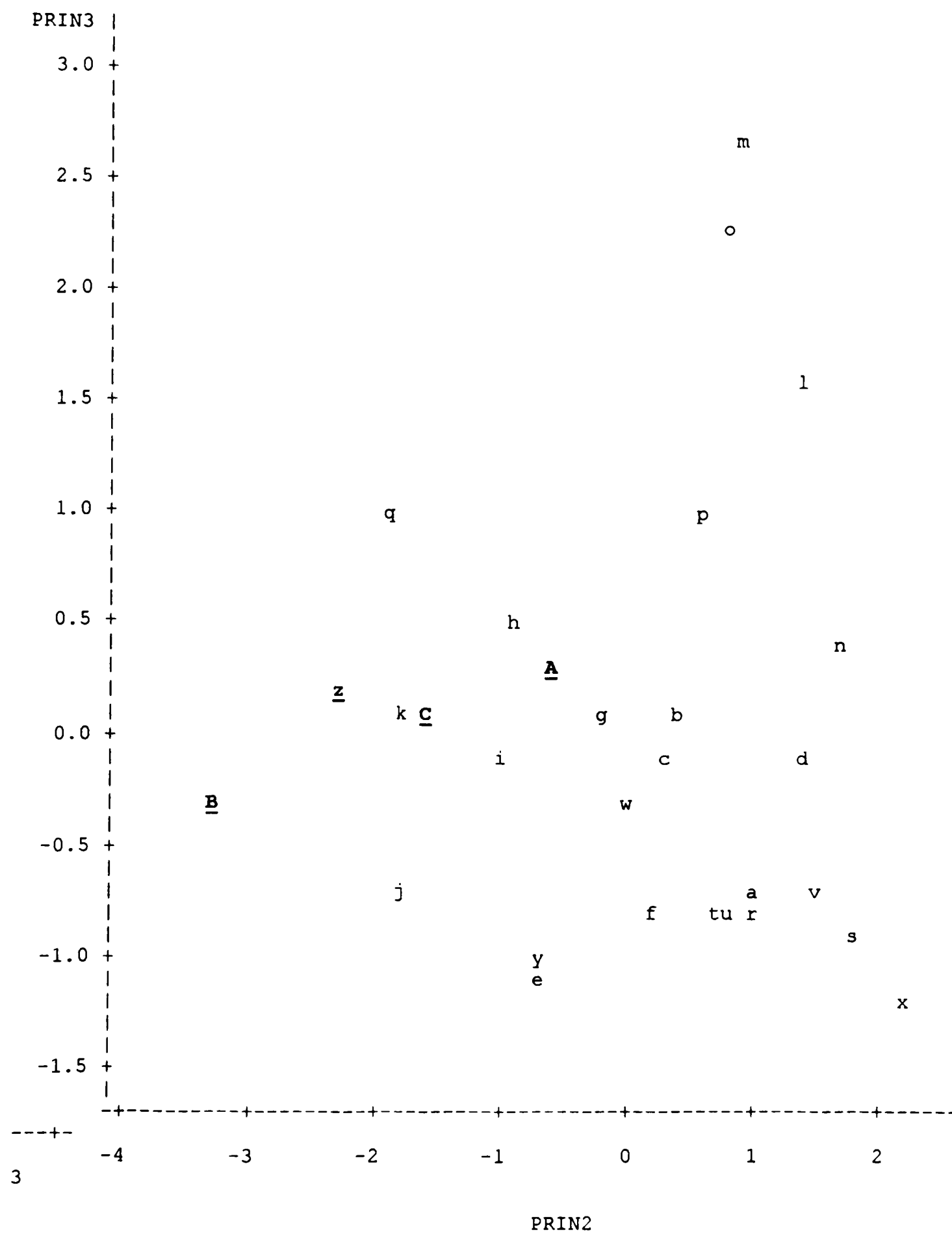


Figure 6.2. Plot of PRIN3*PRIN2, TOTTURT Data.. Bold, underlined characters are standards used, which include *Basilemys* sp. TMM 42335-5 (**z**), *Aspideretes* sp., Javelina Formation TMM42874-1(**A**), Trionychidae(a) TMM 42876-1 (**B**), and Trionychidae(b) TMM 42876-1 (**C**).



Random Data Analysis

Random data generated separately did not plot similarly to the trionychid data (Figures 6.3, 6.4). Loadings are shown in Table 6.3. When the random data were merged with the real data (with constraints) PC1 accounted for ~43% of the total variance, PC2 for ~23%, and PC3 for ~17% (Table 6.4). Loadings were very similar to that of the real data. When the data are plotted according to PC1 versus PC2, and PC2 versus PC3, the random data and the real data appear to plot similarly in morphospace (Figures 6.5, 6.6).

Discussion and Conclusion

Discussion

In the analysis of the real trionychid data there were no discernable differences in the numerical or graphical results of the analyses between the data set of coalesced pits and the data set in which this factor had been removed. This suggests that the coalescence of pits as a factor is too small to be measured as a component of variance in this data set. However, coalescence of pits appears to typically occur along the margins of carapaces, so it is possible that with a larger data set, this component could take on more significance as an indicator of location of the specimens on the carapace. Consequently, it would be advisable to continue measuring coalesced pits separately and using them for comparison with a data set in which this factor is removed. Two

Table 6.3. RANDTURTNC Data.

| | M_AREA | S_AREA | M_PERIM | S_PERIM | SQCOV |
|------|--------|--------|---------|---------|--------|
| Mean | 1.4064 | 0.1777 | 2.293 | 0.0966 | 0.0223 |
| StD | 0.0448 | 0.0585 | 0.0251 | 0.0201 | 0.0737 |

Correlation Matrix

| | M_AREA | S_AREA | M_PERIM | |
|---------|--------|--------|---------|----------------------------------|
| M_AREA | 1.0000 | 0.6114 | 0.1159 | the mean, LOGAREA |
| S_AREA | 0.6114 | 1.000 | 0.1189 | the standard deviation, LOGAREA |
| M_PERIM | 0.1159 | 0.1189 | 1.0000 | the mean, LOGPERIM |
| S_PERIM | -.0530 | 0.1127 | -.1299 | the standard deviation, LOGPERIM |
| SQCOV | 0.0539 | 0.3837 | -.1669 | |

| | S_PERIM | SQCOV | |
|---------|---------|--------|----------------------------------|
| M_AREA | -.0530 | 0.0539 | the mean, LOGAREA |
| S_AREA | 0.1127 | 0.3837 | the standard deviation, LOGAREA |
| M_PERIM | -.1299 | -.1669 | the mean, LOGPERIM |
| S_PERIM | 1.0000 | 0.4290 | the standard deviation, LOGPERIM |
| SQCOV | 0.4290 | 1.0000 | |

Eigenvalues of the Correlation Matrix

| | Eigenvalue | Difference | Proportion | Cumulative |
|-------|------------|------------|------------|------------|
| PRIN1 | 1.821 | 0.3642 | 0.3641 | 0.3641 |
| PRIN2 | 1.457 | 0.5903 | 0.2913 | 0.6555 |
| PRIN3 | 0.8662 | 0.3002 | 0.1732 | 0.8287 |
| PRIN4 | 0.5659 | 0.2755 | 0.1132 | 0.9419 |

Eigenvectors

| | PRIN1 | PRIN2 | PRIN3 | PRIN4 | |
|---------|---------|--------|---------|--------|---------------------|
| M_AREA | 0.4935 | 0.4581 | -.2976 | 0.3861 | mean, LOGAREA |
| S_AREA | 0.6436 | 0.2398 | -.07284 | -.1427 | std. dev., LOGAREA |
| M_PERIM | 0.01293 | 0.4938 | 0.8562 | -.1028 | mean, LOGPERIM |
| S_PERIM | 0.3128 | -.5454 | 0.3992 | 0.6631 | std. dev., LOGPERIM |
| SQCOV | 0.4942 | -.4374 | 0.1170 | -.6167 | |

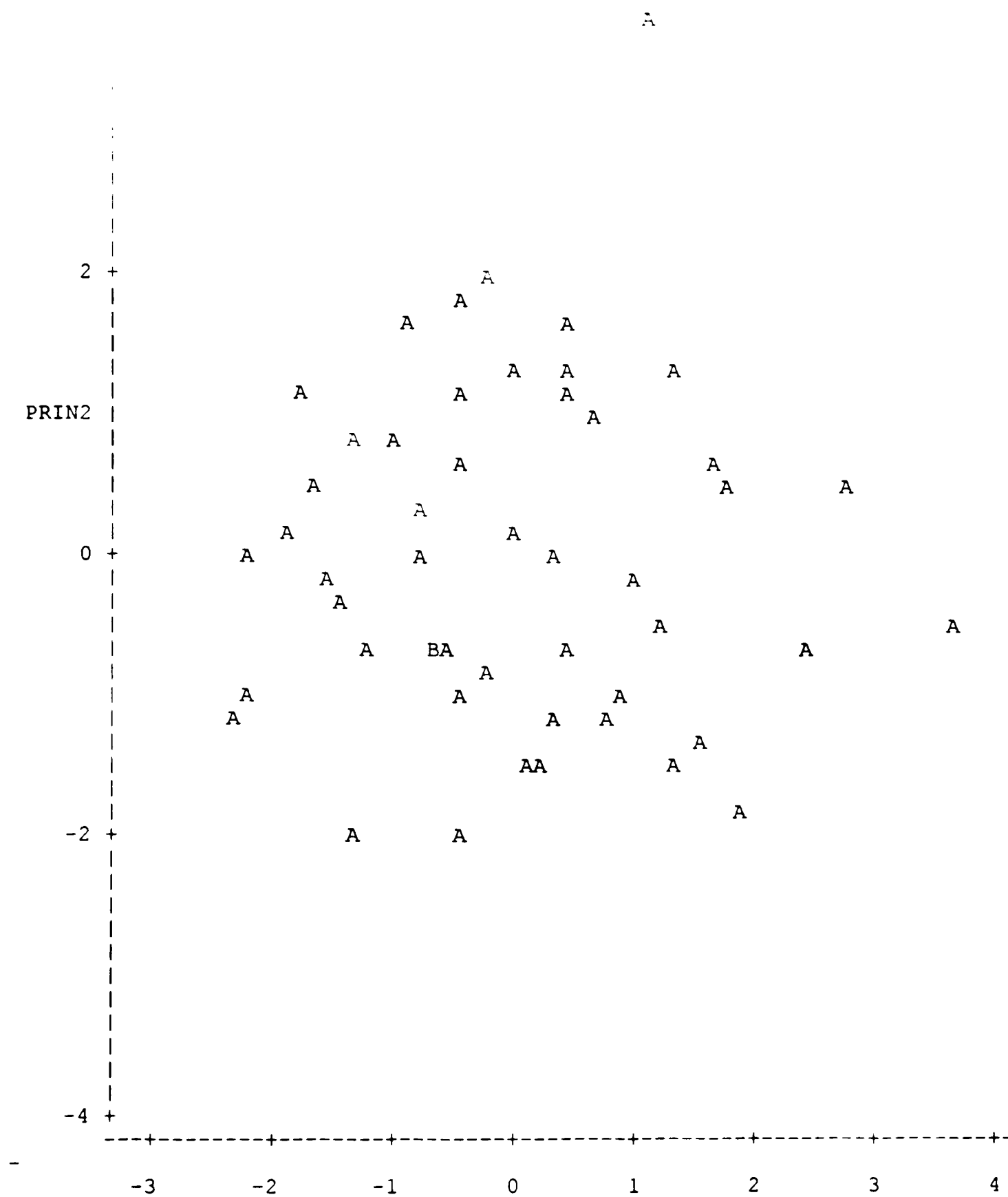


Figure 6.3. Plot of PRIN2*PRIN1, RANDTURTNC Data. Legend: A = 1 obs, B = 2 obs, etc.

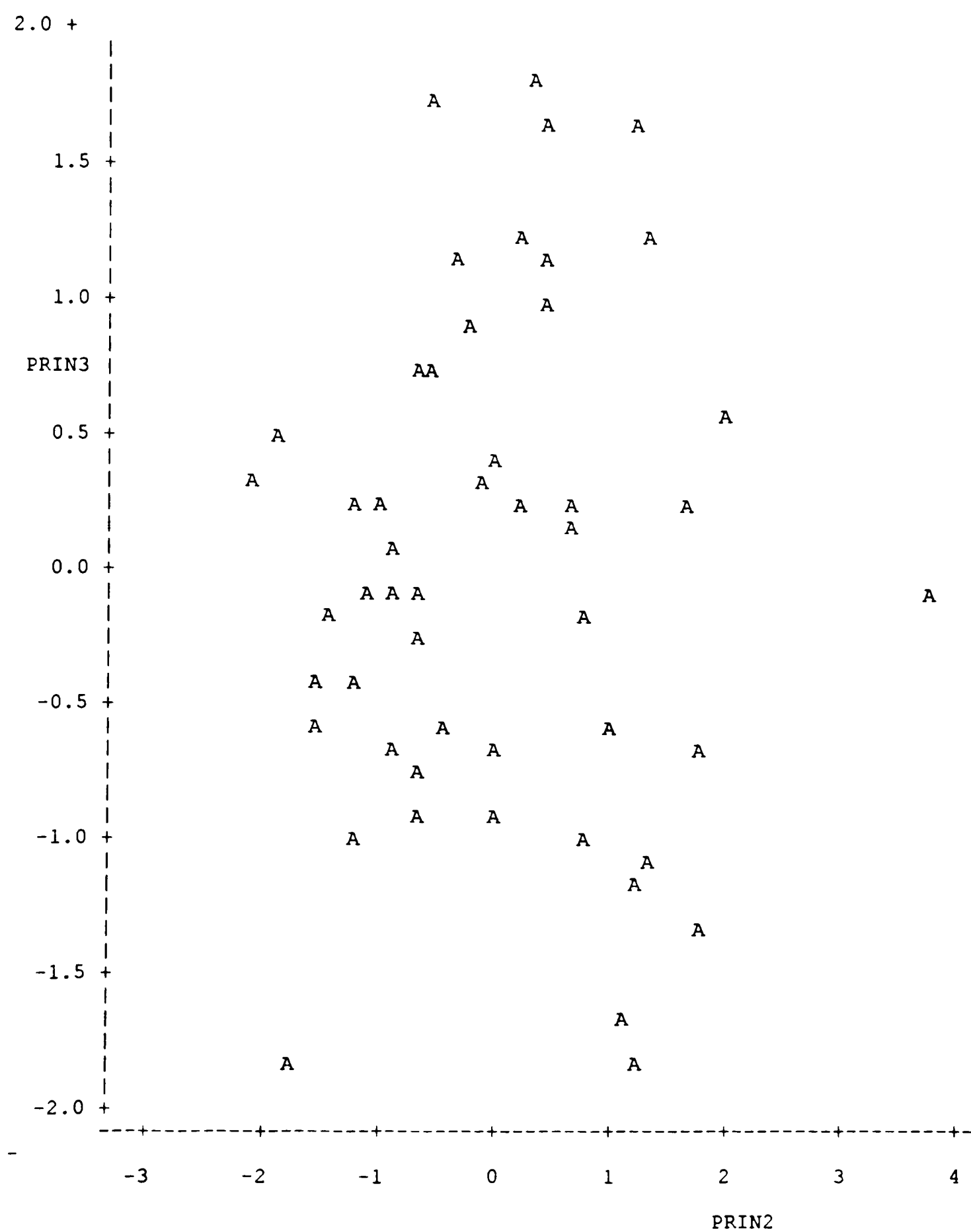


Figure 6.4. Plot of PRIN3*PRIN2, RANDTURTNC. Legend: A = 1 obs, B = 2 obs, etc.

Table 6.4. ALLDATA Data.

| M_AREA | S_AREA | M_PERIM | |
|--------|---------|---------|--------|
| Mean | 1.232 | 0.2402 | 2.272 |
| StD | 0.3422 | 0.0958 | 0.172 |
| | S_PERIM | SPACE | SQCOV |
| Mean | 0.2329 | 46.72 | 0.1543 |
| StD | 0.1233 | 21.64 | 0.1494 |

Correlation Matrix

| | M_AREA | S_AREA | M_PERIM | |
|---------|--------|--------|---------|----------------------------------|
| M_AREA | 1.0000 | -.0688 | 0.4769 | the mean, LOGAREA |
| S_AREA | -.0688 | 1.0000 | 0.0591 | the standard deviation, LOGAREA |
| M_PERIM | 0.4769 | 0.0591 | 1.0000 | the mean, LOGPERIM |
| S_PERIM | -.3396 | 0.4155 | -.2003 | the standard deviation, LOGPERIM |
| SPACE | -.3087 | 0.1481 | 0.0944 | |
| SQCOV | -.4731 | 0.6931 | -.0050 | |

| | S_PERIM | SPACE | SQCOV | |
|---------|---------|--------|--------|----------------------------------|
| M_AREA | -.3396 | -.3087 | -.4731 | the mean, LOGAREA |
| S_AREA | 0.4155 | 0.1481 | 0.6931 | the standard deviation, LOGAREA |
| M_PERIM | -.2003 | 0.0944 | -.0050 | the mean, LOGPERIM |
| S_PERIM | 1.0000 | 0.1664 | 0.7034 | the standard deviation, LOGPERIM |
| SPACE | 0.1664 | 1.0000 | 0.3192 | |
| SQCOV | 0.7034 | 0.3192 | 1.0000 | |

Eigenvalues of the Correlation Matrix

| | Eigenvalue | Difference | Proportion | Cumulative |
|-------|------------|------------|------------|------------|
| PRIN1 | 2.5880 | 1.2070 | 0.4313 | 0.4313 |
| PRIN2 | 1.3800 | 0.3900 | 0.2301 | 0.6614 |
| PRIN3 | 0.9905 | 0.4810 | 0.1651 | 0.8265 |
| PRIN4 | 0.5095 | 0.0840 | 0.0849 | 0.9114 |
| PRIN5 | 0.4255 | 0.3196 | 0.0709 | 0.9823 |

Table 6.4 Continued. ALLDATA Data.

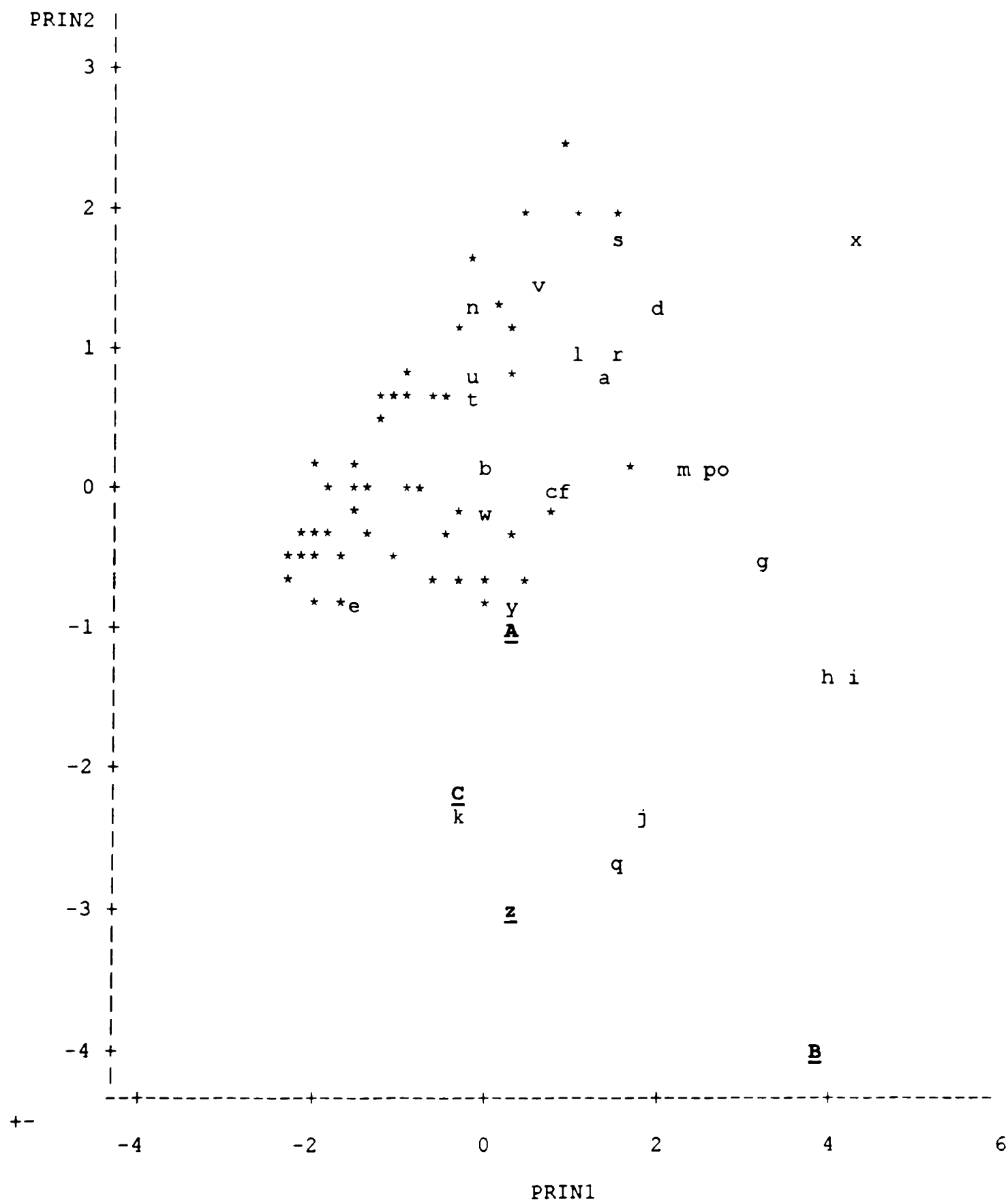
Principal Component Analysis

Eigenvectors

| | PRIN1 | PRIN2 | PRIN3 | |
|---------|--------|---------|---------|----------------------------------|
| M_AREA | -.3932 | 0.51280 | -.24540 | the mean, LOGAREA |
| S_AREA | 0.4168 | 0.41270 | -.29260 | the standard deviation, LOGAREA |
| M_PERIM | -.1505 | 0.72230 | 0.25860 | the mean, LOGPERIM |
| S_PERIM | 0.4949 | 0.00740 | -.25790 | the standard deviation, LOGPERIM |
| SPACE | 0.2735 | 0.08856 | 0.84620 | |
| SQCOV | 0.5737 | 0.19250 | -.06868 | |

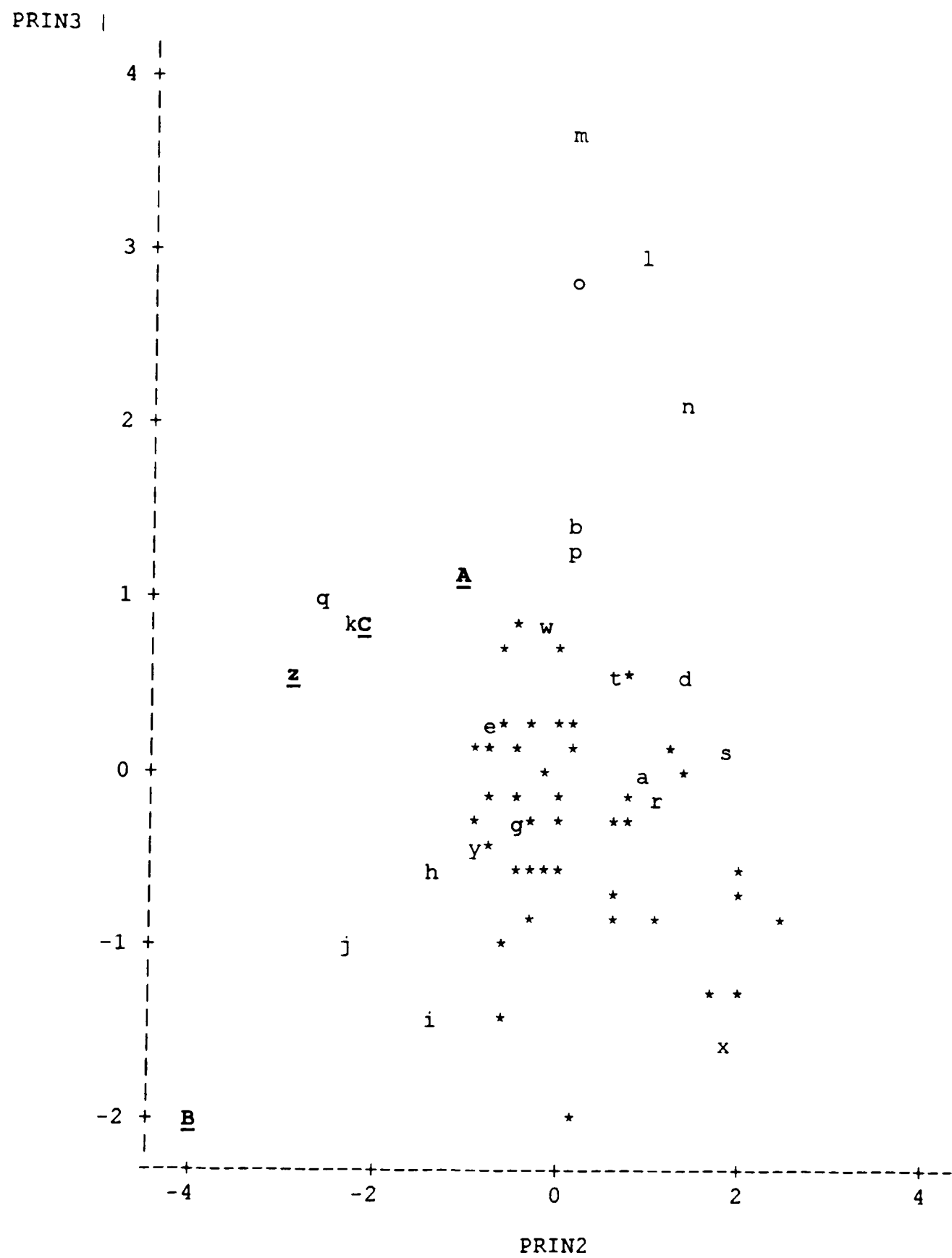
| | PRIN4 | PRIN5 | |
|---------|---------|---------|----------------------------------|
| M_AREA | 0.05945 | 0.61390 | the mean, LOGAREA |
| S_AREA | -.64250 | 0.10260 | the standard deviation, LOGAREA |
| M_PERIM | 0.31800 | -.47730 | the mean, LOGPERIM |
| S_PERIM | 0.68770 | 0.33700 | the standard deviation, LOGPERIM |
| SPACE | -.08930 | 0.43950 | |
| SQCOV | 0.04036 | -.27940 | |

Figure 6.5. Plot of PRIN2*PRIN1, ALLDATA. Bold, underlined characters are standards used, which include *Basilemys* sp. TMM 42335-5 (**z**), *Aspideretes* sp., Javelina Formation TMM42874-1(**A**), Trionychidae(a) TMM 42876-1 (**B**), and Trionychidae(b) TMM 42876-1 (**C**). Randomly generated data are represented by an asterisk (*). PRIN1 represents variability in pit size for the trionychid data; PRIN2 represents overall pit size in the trionychid data.



NOTE: 4 obs hidden.

Figure 6.6. Plot of PRIN3*PRIN2, ALLDATA. NOTE: 13 obs hidden. Bold, underlined characters are standards used, which include *Basilemys* sp. TMM 42335-5 (**z**), *Aspideretes* sp., Javelina Formation TMM42874-1(**A**), Trionychidae(a) TMM 42876-1 (**B**), and Trionychidae(b) TMM 42876-1 (**C**). Randomly generated data are represented by an asterisk (*).



plots were produced as a result of the analysis of the trionychid data (Figures 6.1 and 6.2). In the first, principle component 1 (PC1) plotted variability of size of the pits against overall size (PC2). One prominent cluster appears in the upper left quadrant of the plot. Specimens with large pits of mostly uniform size appear in this area. A check of the specimens against the plot confirms this. A less well defined cluster of outliers appears in the lower left quadrant of the plot. Two of these were standards used for comparison to the 24 Aguja specimens. According to the plot, these specimens have small pits that are mostly uniform in size, which is apparent in actual specimens. A check of the other specimens which appear as outliers on the plot confirm that their positions in morphospace are consistent with the pit patterns.

PC2 and PC3 characterize the overall size of the pits with the space between the pits. Specimens with large spaces between small pits plot in the upper left quadrant. A check of the specimen labeled "q" confirms this. Likewise, a specimen with large pits and little space between them plots in the lower right, as does specimen "x".

Having already determined from the real data that the *variability* of the pit size was a function of the *overall* pit size, two sets of random forms were generated. The first (named "RandataNC") was to determine whether numbers that fell within a reasonable range of constraints, and would produce pits of comparable size and number for imagined species, would produce the same results as real data. These random data did not closely mimic the real data (Figures 6.3, 6.4).

The second set, "Alldata", merged the random data with the real data, and placed biological constraints on the random data. The second data set confirmed that the biological constraints on the placement of the pits in morphospace were, in fact, the variability in the size of the pits compared to their overall size. The loadings and proportions of the principle components are very similar to the real data set (Table 8), and the plots of PC1 versus PC2, and PC2 versus PC3 demonstrate that the random data seem to plot in the same area in morphospace (Figures 6.5, 6.6).

Conclusions and Future Work

This exploratory use of principle components analysis is promising, but far from complete. The purpose of this exercise was to determine whether a model could be developed which might ultimately determine whether the observed pit patterns were significantly non-random and, and if so, where they could be expected to appear in morphospace. This was successfully done, with the results shown here indicating that definite patterns are apparent in the pits on trionychid shells.

It is not possible to determine from these results whether the patterns are related to ontogenetic variables, placement of the pits on the shells, taphonomic influences, sexual dimorphism, or whether these patterns reflect real taxonomic differences. Several things might help determine the origin of the pattern. The next step in the study would be to increase the size of the original data set with more specimens from the same locality, and to provide a more comprehensive set of standards. With an increased data set, and more standards to use for comparison, it

might be possible to determine influences on variance. The standards should include not only specimens that are known to represent different genera and species, but also specimens originating from different positions on the shells. These standards should include specimens that are stratigraphically comparable.

Modern trionychid specimens should also be used as standards. The modern specimens should include different genera, different species of the same genus, and several individuals representing the same species (this last in order to determine what variability is truly individual). Once individual variability is accounted for, then ontogeny, sexual dimorphism, and pit position can be studied in both modern and paleontologic specimens. Taphonomic bias can then be studied by analyzing the influence of abrasion on modern specimens.

By increasing the size of the data set and providing more standards for comparison, presumably denser clusters can be produced, and, with the other sources of “noise” such as pit position, and taphonomic, sexually dimorphic, and ontogenetic bias muted, these clusters in turn might indicate taxonomic separation. Actual use of morphometrics on trionychid shell pits for systematic studies may not be possible. However, it would be useful for studies in diversity if it could be determined that there were more than one species present on a stratigraphic level. Preliminary results from quantitative analysis of these pits are therefore promising.

REFERENCES

- Adkins, W.S., 1933. Mesozoic system in Texas, *In* E.H. Sellards, W.S. Adkins, and F.B. Plummer (eds.), *The Geology of Texas*, vol. 1, Stratigraphy, The Univ. of Texas Bull. 3232. pp. 240-518.
- Archibald, J.D., 1977. Fossil mammalia and testudines of the Hell Creek Formation, and the Geology of the Tullock and Hell Creek Formations, Garfield County, Montana, 2 vols. Unpubl. Ph.D. dissertation, Univ. Cal., Berkeley. 694 pp.
- Bookstein, F.L., Chernoff, B., Elder, R.L., Humphries, Jr., J.M., Smith, G.R., Strauss, R.E., 1985. *Morphometrics in evolutionary biology*. Acad. Nat. Sci. Philadelphia Spec. Pub. No. 15. 277 pp.
- Brinkman, D., and Nicholls, E. L., 1993. New Specimen of *Basilemys praeclara* Hay and its bearing on the relationships of the *Nanhsiungchelyidae* (Reptilia: Testudines). *J. Paleont.*, vol. 67(6), pp. 1027-1031.
- Cope, E.D., 1870. On the Adocidae. *Proc. Am. Phil. Soc.*, vol. 11, pp. 547-553.
- _____, 1871. On the homologies of some of the cranial bones of the reptilia, and on the systematic arrangements of this class. *Proc. Amer. Assoc. Adv. Sci.*, 19th meeting, August, 1870, pp. 194-247.
- _____, 1882. Contributions to the history of the vertebrata of the Lower Eocene of Wyoming and New Mexico, made during 1881. *Proc. Amer. Phil Soc.* Vol. 17, pp. 139-197.
- Davis, J.C., 1986. *Statistics and data analysis in geology*. 2nd ed. Wiley and Sons, New York.
- Dixon, J.R., 1987. *Amphibians and reptiles of Texas*. Texas A&M University Press, College Station. 425 pp.
- Ernst, C.H., and Barbour, R.W., 1989. *Turtles of the world*. Smithsonian Institution, Washington D.C. and London. 313 pp.
- Ernst, C.H., Lovich, J.E., and Barbour, R.W., 1994. *Turtles of the United States and Canada*. Smithsonian Institution Press, Washington and London. 578 pp.

- Fasset and Hinds, 1971. Geology and fuel resources of the Fruitland Formation and Kirtland Shale of the San Juan Basin, New Mexico and Colorado. Geol. Surv. Prof. Pap. 676. Washington. 76 pp.
- Fisher, R.A., Corbet, A.S., and Williams, C.B., 1943. The relation between the number of species and the number of individuals in a random sample of an animal population. J. Anim. Ecol., vol. 12, pp. 42-58.
- Gaffney, E.S., 1965. The genus *Taphrosphys* Cope (Pelomedusidae: Reptilia). Unpublished undergraduate thesis. Rutgers University, New Brunswick, New Jersey. 71 pp.
- _____, 1972. The systematics of the North American family Baenidae (Reptilia, Cryptodira). Bull. Am. Mus. Nat. Hist. vol. 147, pp.245-315.
- _____, 1975a. A phylogeny and classification of the higher categories of turtles. Bull. Am. Mus. Nat. Hist. vol. 155, pp.387-436.
- _____, 1975b. A revision of the side-necked turtle *Taphrosphys sulcatus* (Leidy) from the Cretaceous of New Jersey. Amer. Mus. Novitates. No. 2571, pp. 1-24
- _____, 1979. Description of a large trionychid turtle shell from the Eocene Bridger Formation of Wyoming. Contr. To Geol. Univ. of Wyoming, vol. 17, no.1, p. 53-57.
- _____, and Meylan, P. A., 1988. A phylogeny of turtles. In M.J. Benton (ed.), The phylogeny and classification of tetrapods, vol. 1, Amphibians, reptiles, birds, pp. 157-219. Oxford:Clarendon Press.
- _____, and Zangerl, R., 1968. A revision of the chelonian genus *Bothremys* (Pleurodira: Pelomedusidae). Fieldiana, Geology, Field Mus. Nat. Hist. vol.16, no.7, pp. 193-239.
- Gardner, J.D., and Russell, A.P., 1994. Carapacial variation among soft-shelled turtles (Testudines: Trionychidae), and its relevance to taxonomic and systematic studies of fossil taxa. N. Jb. Geol. Palaont., Abh., vol. 193, pp. 209-244. Stuttgart.
- Gardner, J.D., Russell, A.P., and Brinkman, D.B., 1995. Systematics and taxonomy of soft-shelled turtles (Family Tionychidae) from the Judith River Group (mid-Campanian) of North America. Can. J. Earth Sci., vol. 32, pp. 631-643.

- Gilmore, C.W., 1916. Contributions to the Geology and paleontology of San Juan County, New Mexico. II. Vertebrate faunas of the Ojo Alamo, Kirtland, and Fruitland formations. U.S. Geol. Surv. Prof. Paper, no. 98-Q. pp. 279-308.
- _____, 1919. Reptilian faunas of the Torrejon, Puerco, and underlying Upper Cretaceous formations of San Juan County, New Mexico. USGS Prof. Paper 119.
- _____, 1935. On the reptilia of the Kirtland Formation of New Mexico, with descriptions of new species of fossil turtles. Proc. U.S. Natl. Mus., vol. 83., pp. 159-188.
- _____, 1949. Reptilian fauna of the North Horn Formation of central Utah. USGS Prof. Paper 210-C.
- Hay, O.P., 1908. Fossil turtles of North America. Carnegie Inst. Wash. Publication vol. 75, pp. 1-568.
- _____, 1910. Descriptions of eight new species of fossil turtles from west of the one hundredth meridian. Proc. U.S. Nat. Mus., vol. 38, pp. 307-326.
- Hiriyama, R., 1994. Phylogenetic systematics of chelonoid sea turtles. The Island Arc, vol. 3, pp. 270-284.
- Holman, J.A.H., 1964. Pleistocene amphibians and reptiles from Texas. Herpetologica, vol. 20, no. 2, pp. 73-83.
- _____, 1969. The Pleistocene amphibians and reptiles of Texas. Publ. of the Mus.-Mich. St. Univ. Biol. Ser. vol. 4, no.5, pp. 161-192.
- Hutchison, J.H. and Archibald, J.D., 1986. Diversity of turtles across the Cretaceous/Tertiary boundary in northeastern Montana. Paleogeography, Paleoclimatology, Paleoecology, 55, pp.1-22.
- Hutchison, J.H., and Bramble, D.M., 1981. Homology of the plastral scales of the Kinosternidae and related turtles. Herpetologica, vol. 37(2), pp. 73-85.
- Image – pro Plus Image Processing System Software, 1992. Media Cybernetics, Silver Springs, MD.
- Kachigan, S.K., 1991. Multivariate Statistical Analysis, 3rd ed. Radius Press, New York. 303 pp.

- Knebusch, W.E., 1981. Evidence for deltaic environment of deposition for Aguja Formation (Upper Cretaceous), southwest Texas. Amer. Assoc. Pet. Geol. Bull. (abstr.), vol. 65, p. 764.
- Kovshak, A.A., 1973. Igneous and structural geology of the Grapevine Hills, Big Bend National Park, Brewster County Texas. Univ. of Texas at Arlington, unpubl. M.S. thesis. 107 pp.
- Lambe, L.M., 1902. On the Vertebrata of the mid-Cretaceous of the Northwest Territory. Contr. Canadian Paleont., vol. 3, pp. 25-81.
- _____, 1906. *Boremys*, a new chelonian genus from the Cretaceous of Alberta. Ottawa Nat., vol. 19, no. 10, pp. 232-234.
- Langston, Jr., W., 1956. The shell of *Basilemys variolosa* (Cope). Bull. Nat. Mus. Canada, No. 142., pp. 155-165.
- _____, Standhardt, B. Stevens, M., 1989. Fossil vertebrate collecting in the Big Bend – History and retrospective. In: A. Buseby III and T. Lehman (eds.), Vertebrate Paleontology, Biostratigraphy and Depositional Environments, Latest Cretaceous and Tertiary, Big Bend Area, Texas. 90 pp.
- Lawson, D.A., 1972. Paleoecology of the Tornillo Formation, Big Bend National Park, Brewster County, Texas. Unpubl. M.S. thesis, The Univ. of Texas at Austin. 182 pp.
- Lehman, T.M., 1985. Stratigraphy, sedimentology, and paleontology of Late Cretaceous (Campanian-Maastrichtian) sedimentary rocks in Trans-Pecos Texas. Unpubl. Ph.D. dissertation, Univ. of Texas at Austin. 310 pp.
- _____, 1988. Stratigraphy of the Cretaceous-Tertiary and Paleocene-Eocene transition rocks of Big Bend: discussion. J.Geol., vol. 96, pp. 627-631.
- _____, 1990. Paleosols and the Cretaceous/Tertiary transition in the Big Bend region of Texas. Geology, vol. 18, pp. 362-364.
- _____, 1991. Sedimentation and tectonism in the Laramide Tornillo Basin of West Texas. Sedimentary Geology, vol. 75, pp. 9-28.

- _____, 1996. Late Campanian dinosaur biogeography in the Western Interior of North America. *In*: D. Wolberg and E. Stump, eds., *Dinofest International. Proceedings of a symposium sponsored by Arizona State University. Special Publication, Academy of Natural Sciences, Philadelphia, PA.* (in press).
- Leidy, J. 1856. Notices of extinct Vertebrata discovered by Dr. F.V. Hayden, during the expedition to the Sioux country under the command of Lieut. G.K. Warren. *Proc. Acad. Nat. Sci. Philadelphia*, vol. 8, pp. 311-312.
- Macon, C.C., 1994. Facies analysis and sedimentology of Transgressive shoreline deposits in the Aguja Formation (upper Cretaceous), Trans-Pecos Texas. Unpubl. M.S. thesis, Texas Tech University, Lubbock. 212 pp.
- Magurran, A.E., 1988. *Ecological diversity and its measurement*. Princeton Univ. Press, Princeton, New Jersey. 179 pp.
- Maxwell, R.A., Lonsdale, J.T., Hazzard, R.T., and Wilson, J.A., 1967. *Geology of Big Bend National Park, Brewster County, Texas*. The University of Texas Publ. No. 6711, Bureau of Economic Geology, Austin. 320 pp.
- Meylan, P.A., 1987. The phylogenetic relationships of soft-shelled turtles (family Trionychidae). *Bull. Am. Mus. Nat. Hist.* vol. 186, pp. 1-101.
- Meylan, P.A., and Gaffney, E.S., 1989. The skeletal morphology of the Cretaceous cryptodiran turtle, *Adocus*, and the relationships of the Trionychidae. *Am. Mus. Novitates*, no. 2941, 60 pp.
- Mlynarski, M. 1976. Testudines. *In* O.Kuhn (ed.), *Handbuch der Paleoherpetologie* 7, pp. 1-130. Gustav Fischer Verlag, Stuttgart.
- Pielou, E.C., 1975. *Ecological diversity*. Wiley, New York. 165 pp.
- Preston, F.W., 1962a. The canonical distribution of commonness and rarity. *Ecology*, vol. 43, pp. 185-215.
- Preston, F.W., 1962b. The canonical distribution of commonness and rarity. *Ecology*, vol. 43, pp. 410-32.
- Raup, D.M. 1966. Geometric analysis of shell coiling: general problems. *J. Paleont.* Vol. 40, pp 1178-1190.
- Ricklefs, R.E., 1990. *Ecology*. 3rd ed. W.H. Freeman and Company, New York. 896 pp.

- Romer, A.S., 1976. Osteology of the reptiles. 3rd ed. University of Chicago Press, 772 pp.
- Rosenzweig, M.L., 1995. Species diversity in space and time. Cambridge University Press, Cambridge, U.K., 436 pp.
- Schiebout, J.A., 1974. Vertebrate paleontology and paleoecology of Paleocene Black Peaks Formation, Big Bend National Park, Texas. Texas Mem. Mus., Bull. 88 pp.
- _____, Rigsby, C.A., Rapp, S.D., Hartnell, J.A., and Standhardt, B.R., 1987. Stratigraphy of the Cretaceous-Tertiary and Paleocene-Eocene transition rocks of Big Bend National Park, Texas. J. Geol., vol. 95, pp. 359-375.
- Sonrel, A., 1857. Young turtles, natural size (lithographs). In: L. Agassiz (author), Contributions to the Natural History of the United States, vol. 2. Little, Brown and Company.
- Standhardt, B.R., 1986. Vertebrate paleontology of the Cretaceous/Tertiary transition of Big Bend National Park, Texas. Unpubl. Ph.D. dissertation, Louisiana State Univ., Baton Rouge, La. 298 pp.
- Straight, W.H., 1996. Stratigraphy and paleontology of the Cretaceous-Tertiary Boundary, Big Bend National Park, Texas. Unpubl. M.S. thesis, Texas Tech University, Lubbock. 102 pp.
- Sugihara, G., 1980. Minimal community structure and explanation of species abundance patterns. American Naturalist, vol. 116, pp. 770-87.
- Udden, J.A., 1907. A sketch of the geology of the Chisos Country, Brewster County, Texas. The Univ. of Texas at Austin Bull. 93. 101 pp.
- Webb, R.G., 1990. *Trionyx*. Catal. Am. Amph. Rept., vol. 487, pp. 1-7
- Wieland, R. 1904. Structure of the Upper Cretaceous turtles of New Jersey: *Adocus*, *Osteopygis* and *Propleura*. Am. J. Sci., vol. 17, pp. 112-132.
- Williams, E.E. 1950. Variation and selection in the cervical central articulations of living turtles. Bull. Amer. Mus. Nat. Hist., vol. 94, pp. 505-562.
- Wiman, C. 1933. Über Schilkkroten aus der oberen Kreide in New Mexico. Nova Acta R. Soc. Sci. Upsaliensis, vol. 9, no. 5, pp. 1-34.

- Zangerl, R., 1948. The vertebrate fauna of the Selma Formation of Alabama, Part 2, The Pleurodiran turtles. Fieldiana Geology, Chicago Nat. Hist. Mus. vol.3, no.2.
- _____, 1953a. The vertebrate fauna of the Selma Formation of Alabama, Part 3, The turtles of the family Protostegidae. Fieldiana Geology, Chicago Nat. Hist. Mus. vol.3, no.3.
- _____, 1953b. The vertebrate fauna of the Selma Formation of Alabama, Part 4, The turtles of the family Toxochelyidae. Fieldiana Geology, Chicago Nat. Hist. Mus. vol.3, no.4.
- _____, 1960. The vertebrates of the Selma Formation of Alabama, Part 5, An advanced cheloniid sea turtle. Fieldiana Geology, Chicago Nat. Hist. Mus. vol. 3, no.5.
- _____, 1969. The turtle shell. In C. Gans and T.S. Parsons (eds.), Biology of the Reptilia, I, pp. 311-339. Academic Press, New York.
- _____, Hendrickson, L.P., and Hendrickson, J.R., 1988. A redescription of the Australian Flatback, sea turtle, *Natator depressus*. Bishop Mus. Bull. Zoology I. Bishop Mus. Press, Honolulu. 69 pp.
- _____, and Johnson, R.G., 1957. The nature of shield abnormalities in the turtle shell. Fieldiana Geology, Chicago Nat. Hist. Mus. vol. 10, no. 29.

APPENDIX

SAS PROGRAM FOR MORPHOMETRIC STUDY

TOTTURT.SAS

```
options linesize=79;
```

```
* Read text file containing one line per pit, grouped by specimen;
```

```
data turtle;  
  infile 'turtle2.dat';  
  input label$ spec$ totarea totperim pit$ area perim;  
  area = log(sqrt(area));  
  perim = log(perim);  
run;
```

```
*proc means data=turtle;  
* run;
```

```
proc sort data=turtle;  
  by spec;  
run;
```

```
* Calculate and save univariate statistics for each specimen, across pits;  
* Save results in individual datasets;
```

```
proc univariate data=turtle noprint;  
  var area;  
  by spec;  
  output out=uniarea mean=m_area std=s_area;  
run;
```

```
proc univariate data=turtle noprint;  
  var perim;  
  by spec;  
  output out=uniperim mean=m_perim std=s_perim;
```

```
run;
```

```
data turtle2;  
  infile 'turtle2.dat';  
  input label$ spec$ totarea totperim pit$ area perim;  
run;
```

```
proc sort data=turtle2;  
  by spec;  
run;
```

```
proc univariate data=turtle2 noprint;  
  var area;  
  by spec;  
  output out=space sum=pitarea;  
run;
```

```
proc print data=space;  
run;
```

```
proc univariate data=turtle2 noprint;  
  var totarea;  
  by spec;  
  output out=totarea mean=totarea;  
run;
```

```
proc print data=totarea;  
run;
```

```
data space;  
  merge space totarea;  
  space = totarea - pitarea;  
run;
```

```
proc print data=space;  
run;
```

- * Calculate and save covar between area,perim for each specimen, across pits;
- * Save results in dataset and filter for covariance only;


```
proc corr data=turtle cov noprint outp=corrdata;
  var area perim;
  by spec;
run;
```

```
data corrdata;
  set corrdata;
  *take square root of covarinace to make units equivalent;
  sqcov = sqrt(abs(perim));
  if (perim < 0) then
    sqcov = -sqcov;
  keep spec sqcov;
  drop area perim _type_ _name_;
  if _type_='COV' and _name_='AREA' then output;
run;
```

* Save the 1-char label for each specimen from original dataset;

```
data label;
  set turtle;
  if _n_=1 then specsave = ' ';
  if spec NE specsave then output;
  specsave = spec;
  * keep spec label totarea totperim;
  keep spec label totarea;
  keep spec label;
  retain specsave;
run;
```

```
proc sort data=space;
  by spec;
run;
```

* Merge all results into common dataset having one line per specimen;

```
data turtle;
  merge label uniarea uniperim space corrdata;
run;
```

```
proc print data=turtle;
run;
```

* Analyses of specimens;

```
proc princomp data=turtle out=scores;  
* VAR M_area S_area M_perim S_perim t_area t_perim SQCOV:  
  VAR M_area S_area M_perim S_perim space SQCOV;  
run;
```

```
proc plot data=scores;  
plot prin2 * prin1 = label;  
plot prin3 * prin2 = label;  
run;
```

RANDTURT.SAS

```
options linesize=75;
```

```
data turtle;  
do spec = 1 to 50;  
  * numbers of pits/specimen vary from approx 6-12, centered on 9;  
  do pit = 1 to round(rannor(0) + 9);  
    * perimeter is normally distributed, with a variance that is inversely  
    * proportional to the number of pits (size), and centered arbitrarily  
    * on 10;  
    * perim = rannor(0) + 10; /*no constraint*/  
    c = 0.2;  
    perim = rannor(0)/(c*pit) + 10; /*constrained*/  
  
    * area of circle having this perimeter;  
    area = perim * perim/(4* 3.1415927);  
  
    * restrict area to within 0.3-0.9 of maximum;  
    area = area*(0.3+ranuni(0)*6)/pit + 10; /*unconstrained*/  
    sarea = sqrt(area);  
    logarea = log(sarea);  
    logperim = log(perim);  
    output;  
  end;  
end;
```

```

*proc print data=turtle;
* run;

*proc chart data=turtle;
* vbar area;
* vbar perim;

proc univariate data=turtle noprint;
  var logarea;
  by spec;
  output out=uniarea mean=m_area std=s_area;
run;

proc univariate data=turtle noprint;
  var logperim;
  by spec;
  output out=uniperim mean=m_perim std=s_perim;
run;

proc corr data=turtle cov noprint outp=corrdata;
  var logarea logperim;
  by spec;
run;

*proc print data=corrdata;
* run;

data corrdata;
  set corrdata;
  * take sqrt of covariance to make units equivalent;
  sqcov = sqrt(abs(logperim));
  if (logperim < 0) then
    sqcov = -sqcov;
  * drop logarea logperim _type_ _name_;
  keep spec sqcov;
  * keep only one line per specimen;
  if _type_='COV' and _name_='LOGAREA' then output;
run;

*proc print data=corrdata;
* run;

```

```

data space;
  do spec = 1 to 50;
    space = 20 + 40*ranuni(0);
    logspace = log(space);
    output;
  end;

data turtle;
  merge uniarea uniperim space corrddata;
run;

*proc print data=turtle;
*run;

proc princomp data=turtle out=scores;
  var m_area s_area m_perim s_perim space sqcov;
run;

proc plot data=scores;
  plot prin2 * prin1;
  plot prin3 * prin2;
run;

```

ALLDATA.SAS

```

options linesize=75;

data turtle;
  do spec = 1 to 50;
    * numbers of pits/specimen vary from approx 6-12, centered on 9;
    do pit = 1 to round(rannor(0) + 9);
      * perimeter is normally distributed, with a variance that is inversely
      * proportional to the number of pits (size), and centered arbitrarily
      * on 10;
      *   perim = rannor(0) + 10; /* no constraint */
      c = 0.2; /* constraint factor, where limit 0 = unconstrained */
      perim = rannor(0)/(c*pit) + 10; /* biological constraint */

```

```

* area of circle having this perimeter;
  area = perim * perim/(4* 3.1415927);

  * restrict area to within 0.3-0.9 of maximum;
  * area constrained to be between 0.3-0.9 of max area for given
  * area = area * ranuni(0); /* unconstrained */
  area = area * (0.2 + ranuni(0)*8)/pit + 10; /* constrained */

  sqarea = sqrt(area);
  logarea = log(sqarea);
  logperim = log(perim);
  output;
end;
end;

proc univariate data=turtle noprint;
  var logarea;
  by spec;
  output out=uniarea mean=m_area std=s_area;
run;

proc univariate data=turtle noprint;
  var logperim;
  by spec;
  output out=uniperim mean=m_perim std=s_perim;
run;

proc corr data=turtle cov noprint outp=corrdata;
  var logarea logperim;
  by spec;
run;

data corrdata;
  set corrdata;
  * take sqrt of covariance to make units equivalent;
  sqcov = sqrt(abs(logperim));
  if (logperim < 0) then
    sqcov = -sqcov;
  keep spec sqcov;

```

```

* keep only one line per specimen;
if _type_='COV' and _name_='LOGAREA' then output;
run;

data space;
do spec = 1 to 50;
    space = 20 + 40*ranuni(0);
    logspace = log(space);
    output;
end;

data randturt;
merge uniarea uniperim space corrddata;
label = '*';
drop spec;
run;

* -----;

* Read text file containing one line per pit, grouped by specimen;

data turtle;
infile 'turtle2.dat';
input label$ spec$ totarea totperim pit$ area perim;

space = totarea - sum (of area);

area = log(sqrt(area));
perim = log(perim);
run;

proc means data=turtle;
run;

*proc print data=turtle;
* run;

* Sort by specimen;

proc sort data=turtle;
by spec;
run;

```

- * Calculate and save univariate statistics for each specimen, across pits;
- * Save results in individual datasets;

```
proc univariate data=turtle noprint;
  var area;
  by spec;
  output out=uniarea mean=m_area std=s_area;
run;
```

```
proc univariate data=turtle noprint;
  var perim;
  by spec;
  output out=uniperim mean=m_perim std=s_perim;
run;
```

```
data turtle2;
  infile 'turtle2.dat';
  input label$ spec$ totarea totperim pit$ area perim;
run;
```

```
proc sort data=turtle2;
  by spec;
run;
```

```
proc univariate data=turtle2 noprint;
  var area;
  by spec;
  output out=space sum=pitarea;
run;
```

```
proc univariate data=turtle2 noprint;
  var totarea;
  by spec;
  output out=totarea mean=totarea;
run;
```

```
data space;
  merge space totarea;
  space = totarea - pitarea;
run;
```

- * Calculate and save covar between area,perim for each specimen, across pits;

* Save results in dataset and filter for covariance only;

```
proc corr data=turtle cov noprint outp=corrdata;  
  var area perim;  
  by spec;  
run;
```

```
data corrdata;  
  set corrdata;  
  sqcov = sqrt(abs(perim));  
  if (perim < 0) then  
    sqcov = -sqcov;  
  drop area perim _type_ _name_;  
  if _type_='COV' and _name_='AREA' then output;  
run;
```

* Save the 1-char label for each specimen from original dataset;

```
data label;  
  set turtle;  
  if _n_=1 then specsave = ' ';  
  if spec NE specsave then output;  
  specsave = spec;  
  keep spec label;  
  retain specsave;  
run;
```

* Merge all results into common dataset having one line per specimen;

```
data realturt;  
  merge label uniarea uniperim space corrdata;  
  drop spec;  
run;
```

* Analyses of specimens;

```
data turtle;  
  set randturt realturt;  
run;
```

```
proc princomp data=turtle out=scores;
```



```
VAR M_area S_area M_perim S_perim Space SQCOV;  
run;
```

```
proc plot data=scores;  
plot prin2 * prin1 = label;  
plot prin3 * prin2 = label;  
run;
```

